Author:
Taylor, Jelena

Title:
Investigation of the potential role of oral pathogens in Parkinson's Disease

Investigation of the potential role of oral pathogens in Parkinson's Disease

By

Jelena Taylor

A dissertation submitted to the University of Bristol in accordance with the requirements for award of the degree of Master of Research in Bristol Dental School in the Faculty of Health Sciences, November 2022

Word Count: 29,924

Abstract

Introduction:

Parkinson's disease (PD) is a progressive neurodegenerative disease, characterised by motor symptoms which are caused by loss of dopaminergic neurons in the substantia nigra (Pradeep *et al.*, 2015; Chen *et al.*, 2017).

Misfolded protein aggregations, mainly comprised of α-synuclein accumulations in PD brains are termed Lewy Bodies (LB) (Outeiro *et al.*, 2019), with LB progression being identified in six stages (Braak *et al.*, 2003). α-synuclein has been found to have antimicrobial properties (Park *et al.*, 2016), and recently questions have been raised as to whether spread of α-synuclein is a response to infection, and whether peripheral infections such as periodontitis could be a risk factor for PD (Ferrari and Tarelli, 2011).

Here, post-mortem PD brain tissue was analysed for presence and abundance of bacterial species compared with controls (C). Presence of α-synuclein has also been investigated to analyse any differences between PD and C.

Methods:

Ten PD and ten C brain tissues were obtained from the South West Dementia Brain Bank (SWDBB). DNA extraction was performed, and concentrations determined. Using quantitative polymerase chain reaction (qPCR) to amplify variable 3 and 4 region of 16S rRNA gene, bacterial DNA was quantified against known standards. PCR product was sent for Next Generation Sequencing (NGS) to determine taxa present in samples. Immunoassays were used to determine α-synuclein concentrations and compared with bacterial concentrations to determine any correlation.

Results:

Higher bacterial concentrations were found in PD brains than C, in particular the midbrain areas. There was no correlation between bacterial and α-synuclein concentration. Seven of the top ten genera identified by NGS were found to be oral, and *Prevotella denticola,* a known pathogen in periodontitis, the most differentially represented species between control and PD in substantia nigra brain area samples, with it being represented significantly more in PD samples ($p < 0.01$).

Word Count: 298

Dedication and acknowledgements

I dedicate this work to my children Noah and Jacob, who have enriched my life beyond comprehension. I hope they too can achieve anything they want and be supported in life to do so.

I want to thank my supervisors Professor Nicola West and Dr Shelley Allen-Birt, and all the team at the Dental Clinical Trials Unit. I thoroughly enjoyed working with the team and feel very grateful for the opportunities forged during my time there. I sincerely want to thank Dr Maria Davies who has been a constant support during the difficult times in my study and for pushing me to complete it when times were hard.

Additionally, the South West Health Protection Team at UKHSA supported me with granting study days to be able to complete my thesis, for this I am very grateful.

Finally, I would like to honour and thank Dr David Emery who sadly passed away before the thesis was submitted. Dave was a brilliant scientist and mentor to me in the laboratory, and his wit and humour alleviated many of my stressful qPCR dramas! I am thankful to have known and learnt from him, he will be missed.

Author’s declaration

I declare that the work in this dissertation was carried out in accordance with the requirements of the University's *Regulations and Code of Practice for Research Degree Programmes* and that it has not been submitted for any other academic award. Except where indicated by specific reference in the text, the work is the candidate's own work. Work done in collaboration with, or with the assistance of, others, is indicated as such. Any views expressed in the dissertation are those of the author.

SIGNED: DATE: 30/11/2022

Contents

List of figures

List of tables

List of abbreviations

AD	Alzheimer's Disease
ALP	Autophagy-Lysosomal Pathway
ALS	Amyotrophic Lateral Sclerosis
AMP	Antimicrobial Peptide
ANOSIM	Analysis of Similarity
ApoA-I	Apolipoprotein A-I
APOE	Apolipoprotein E
ASP	α-synucleinopathies
ATP	Adenosine Triphosphate
Aβ	Amyloid Beta
BB	Brain Bank
BBB	Blood Brain Barrier
BCA	Bicinchoninic Acid
BCSFB	Brain-Cerebrospinal Fluid Barrier
BG	Betaglobin
BMVEC	Brain Microvascular Endothelial Cells
bp	Base Pairs
BS	Brain Stem
BSA	Bovine Serum Albumin
CAA	Cerebral Amyloid Angiopathy
CERAD	Consortium to Establish a Registry for Alzheimer's Disease
CNS	Central Nervous System
COD	Cause of death
CP	Choroid Plexus
CPITN	Community Periodontal Index for Treatment Needs
CSF	Cerebral spinal fluid
CT	Computerised Tomography
Ct	Cycle Threshold
CVD	Cardiovascular Disease
DA	Dopaminergic Neurons
DAMPs	Damage-Associated Molecular Patterns
DBS	Deep Brain Stimulation

DCE-MRI	Dynamic Contrast-Enhanced Magnetic Resonance Imaging
DLB	Dementia with Lewy Bodies
DMSO	Dimethyl Sulfoxide
DNH	Dorsal Nigral Hyperintensity
dsDNA	Double Stranded DNA
EC	Entorhinal Cortex
EDTA	Ethylenediaminetetraacetic Acid
ELISA	Enzyme-Linked Immunosorbent Assay
ENS	Enteric Nervous System
ERH	Entorhinal Cortex/Hippocampus region
GI	Gastrointestinal
HDL	High Density Lipoprotein
HOMD	Human Oral Microbiome Database
HSV-1	Herpes Simplex Virus 1
HTA	Health Tissue Authority
IL	Interleukin
iRBD	idiopathic Rapid Eye Movement Sleep Behaviour Disorder
LB	Lewy Body
LBP	Lewy Body Pathology
LC	Locus Coeruleus
LDA	Linear Discriminant Analysis
L-dopa	Levodopa
LN	Lewy Neurite
LP	Lewy Pathology
LPS	Lipopolysaccharide
LRRK2	Leucine-Rich Repeat Serine/Threonine-Protein Kinase 2
MAOBI	Monoamine Oxidase Type B Inhibitor
MARS	Multivariate Adaptive Regression Spline
MCI	Mild Cognitive Impairment
MDS-PD	International Parkinson and Movement Disorder Society
MED	Minimum Entropy Decomposition
MHC	Major Histocompatibility Complex
MMSE	Mini-Mental State Examination
MRI	Magnetic Resonance Imaging

MRPP	Multi-Response Permutation Procedure
MSA	Multiple System Atrophy
MTS	Mitochondrial Targeting Sequence
NaCl	Sodium Chloride
NCI	Non-Cognitively Impaired
NGS	Next Generation Sequencing
NLR	Nod-Like Receptors
NLRC	NLR family CARD domain
NLRP	Nod-Like Receptor Protein
NMDS	Non-Metric Multidimensional Scaling
NMS	Non-Motor Symptoms
NSAID	Non-Steroidal Anti-Inflammatory Drug
NTC	No Template Control
OTU	Operational Taxonomic Unit
PAMPs	Pathogen-Associated Molecular Pattern Molecules
PBS	Phosphate Buffered Saline
PC3	Prostate Cancer cells
PCA	Principal Component Analysis
PCoA	Principal Co-Ordinate Analysis
PCR	Polymerase Chain Reaction
PD	Parkinson's Disease
PDD	Parkinson's Disease with Dementia
PDQ-39	Parkinson's Disease Questionnaire
PE	Paired-end
PET	Position Emission Tomography
PMD	Post Mortem Delay
PMI	Post Mortem Interval
PRR	Pattern Recognition Receptors
PSP	Progressive Supranuclear Palsy
QoL	Quality of Life
REM	Rapid Eye Movement
RIPA	Radio Immuno Precipitation Assay
ROS	Reactive Oxygen Species
SCFA	Short Chain Fatty Acid

SIP	Sickness Impact Profile
SN	Substantia Nigra
SNCA	Synuclein Alpha gene
SNpc	Substantia Nigra pars compacta
SPECT	Single-Photon Emission Computed Tomography
STN	Subthalamic Nuclei
SVD	Small Vessel Disease
SWDBB	South West Dementia Brain Bank
SWI	Susceptibility-Weighted Imaging
TAE	Tris-Acetate-EDTA
Tm	Melting Temperature
TNFα	Tumour Necrosis Factor alpha
TOM	Translocase of the Outer Membrane
TSE	Transmissible Spongiform Encephalopathies
UKPDBBDC	UK Parkinson's Disease Brain Bank Clinical Diagnostic Criteria
UPGMA	Unweighted Pair-Group Method with Arithmetic Means
UPS	Ubiquitin Proteasome System
WGCNA	Weighted Gene Co-expression Network Analysis

Chapter 1 Introduction

1.1. Parkinson's Disease (PD): An overview

1.1.1 Introduction and history

Parkinson's disease (PD) is a progressive neurodegenerative disease characterized mainly by three motor symptoms: tremor, rigidity, and bradykinesia (Dickson *et al.*, 2009). James Parkinson first described some of the key symptoms of PD in 1817, and later Jean-Martin Charcot provided a more thorough description and identified bradykinesia also as a key feature of PD (Parkinson, 1817; Charcot, 1872). However, it was Édouard Brissaud who first hypothesised in 1895 that damage to the Substantia Nigra (SN-rich in dopaminergic neurons) in the mid-brain was a cause of the typical PD tremors (Brissaud, 1899; Goetz, 2011). Brissaud's hypothesis was validated in 1919 by Konstantin Trétiakoff by a post-mortem study of the midbrain which associated changes in pathology in this region with PD symptoms (Tretiakoff, 1919; Parent and Parent, 2010; Goetz, 2011). It is now known that PD is an α-synucleopathy, whereby α-synuclein accumulates in Lewy bodies (LB) and Lewy neurites (LN) in the brain leading to neurodegeneration (Dickson, 2012). In addition to the extrapyramidal (motor) symptoms, there are also many non-motor symptoms (NMS) and characteristics of PD, such as sleep-disturbance, anosmia, and dementia (Martinez-Martin *et al.*, 2015), making it a heterologous disease. PD mainly occurs sporadically (with no known specific cause), however there are also familial or 'inheritable' cases which account for 10-15% of all cases (Scott *et al.*, 2018), and mutations in several genes such as Parkin, SNCA (synuclein alpha) and LRRK2 (Leucine-rich repeat kinase 2) have been associated with increased susceptibility to PD (Emamzadeh and Surguchov, 2018). The onset of motor symptoms in sporadic cases of PD are usually witnessed at around 55 years of age (Meade *et al.*, 2019), however the disease has a long pre-clinical phase (Yilmaz *et al.*, 2019) and it is estimated that at time of diagnosis around 60% of the dopaminergic neurons have been lost (Balestrino and Schapira, 2020).

1.1.2 Prevalence and incidence of PD

PD is the second most common neurodegenerative disease after Alzheimer's Disease (AD) (Chai and Lim, 2014). Approximately 1% of the adult population over 60 years has PD (Reeve *et al.*, 2014; Tysnes and Storstein, 2017), and the Global Burden of Disease Study estimates that there are 6.2 million people worldwide affected with the disease (Dorsey and Bloem, 2018). Age is the greatest risk factor for PD, with prevalence rising to 3% among the 80 years and over demographic (Scott *et*

al., 2018; Blauwendraat *et al.*, 2022). Due to the ageing population, prevalence is increasing and the incidence of PD diagnoses is expected to double by 2030 (Elbaz *et al.*, 2015; Rey *et al.*, 2018). Prevalence rates differ from study to study, due to the differences in the study methods, however most agree on an overall prevalence rate of between 1 and 2 per 1000 (Tysnes and Storstein, 2017).

European incidence rates of PD generally range from 11 to 19 per 100,000 per year (Balestrino and Schapira, 2020), although a 2005 study of individual nations found rates ranged between 5 and 346 per 100,000, likely reflecting differences in methods used as well as environmental or genetic factors (Von Campenhausen *et al.*, 2005).

1.1.3 Risk factors for PD

In addition to age, there are a number of other risk factors for PD. Environmental factors such as pesticide exposure, are thought to play a role in the increased risk of developing PD although evidence for causality in most cases is not conclusive (Pang *et al.*, 2019). There is also increasing evidence from studies of sport professionals who encounter repeated head injuries, such as boxers and rugby players, suggesting that they are at increased risk of developing parkinsonism and dementia (Noyce *et al.*, 2016). Conversely, there have been studies which show a negative association or benefit of certain chemicals/habits. For example lifestyle factors such as caffeine and alcohol drinking and smoking have shown to be associated with a reduced risk of developing PD (Noyce *et al.*, 2016), whether these chemicals are neuroprotective remains to be seen however. An initial pilot clinical trial investigating nicotine therapy improved motor scores in PD patients (Villafane *et al.*, 2007), however no significant difference in motor scores was detected in a follow up randomised controlled trial (Villafane *et al.*, 2018).

Gender also influences risk. 'A manual of disease of the nervous system' published in 1888 by William Gowers, first reported a higher rate of PD incidence in males than females, (Gowers, 1888; Goetz, 2011), and in the present day males are 1.5 times more likely to be diagnosed with PD than females (Miller and Cronin-Golomb, 2010; Elbaz *et al.*, 2015). Some symptoms are more commonly experienced by one gender than the other, for example, men with PD are more likely to suffer from rigidity while women are more likely to suffer from dyskinesias (Miller and Cronin-Golomb, 2010). In addition, women are on average diagnosed 2 years later than men, and it is suggested that there is a potential PD protective effect of oestrogen in women (Miller and Cronin-Golomb, 2010). Studies into PD gender differences are ongoing (Song *et al.*, 2020).

As mentioned above, there are gene mutations which increase the susceptibility of developing PD. Close family members of a PD patient have a 2 to 3-fold increase of developing PD themselves, and

around 5-10% of all patients have a monogenic form of the disease (Lill, 2016; Tysnes and Storstein, 2017).

1.1.4 Parkinson's Disease with Dementia (PDD) and Lewy Body Dementia (LBD)

Cognitive impairment is a common symptom of PD. At initial diagnosis of PD, around 30% of patients will have some cognitive impairment, however this increases to 80% as the disease progresses (Aldridge *et al.*, 2018). Dementia occurs in Parkinson's Disease with Dementia (PDD) and Dementia with Lewy Bodies (DLB)(Van Den Berge *et al.*, 2012), which share many pathological features, such as the presence of α synuclein, Lewy bodies, and also β amyloid and tau pathologies (Jellinger and Korczyn, 2018). However, the clinical features and time-course of the symptoms differ between the two (Emre *et al.*, 2007). It is suggested that the two diseases are likely to be sub-types within a spectrum of LB diseases that range from incidental LBP (Lewy Body Pathology), where there are no PD symptoms, to DLB, where AD is present (Jellinger and Korczyn, 2018). A diagnosis of PDD is made when dementia develops in established PD, conversely a DLB diagnosis is made when dementia precedes or begins within one year of Parkinsonism motor symptoms (Gomperts, 2016; McKeith *et al.*, 2017).

1.1.5 Diagnosis of PD

Although Parkinson and Charcot first identified the cardinal symptoms of PD in the early 19th century, it was only in the early 1990s that formal diagnostic criteria were introduced, improving diagnostic accuracy from ~75% to 82% (Marsili *et al.*, 2018). The first formal criteria for the diagnosis of PD were set out by the 'UK Parkinson's Disease Brain Bank Clinical Diagnostic Criteria' (UKPDBBDC) and followed a 3-step process. Firstly parkinsonian syndromes were identified, then diseases that are not PD were excluded, and finally criteria that support a PD diagnosis were reviewed (Marsili *et al.*, 2018). Criteria were updated by Gelb and colleagues in 1999 (Gelb *et al.*, 1999) which allowed diagnosis to be categorised as probable or possible PD. More recently, the International Parkinson and Movement Disorder Society (MDS-PD) diagnostic criteria are used, which incorporate NMS as well as motor symptoms (Marsili *et al.*, 2018). Similar to the UKPDBBDC and criteria of Gelb (1999), the MDS-PD criteria are designed to minimise diagnostic error through misdiagnosis of other Parkinsonism disorders or other pathologies causing neurodegeneration such as, Multiple System Atrophy (MSA) and Progressive Supranuclear Palsy (PSP) (Postuma *et al.*, 2015). In addition to the diagnosis of Parkinsonism to include bradykinesia as well as either tremor or rigidity (step 1), there are exclusion criteria (step 2), supportive criteria (step 3), and red flags (step

4), which are characteristics and which are strongly suggestive of a non-PD diagnosis (Scott *et al.*, 2018). Using the above criteria and with subsequent follow up appointments with patients, diagnostic accuracy is increasing; confirmation of diagnosis of PD however can currently only be obtained through post-mortem neuropathology (Beach and Adler, 2018). Post-mortem studies have shown that clinical accuracy of PD diagnosis is 81%, with the most common misdiagnosis post-mortem being either PSP or MSA (Beach and Adler, 2018; Kobylecki, 2020).

Currently, PD diagnosis is still obtained through clinical tests made by neurologists and movement-disorder specialists, meaning that clinical symptoms, usually motor symptoms, must be present. However, this is a late stage of PD (Noyce *et al.*, 2016). Finding prodromal markers or a biomarker for diagnosis that can be detected during the prodromal stage could greatly improve prognosis in PD patients as treatment could then start early before motor symptoms develop. In addition, a biomarker(s) would help improve diagnostic accuracy (Miller and Callaghan, 2014).

There are prodromal markers currently in use clinically, which are: slight motor impairment, changes in olfaction, rapid eye movement, and detection of reduced nigrostriatal radioligand uptake in a single photon emission computed tomography (SPECT) scan (Yilmaz *et al.*, 2019). While SPECT scans are included in diagnostic criteria for prodromal PD, there are now other imaging biomarkers that have also shown great promise such as reduction or absence of dorsal nigral hyperintensity (DNH) of the SN using susceptibility-weighted imaging (SWI) (Yilmaz *et al.*, 2019). A study conducted by De Marzi and colleagues found that DNH was lacking in 92% of individuals who had idiopathic rapid eye movement sleep behaviour disorder (iRBD) compared to 3% of healthy controls, suggesting that DNH could be a good biomarker for prodromal PD (De Marzi *et al.*, 2016). Imaging markers are also evolving that might help in differentiating between DLB and PDD, which is challenging, and DLB remains clinically underdiagnosed (Orad and Shiner, 2022). Methods such as SWI can aid in the diagnosis of these two diseases and can also exclude other possible causes of these symptoms such as tumours or inflammatory changes. A differential diagnosis algorithm using different scan combinations to confirm AD, DLB or PDD has been proposed (Orad and Shiner, 2022).

Although neuroimaging is improving and becoming reliable for PD diagnosis, scanners remain costly and still lack specificity (Chelliah Sundramurthi *et al.*, 2022), thus the search for biomarkers remains important. There are some promising biomarkers available for PD, however they are still not specific enough for PD to be used in diagnosis, unlike biomarkers that have been used for AD for some time now (Yilmaz *et al.*, 2019). A systematic review conducted by Chelliah and colleagues for proteomic biomarkers in blood and cerebrospinal fluid (CSF), found Apolipoprotein A-I (ApoA-I) to be the most reliable and replicable biomarker for diagnosing PD early. ApoA-I is found in high density lipoprotein

(HDL), whose role is to eliminate excess cholesterol. A reduction in ApoA-I leads to a reduction in HDL, as seen in cardiovascular disease and neurodegenerative diseases (Chelliah Sundramurthi *et al.*, 2022). ApoA-I could therefore be used as a blood-based, non-invasive biomarker for prodromal PD.

1.1.6 Braak staging of PD

A post-mortem staging scheme for PD was developed by Braak and colleagues to characterize PD disease progression for the purposes of diagnosis and research, by identifying the presence of LB pathology in different areas of the brain (Braak *et al.*, 2003). This is a six-stage scheme, which is distinct from the one developed for AD, although both visualise aggregations caused by protein misfolding of A-beta (Aβ) in AD, and α-synuclein, a pre-synaptic neuronal protein, in PD (Braak and Braak, 1995). Lewy bodies are intraneuronal protein inclusions that accumulate progressively in PD, and mainly consist of misfolded α-synuclein (Outeiro, 2019). These inclusions can be easily distinguished from other neuropathological diseases based on their components and their pattern of spread into susceptible brain regions specific to PD (Braak *et al.*, 2004). The initial study used post-mortem stained brain sections from 41 individuals clinically diagnosed with either PD, LB or LN but no PD symptoms or without LB or LN (19 females and 22 males) (Braak *et al.*, 2003). Heiko Braak and colleagues were able to visualise LB and LN and determine specific sites of origin and the brain areas that subsequently became affected (populated by LB and LN) as PD progressed. Six stages of PD pathology were identified and it was shown that in stages 1/2, Lewy pathology originated in either or both of the dorsal motor nuclei of the vagal and glossopharyngeal nerve in the brainstem, and the anterior olfactory nucleus. In stages 3/4, Lewy pathology was shown to progress into neighbouring midbrain areas, eventually reaching the neocortex in stages 5/6, at which point the individual would most likely be suffering with dementia (Braak *et al.*, 2003).

1.1.7 PD symptoms and their effects on quality of life (QoL)

The measurement of QoL in diseases mainly depends on self-reported patient assessments, primarily through questionnaires such as the Sickness Impact Profile (SIP) and the 39 item Parkinson's Disease Questionnaire (PDQ-39) (Opara *et al.*, 2012). These questionnaires are designed to address a patient's satisfaction levels with daily activities such as eating and sleeping, and the data derived from them are used to improve rehabilitation in patients with chronic conditions such as PD (Karlsen *et al.*, 1999). In a study to determine the most troublesome PD symptoms, patients diagnosed within the previous 6 years ranked as highest the motor symptoms of slowness/tremor/stiffness followed by pain and loss of smell/taste, and those diagnosed longer ago rated the treatment, on-off

fluctuations of their motor features and dyskinesia highest followed by mood changes, drooling and sleep problems (Politis *et al.*, 2010). Thus, QoL has been shown to be affected by both motor and NMS. Furthermore, in recent years evidence has suggested that NMS may be more important than motor symptoms when considering impacts on daily living (Barone *et al.*, 2017). Most patients with PD present with various NMS, yet NMS are often under-recognised by professionals (Chaudhuri *et al.*, 2011). Some examples of common non-motor symptoms are depression, incontinence, constipation, dysphagia, drooling, and sleep disorders such as insomnia and Rapid Eye Movement (REM) sleep behaviour disorder (Adler, 2005). That depression is among the main predictors of poor QoL has been a consistent finding in several studies, even when using different study methods (Shibley *et al.*, 2008; Santos-García and De La Fuente-Fernández, 2013). Dysphagia, drooling, and xerostomia are conditions of the oral cavity and combined with compromised manual dexterity, PD patients often are unable to sustain good oral hygiene. This results in dental caries and periodontitis, which affect their ability to eat (Nakayama *et al.*, 2004; Packer *et al.*, 2009).

1.1.8 Current treatments for PD

There are different types of therapies available to individuals with PD that are often based on the severity of the disease at diagnosis and the age of the patient, with an aim to improve QoL, as there are currently no treatments that can slow down PD progression or prevent it from occurring (Scott *et al.*, 2018). Most treatments aim to restore dopamine depleted in PD, and the most effective treatment, established over 50 years ago, is Levodopa, or L-Dopa, a precursor to dopamine that can cross the blood-brain-barrier (BBB) and increase dopamine levels in the brain (Connolly and Lang, 2014). This treatment is suitable at all stages of PD, and considering both its effect, short-term side effects and evidence that it has also substantially increased QoL in patients with PD, L-Dopa is often hailed as the best treatment for PD (Oertel and Schulz, 2016).

Other treatments that target different parts of the dopamine pathway may also be prescribed, but usually to younger patients or those with mild motor symptoms (Scott *et al.*, 2018). Agonists that activate the dopamine receptor can be given in formulations such as patches where release is prolonged. However these also have side effects some of which are serious including the development of compulsive behaviours which can include gambling, compulsive shopping or overeating (Moore *et al.*, 2014). For treatment of mild motor symptoms, a monoamine oxidase type B inhibitor (MAOBI) that targets enzymes that degrade dopamine is usually the initial choice for treatment as it is less potent than the conventional dopamine agonists and Levodopa therapies (Connolly and Lang, 2014). Starting with MAOBI instead of Levodopa also delays motor

complications such as freezing episodes and speech impairment, which are often seen once the benefit of Levodopa becomes limited (Thanvi and Lo, 2004).

In the 1990s, there was a surge in Deep Brain Simulation (DBS) procedures for the treatment in PD, due to concerns of the adverse effects seen in surgical treatments such as pallidotomy that were popular prior to Levodopa coming to market (Bronstein *et al.*, 2011). The subthalamic nuclei (STN), which is a key area of motor control in basal ganglia, and the globus pallidus interna are the effective targets for DBS. The high frequency chronic stimulation of these areas suppresses PD symptoms (Benabid, 2003; Bronstein *et al.*, 2011). Careful patient selection is necessary for DBS as it is only suitable for certain cases, and it requires a multidisciplinary team of movement disorder specialists, neurosurgeons, and psychiatrists. The best DBS results are most often seen in individuals with advanced PD who also are of younger age, have a good response to Levodopa and have little or no cognitive impairment (Bronstein *et al.*, 2011).

There are still some controversial aspects to treatment of PD using DBS, with infection and migration of hardware leads being a common cause of issues. However there have been long term improvements of up to 5 years in PD patients treated with DBS and it has also been found to alleviate psychiatric fluctuations, and improve quality of sleep and autonomic functions (Bronstein *et al.*, 2011; Hartmann *et al.*, 2019). However, PD still progresses in individuals who have received DBS and there is little evidence that it may alter the disease progression; furthermore just like Levodopa, patients develop a resistance such as freezing of gait (Bronstein *et al.*, 2011).

Treatment of NMS is still to this day often an un-met need for patients with PD and their families. Neuropsychiatric symptoms such as depression can be severely debilitating in the PD population, and while reported depressive symptoms vary widely, their prevalence has been said to be as high as 76% (Veazey, 2005). There is also evidence to suggest that depression in PD patients can exacerbate cognitive and motor symptoms (Marsh, 2013; Vanle *et al.*, 2018), hence the importance of more research into effective treatments available for NMS.

1.2 Pathology of Parkinson's Disease

There are marked anatomical differences in the PD brain compared to non-diseased brain. The loss of neurons in the substantia nigra (SN) and locus coeruleus (LC) of the midbrain is noticeable in PD post-mortem brain due to neuromelanin pigment loss (Dickson *et al.*, 2009). The loss of pigment correlates with the amount of neuromelanin containing dopaminergic neuron death in the SN, and the noradrenergic neuron death in the LC (Scott *et al.*, 2018).

Below in figure 1.1 shows (a) the lateral view of the left hemisphere of the brain and (b) a mid-sagittal view of the right hemisphere. Both are annotated with Brodmann areas; numbered areas around the cerebral cortex based on their histological and anatomical aspects as developed by Korbinian Brodmann, the figure was taken from Bruner, 2022 (Bruner, 2022) and http://websites.umich.edu/~cogneuro/jpg/Brodmann.html.

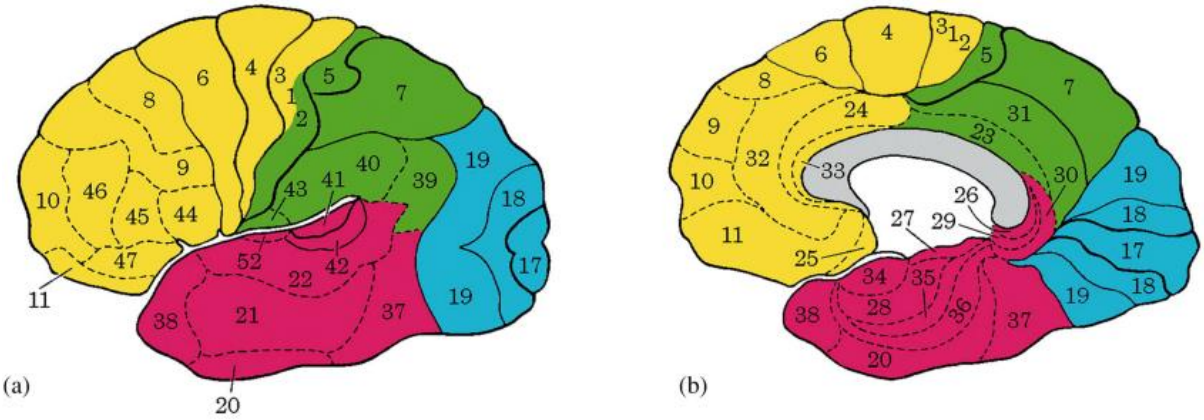

Figure 1.1: A & B: Lateral and mid-sagittal view of the human brain annotated with Brodmann areas
Legend: Lobes Frontal – yellow, Parietal – green, Temporal – red, Occipital – blue.

Brodmann areas are often employed within scientific and medical research as they are similar to the macroanatomical boundaries of the sulci and gyri regions, and so although there are limitations with using Brodmann areas, they are still often used due to ease of identifying topology of brain areas (Bruner, 2022).

Figure 1.2 below is a drawing of (a) the cerebral cortex and brainstem, alongside (b) a cross-section of the caudal midbrain annotated with areas affected by PD pathology and neurodegeneration. Figure 1.2 (b) has been adapted from Clark *et al* (Clark *et al.*, 2018)

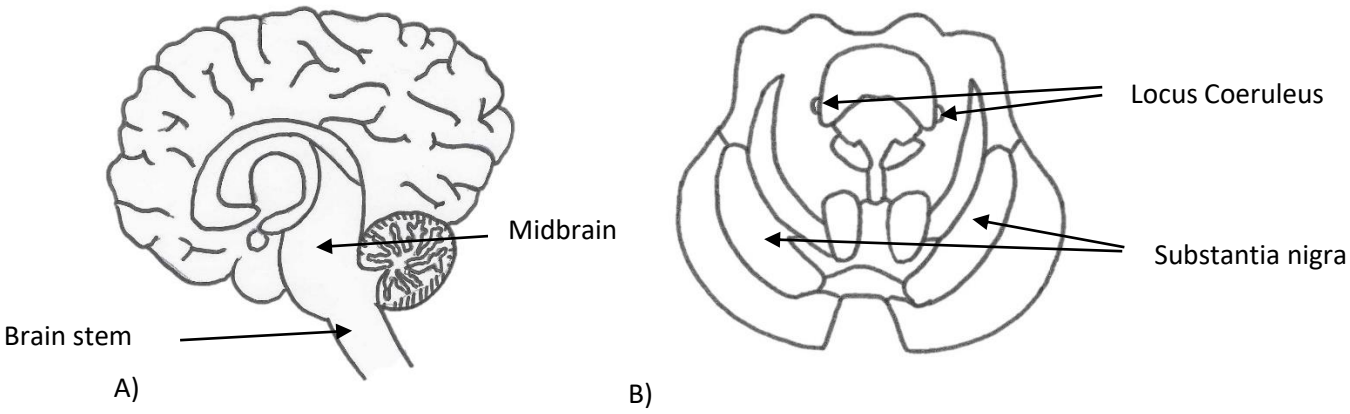

Figure 1.2: A & B: Brainstem and midbrain components

1.2.1 Loss of dopaminergic neurons

Dopamine (3,4-dihydroxyphenylethylamine), secreted by the dopaminergic neurons, is a neurotransmitter that controls our ability to move, our thought processes, regulates our emotions, reinforces behavioural circuits, and is involved in memory (Trutti *et al.*, 2019). There are four dopaminergic pathways in the brain; the mesolimbic, mesocortical, nigrostriatal, and tuberoinfundibular (Habibi, 2017). Dopamine is synthesised in different areas of the brain in each of the four pathways and transmitted to various regions of the brain to carry out its role (Klein *et al.*, 2019). Dopamine synthesized in the SN is transmitted to the dorsal striatum in the nigrostriatal pathway, which is associated with movement (Luo and Huang, 2016). However, recent studies have shown that this pathway is also involved in reward systems and addiction (Wise, 2009). Loss of the dopaminergic cells in the SN of the midbrain thus reduces nigrostriatal pathway signalling and is consequently what initiates the classic motor symptoms present in individuals with PD (Seyfried *et al.*, 2018). The loss of these dopamine producing cells is ultimately the focus of many drug therapies, both commercially available and undergoing clinical trials.

1.2.2 Loss of noradrenergic neurons

The dopaminergic neurons of the SN are not the only neurons to be affected in the brain in PD. Neurodegeneration also affects the noradrenergic, cholinergic, and serotonergic pathways, each of which interacts with dopamine (Meder *et al.*, 2019). This involvement of multiple pathways gives rise to the debilitating NMS and their variety often seen in PD patients, which are not alleviated by dopamine therapy (Braak *et al.*, 2003; Hawkes *et al.*, 2010; Meder *et al.*, 2019). Braak and colleagues

discovered in their post-mortem studies that the LC develops LB pathology in stage 2 of PD, before the SN is impacted (Braak *et al.*, 2004), suggesting an early role for this brain area. The LC is comprises noradrenergic neurons containing neuromelanin, which supply a network of areas in the brain such as the olfactory bulb, hippocampus, and the SN (Paredes-rodriguez *et al.*, 2020). The LC has a range of functions, for instance involving the sleep-waking cycle, control of autonomic functions and the stress response (Gesi *et al.*, 2000). Post-mortem studies have also demonstrated that in PD there is a moderate to severe loss of cells in the LC alongside LB pathology (Giguere *et al.*, 2019). It is now considered that degeneration of the noradrenergic system is associated with a broad spectrum of NMS in PD and plays a key part in the progression of neurodegeneration and LB pathology (Paredes-rodriguez *et al.*, 2020).

1.2.3 α-synuclein

The α-synuclein protein is 140-amino acids in length and in its native state is unfolded and expressed abundantly in the brain and periphery (George *et al.*, 2013). It is thought that α-synuclein in its natural state is involved in vesicular and neurotransmitter trafficking and release, due to its presence in synaptic membranes (George *et al.*, 2013; Fitzgerald *et al.*, 2019). The presence of hyperphosphorylated, misfolded and fibrillized α-synuclein protein, in the central nervous system is a hallmark of α-synucleinopathies (ASP), which include PD, PDD, DLB and multiple system atrophy (MSA), however inclusions of fibrillized α-synuclein affect different cell types in the different diseases (Brück *et al.*, 2016). In addition to α-synuclein there are other protein aggregates that are also present in PD patients (such as tau and ubiquitin), and together they are termed Lewy bodies (LB) when present in the neuron soma, or Lewy neurites (LN) when present in the axon α-synuclein is, however, the major component (Bieri *et al.*, 2018). LN and LB have distinctly different morphologies, with LB being largely spherical and LN more rod like (Valdinocci *et al.*, 2017).

When present in LB and LN, α-synuclein mimics the characteristics of misfolded amyloid protein and is assembled into highly ordered fibrils (Spillantini *et al.*, 1998; Bieri *et al.*, 2018). Amyloid fibrils, such as the insoluble α-synuclein aggregates, are assembled in a way that make them resistant to degradation, and a well-known example of amyloid disease is AD (Rambaran and Serpell, 2008). The hallmark pathologies of AD, Aβ plaques and tau neurofibrillary tangles, are also often found in PD patients and correlate with cognitive decline in PDD and DLB (Irwin *et al.*, 2013). Around 50% of patients with PDD develop a secondary diagnosis of AD (Jellinger and Attems, 2006; Irwin *et al.*, 2013). Hallmark symptoms of PD do not occur until accumulation of α-synuclein fibrils are already advanced, and it is thought that the several early NMS are caused as a result of LB within the

olfactory system and enteric nervous system, giving rise to prodromal symptoms such as hyposmia and constipation (Fahn, 2003; Tyson *et al.*, 2016).

1.2.4 Lewy pathology

Chapter 1 Heiko Braak and colleagues described the staging of PD associated with the spread of LB pathology (Braak *et al.*, 2003). Following this initial publication, the group went on to postulate that a neurotropic pathogen induces PD and termed this the 'dual-hit hypothesis' (Braak *et al.*, 2003; Hawkes *et al.*, 2007). In this hypothesis the mode of entry for the pathogen would be through exposed olfactory and enteric systems from which the pathogen would travel into the central nervous system (CNS) anterogradely or retrogradely, respectively (Braak *et al.*, 2003; Hawkes *et al.*, 2007). Supporting this model, early symptoms of PD are anosmia and gastrointestinal (GI) such as constipation (Poewe, 2008). Furthermore, presence of α-synuclein in the enteric nervous system has been found to have a causal relationship with gastrointestinal symptoms such as reduced colonic motility in animal models (Fitzgerald *et al.*, 2019; Manfredsson *et al.*, 2019). The Braak staging system is outlined in Figure 1.1

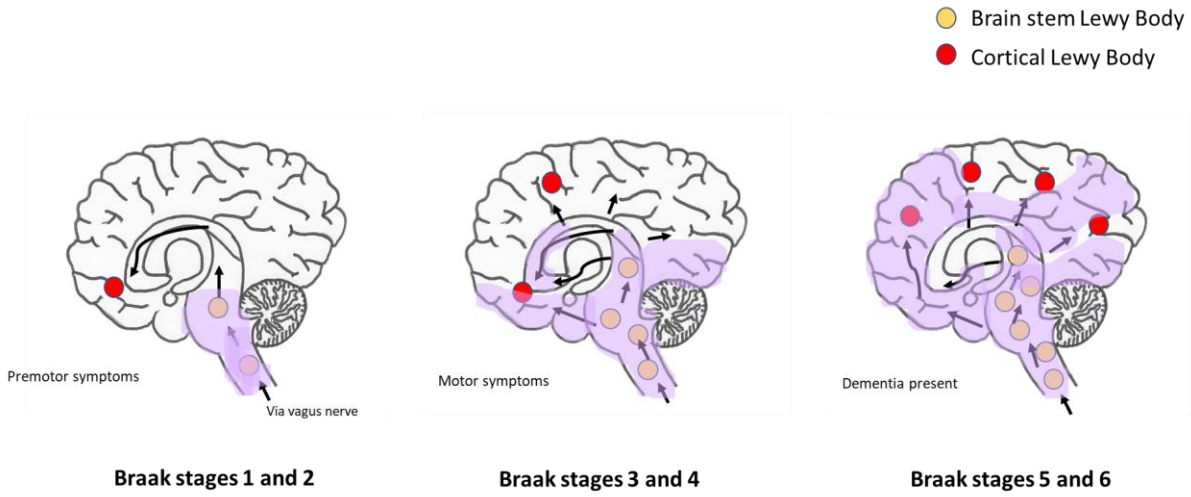

Figure 1.3: Braak stages in PD
A visual diagram of the 6 Braak stages of LB progression in PD, adapted from *Olfactory dysfunction in Parkinson Disease* (Doty, 2012)

As depicted in the diagram above, the Braak staging scheme has 6 stages with progression of LB pathology spreading from a caudal to a rostral pattern. There are two parts to the staging of PD, the pre-symptomatic phase, and the symptomatic phase. In Braak stages 1, 2, and 3, LN and LB are confined to the dorsal motor nucleus of the vagus nerve, the olfactory bulb, and the glossopharyngeal nerve, beginning to first deposit in the substantia nigra pars compacta (SNpc) at

stage 3. LN and LBs travel up the brain stem and progress into specific areas of the cerebral cortex in stage 4 (namely between the neocortex and allocortex). LNs are also found in the second sector of Ammon's Horn at Braak stage 4 and then proceed to the first and third sector at stages 5 and 6. In Braak stages 5 and 6, the cells of the SNpc are unmistakeably degenerated and pale in comparison to controls due to loss of dopaminergic cells, and LN and LB appear in the temporal mesocortex and throughout the neocortex. Braak stages 4, 5 and 6 are the symptomatic phases of PD.

The Braak staging scheme has been widely accepted, however only around 50% of people with PD have a Lewy Pathology (LP) that is consistent with Braaks' staging (Surmeier *et al.*, 2017). It should also be noted that Braak and colleagues (Braak *et al.*, 2003) did not include patients with DLB in their staging study, and other groups have found that brain tissue from patients with DLB did not correlate with the Braak staging scheme (Burke *et al.*, 2008; Parkkinen *et al.*, 2008). Furthermore, the concept of the caudo-rostral trajectory in the lower brain stem and the suggestion that LP seeds into other brain areas in a 'prion like' manner due to the connectiveness and similarity between anatomical sites is widely questioned as there are areas highly innervated by the SNpc that remain unaffected (Tredici and Braak, 2020).

Braak and colleagues described how the use of the Braak staging scheme, whether for clinical or research purposes, will influence the application of it, and different methods of tissue processing and different staining protocols, for example, will all account for variability in assessments (Tredici and Braak, 2020). They concluded that it is for these reasons and much more, that it is important that there is a central setting where staging schemes can be regularly discussed and updated in light of new research. However, in the absence of this, Braak staging for PD is in use and may be used in the future alongside *in vivo* neuroimaging and genetics to expand and create a more individualised profiling (Tredici and Braak, 2020).

Currently, there is no international agreement of staging schemes and Braak staging for AD and PD is still used as the gold standard, with few immunohistochemical and biochemical improvements since the original 1991 staging scheme, and its accuracy remaining a subject of debate (Tredici and Braak, 2020).

1.3 α-synuclein, accumulation in PD and effects on neurodegeneration

1.3.1 Normal function of α-synuclein

Under normal physiological conditions, α-synuclein is abundant in the brain but is also located to a lesser extent in the periphery, such as in the enteric nervous system and red blood cells (Marques

and Outeiro, 2012; Anis *et al.*, 2022). Data from many studies have now suggested that α-synuclein is involved in the release of neurotransmitters (due to the accumulation of α-synuclein at presynaptic vesicles), as well as having a role in synaptic plasticity and maintenance of the synaptic vesicle pool (Guo *et al.*, 2022). Various studies have used in vitro methods to investigate the true native structure of α-synuclein. The answers, however, have remained elusive. A possible reason for the differing outcomes of these studies are the different methods and buffer solutions used, which could potentially alter its structure (Meade *et al.*, 2019). It is thought, however, that in healthy neurons, α-synuclein exists as a soluble monomer or tetra helical form and various studies have found that it develops a helical structure when bound to membranes (Moussaud *et al.*, 2014; Meade *et al.*, 2019).

In light of studies by Soscia and colleagues (Soscia *et al.*, 2010), which reported that amyloid-β was an antimicrobial peptide (AMP), Park and colleagues sought to investigate whether α-synuclein, which shares similar characteristics to amyloid-β, could also be an AMP (Park *et al.*, 2016). Their study found that α-synuclein exhibited antimicrobial activity against a range of bacteria and some fungal strains (Park *et al.*, 2016). AMPs are a key part of the immune system and considered the first line of defence against pathogens (Oliva *et al.*, 2021). The discovery that amyloids have an antimicrobial role has initiated many clinical trials to investigate whether they could be used clinically as topical or systemic antibiotics (Kumar *et al.*, 2016). Whilst the true role of amyloids such as Aβ and α-synuclein are not fully understood, it is evident that they (and others such as tau peptides) have protective effects for cells. However, dysregulation or overexpression of AMPs has been shown to lead to cell toxicity, chronic inflammation and degenerative effects and is implicated in a range of chronic diseases (Kumar *et al.*, 2016; Lee *et al.*, 2020).

1.3.2 Accumulation of α-synuclein

In PD, α-synuclein can be monomeric, but also exists in oligomeric, fibrillar or in ribbon form (Guo *et al.*, 2022). The monomeric and oligomeric forms of α-synuclein precede the fibrillar form, however their role in the formation of the fibril form and how these α-synuclein species spread is still unclear (Surmeier *et al.*, 2017; Fitzgerald *et al.*, 2019). The fibrillar species of α-synuclein is the most prevalent conformation found within LB (Fitzgerald *et al.*, 2019). It was assumed that as the fibrillar form was the major component of LB that it was also the most toxic. However, PD model systems found no correlation between fibril and inclusion body formation with neurotoxicity (Karpinar *et al.*, 2009). Data from rodent studies and in vitro cell based studies have led to the widely accepted belief that the oligomer species of α-synuclein is the most toxic to cells and can result in the degeneration of the SN (Scott *et al.*, 2018; O'Hara *et al.*, 2020).

The oligomeric form of α-synuclein has been found to influence the 'seeding' and increased abnormal aggregation of α-synuclein (Danzer *et al.*, 2012; Scott *et al.*, 2018). There are many factors that have been shown to influence the relative levels of different species of α-synuclein and consequent abnormal aggregation such as phosphorylation of Ser-129 or C-terminal truncation of SNCA that encodes α-synuclein, ubiquitination, oxidative stress and the presence of fatty acids, to name a few (Scott *et al.*, 2018; O'Hara *et al.*, 2020). Phosphorylation of α-synuclein has been shown to favour the formation of α-synuclein oligomers, and in healthy individuals only approximately 4% of α-synuclein is phosphorylated (Rocha Sobrinho *et al.*, 2018). By contrast, phosphorylated α-synuclein at Ser-129 accounts for up to 90% of aggregated α-synuclein in LB in PD brains (O'Hara *et al.*, 2020). The point mutations E46K and A53T in SNCA have also been found to increase the oligomeric and fibrillar forms of α-synuclein (George *et al.*, 2013).

Accumulation of α-synuclein can also be due to a failure to remove it from the brain. Degradation and removal of misfolded proteins from the brain occurs through two pathways: the Autophagy-Lysosomal Pathway (ALP) and the Ubiquitin Proteasome System (UPS), which are independent systems but work in symbiosis (Lopes da Fonseca *et al.*, 2015). The UPS system involves attaching molecules of ubiquitin to α-synuclein and transporting it to the proteosome for degradation and removal. This method can be directly or indirectly impaired through various conditions such as oxidative stress (Betarbet *et al.*, 2005). The ALP comprises three pathways, and each pathway has a role in the engulfing, fusing and breakdown of proteins within the lysosome (Scott *et al.*, 2018). The native form of α-synuclein is mainly cleared by both systems, and activity of these pathways has been found to be reduced in PD brain compared to healthy brain tissue. This has also been observed in animal models of PD (Scott *et al.*, 2018).

1.3.3 Spread of α-synuclein

The molecular mechanisms of α-synuclein spread remain unclear. However, mouse model and post-mortem studies are consistent with cell-to-cell transmission through interconnected brain areas (Bras and Outeiro, 2021). The evidence for cell-to-cell transmission first arose through a trial involving PD patients who received donor dopamine neuronal grafts from healthy donors to alleviate symptoms (Killinger and Kordower, 2019). Over 10 years later in post-mortem histological analysis of the recipient's brain tissue, it was found that the transplanted donor tissue had LP, and that the longer the recipient had had the donated tissue the higher the percentage of donor tissue affected with LP (Kordower *et al.*, 2008). It is, however, controversial to label PD as a prion disease as there is no evidence showing direct transmission of neurogenerative diseases between individuals such as in

the case of transmissible spongiform encephalopathies (TSE). Instead, the progression of α-synuclein is termed 'prion-like' or 'prionoid' (Bras and Outeiro, 2021). The different aggregated forms of α-synuclein, or 'strains', have been shown to display different effects and seeding capacity in cells, which possibly lead to the different synucleinopathies such as MSA and PSA (Bras and Outeiro, 2021).

1.3.4 α-synuclein mutations in PD

There have been over 100 loci identified through genetic research and the genes found to potentially cause PD are named PARK followed by a number (Scott *et al.*, 2018; Jankovic and Tan, 2020). The gene that codes for α-synuclein is SNCA, and there are several point mutations (as well as duplication and triplication of SNCA) that are associated with familial PD (Jan *et al.*, 2021). Mutations can either be autosomal dominant or autosomal recessive (Scott *et al.*, 2018). The point mutation A53T in the SNCA gene is associated with an earlier onset of familial PD, and individuals with triplication of the SNCA gene have a more rapid disease progression (Guo *et al.*, 2022). Point mutations in the gene LRRK2, which encodes for leucine-rich repeat serine/threonine-protein kinase 2, are the most common autosomal-dominant cause of PD (Surmeier *et al.*, 2017). A common point mutation in this gene, G2019S, has been identified in both familial and sporadic PD; however it is less common in the latter (Jankovic and Tan, 2020). Recessive mutations linked to early onset PD are in genes PINK1, PARK2, and PARK7. These are all loss of function mutations and PARK2 is the most common recessive form of PD (Surmeier *et al.*, 2017).

The mutations found within the SNCA gene to date, all lead to either an increase in aggregation, a change to the oligomeric state, or a decrease in the normal ratio between monomer to tetramer conformations of α-synuclein, which then facilitates these changes (Meade *et al.*, 2019). It has been postulated that a disruption of the ratio of the different forms of α-synuclein leads to PD pathology, rather than the presence of them alone, considering that monomer and oligomer forms have been seen in native conditions (Fitzgerald *et al.*, 2019).

1.3.5 Mitochondrial dysfunction in PD

Mitochondrial dysfunction in PD is well established in the literature (Rocha Sobrinho *et al.*, 2018), and the discovery of the role of familial genes PINK1 and PRKN in PD has established its importance in the disease as they mediate mitochondrial quality control (Malpartida *et al.*, 2021). However, the exact role of mitochondrial dysfunction in PD, whether it acts as an initiator or propagator, remains

unclear (Malpartida *et al.*, 2021). Various studies have demonstrated that α-synuclein could cause mitochondrial impairment. Nuclear-encoded mitochondrial proteins have a mitochondrial targeting sequence (MTS) that interacts with the mitochondria's translocase of the outer membrane (TOM) complex and allows them to enter the mitochondria. Data indicates that α-synuclein also has an MTS, and that via an interaction with TOM can disrupt normal protein transport into the mitochondria, an interaction that has been associated with increased reactive oxygen species (ROS) production and impaired mitochondrial function (Devi *et al.*, 2008; Di Maio *et al.*, 2016). Oxidative stress (when ROS disrupts a cell's defence mechanism and function leading to cell death), is thought to be a key event in neurodegeneration in PD (Berg *et al.*, 2005). It has also been shown that proteins that have been modified due to being oxidised by free radicals are more prone to aggregation (Souza *et al.*, 2000).

Evidence also suggests that α-synuclein can disrupt mitochondrial dynamics such as fusion and autophagic degradation, which are required for cells to remain healthy, this disruption being associated with PD (Rocha Sobrinho *et al.*, 2018). In addition, there are studies that suggest that α-synuclein interferes with the cytoskeleton. Tubulin is a major constituent of the cytoskeleton of a cell, and cellular processes such as intracellular transport and metabolism depend on the dynamics of the cytoskeleton (Rocha Sobrinho *et al.*, 2018). In 2010, Zhou and colleagues showed that α-synuclein was able to interact with tubulin, inhibit the formation of microtubules and negatively impact the cellular transport and distribution of mitochondria (Zhou *et al.*, 2010). Interestingly, Alim and colleagues (Alim *et al.*, 2002) demonstrated in vitro that tubulin could promote α-synuclein fibril formation, but this has not been confirmed yet in vivo.

Brain cells demand high energy for neuronal functions, and most of the adenosine triphosphate (ATP) demands are derived from mitochondrial oxidative phosphorylation (Faria-pereira and Morais, 2022). It has been shown in vitro that both endogenous and oligomeric α-synuclein decrease mitochondrial respiration (Di Maio *et al.*, 2016). When comparing brain areas, defects in respiration were located in the midbrain, affecting the nigrostriatal dopaminergic neurons, and were accompanied by increased oxidative stress (Subramaniam *et al.*, 2014). There is also good evidence that α-synuclein plays a specific role in modulating complex 1 inhibition. Complex 1, as the first enzyme in the chain that leads to the generation of ATP by the mitochondria, is critical for its function (Sharma *et al.*, 2009). It has been shown that α-synuclein can be transported inside the mitochondria and disrupt complex 1 activity (Liu *et al.*, 2009), and that prefibrillar oligomeric forms of α-synuclein cause complex 1 dysfunction (Luth *et al.*, 2014). By contrast, data from other studies have suggested other mechanisms by which α-synuclein interferes with complex 1 activity, and are not consistent with regards to the form of α-synuclein that is most damaging. However, taken

together, the body of evidence supports a role for α-synuclein in regulating complex 1 (Rocha Sobrinho *et al.*, 2018).

Lastly, α-synuclein activates microglia, which are the macrophages of the brain that sense cellular damage (Rocha Sobrinho *et al.*, 2018). Evidence suggests that microglia can directly engulf α-synuclein to clear it from the extracellular space. This then leads to proinflammatory changes that create neurotoxicity such as increased production of ROS, which further exacerbates mitochondrial dysfunction in dopamine cells and can lead to cell death (Rocha Sobrinho *et al.*, 2018).

1.4 Pathogens, inflammation, and their association with PD

1.4.1 Microbiota-Gut-Brain-Axis

The Microbiota-Gut-Brain-Axis describes the bidirectional communication via the microbiota between the gut (enteric nervous system or ENS) and the brain (CNS). There are two collective terms used within the literature: *microbiome*, which refers to the genomes of microorganisms in an environment, and *microbiota*, which refers to the collective species names of all the microorganisms in an environment (Valdes *et al.*, 2018).

Humans harbour trillions of microbes on and inside the body that display a symbiotic host-microbial relationship in the absence of disease (Lloyd-price *et al.*, 2016). Infants first become colonised by microorganisms once they are born, and their microbiome undergoes various changes due to diet and exposure to environments reaching a steady equilibrium in adulthood, until changes start to occur in old age (over 65 years) (Sharon *et al.*, 2016). The gut microbiota is diverse with between 400 and 1000 species being reported (Rhee *et al.*, 2009) and is known to play a central role in gut homeostasis, being involved in digestion, immunity, inflammation, and energy metabolism (Valdes *et al.*, 2018). In healthy individuals the microbiota of the gut at the phyla level mainly comprises Proteobacteria, Bacteroidetes, Firmicutes, Clostridiales and Lactobacillales, which are a mix of Gram positive and Gram negative bacteria (Kamada *et al.*, 2013).

Bacteria in the gut have now been shown to actively communicate with the brain through three key routes that work in parallel and are interconnected: neuronal, endocrine/systemic and immune (Agirman and Hsiao, 2021). Through the immune pathway, some components of microbes (such as polysaccharide A, a capsular carbohydrate from the gut commensal *Bacteroides fragilis*), and metabolites that are released such as short chain fatty acids (SCFA), can influence the homeostasis of the immune system and local immune responses (Alvarez *et al.*, 2020; Agirman and Hsiao, 2021). In mice, Erny and colleagues demonstrated that gut microbiota and the SCFA released regulated the

homeostasis of brain microglia, and suggested they have a role in regulating the microglial maturation and function (Erny *et al.*, 2016). Some gut bacteria have the ability to directly synthesise neurotransmitters (such as dopamine and noradrenaline) or neuromodulators, and if released into the periphery these can directly influence the activity of the CNS, while other bacteria modulate the secretion of hormones such as serotonin by enteroendocrine cells, both bacterial groups acting through the endocrine/systemic pathway (Sherwin *et al.*, 2018; Agirman and Hsiao, 2021). The gut is highly innervated and there are four levels to the neural network that are integrated to allow the control of gut function, such as movement of the GI tract (Dong *et al.*, 2022). In the neuronal pathway, microbial products such as SCFA supply energy and have neuroactive properties by directly interacting with enteric neurons, in particular the vagal and spinal efferents. These signals are then passed through sensory circuits to specific brain regions involved in cognition, mood and emotional response (Fuente-Nunez *et al.*, 2018; Agirman and Hsiao, 2021).

In the reverse direction, the brain has been shown to influence the gut microbiome. Signalling molecules released by neurones, which are controlled by the brain, are suggested to be able to affect the microbiota (Carabotti *et al.*, 2015). Binding sites for host derived enteric neurotransmitters have been found on bacteria, and some studies have found that this could cause increased susceptibility to inflammation and infection and could alter the function of elements in the gut microbiota (Hughes and Sperandio, 2008; Carabotti *et al.*, 2015). The brain can directly influence the gut composition through secretion of signalling molecules and immune cells and the communication between CNS and enteric bacteria relies on neurotransmitter receptors on bacterial cell walls (Carabotti *et al.*, 2015). Enterochromaffin cells, which are distributed along the intestinal tract and are considered important in regulating the bidirectional communication between the gut lumen and CNS, are in direct contract with afferent and efferent nerve terminals as well as the gut microbiota, and they also express lots of receptors, such as for serotonin (regulated by the brain), in response to stimuli such as bacterial toxins (Rhee *et al.*, 2009).

Studies using a variety of mouse models have found associations between dysbiosis of the gut microbiome and multiple systemic disorders such as depression and autism (Sharon *et al.*, 2016), and in a key study it was shown that germ free mice developed the motor symptoms of PD after being fed metabolites from bacteria (Sampson *et al.*, 2016). In PD, gastrointestinal disturbances, such as constipation are common, often beginning many years before the onset of typical PD symptoms and worsen over the course of the disease (Sherwin *et al.*, 2018). Studies such as those by Scheperjans *et al* (Scheperjans *et al.*, 2015) have shown differences in faecal microbial populations in PD patients, with a decrease in *Prevotellaceae* and an increase in *Lactobacilliaceae* species compared with controls. In the same study this group was also able to distinguish between different forms of

PD based on levels of faecal *Enterobacteriaceae;* PD patients with a tremor-dominant form had lower abundance of this species than patients who had more severe postural and gait instability (Scheperjans *et al.*, 2015). Interestingly, *Prevotella* species, which were found to be reduced in faecal matter of PD patients, produce mucin whose role in the ENS is to maintain the tight junctions of the intestinal barrier (Sherwin *et al.*, 2018). Therefore a reduction of *Prevotella* species, in addition to a change in the microbiome, may lead to intestinal permeability and translocation of enteric bacteria contributing to intestinal inflammation, which has been proposed to contribute to the induction of misfolding of α-synuclein in the gut (Mulak and Bonaz, 2015; Sherwin *et al.*, 2018).

These findings fit with the dual-hit hypothesis' that Heiko Braak and colleagues proposed in which, in PD, a neurotropic pathogen enters the brain via two routes, one of which is the olfactory route, the other the enteric route and nasal secretions swallowed in saliva (Hawkes *et al.*, 2007, 2009). In the enteric route, Braak and colleagues proposed that the pathogen disrupted the epithelial lining of the GI tract and triggered α-synuclein mis-folding and accumulation. Misfolded α-synuclein would be able to penetrate the epithelial lining and enter the CNS via transsynaptic transmission to the vagus nerve, allowing entry into the medulla, onto the pons, and then through the midbrain into the SNpc where the onset of neurodegeneration would occur (Hawkes *et al.*, 2007).

There are now many studies that support the view of Braak and colleagues that the gut is the primary site at which PD is initiated since the gut is one of the first sites of LB pathology and the changes in the gut microbiota seen in PD patients and their downstream effects such as increased intestinal permeability can cause the GI disturbances seen in PD patients (Hawkes *et al.*, 2007). However, it is still to be elucidated whether the differences in gut microbiota are causal or exacerbates the disease, and so further research is needed.

1.4.2 Neuroinflammation

Neuroinflammation is inflammation of the CNS resulting from an immune response to harmful agents, and it is posited that this is a key driver in the pathology of neurodegenerative diseases such as PD (Sharon *et al.*, 2016).

The major risk factor for PD is increased age since the individual becomes more prone to infection due to changes in the immune system. This includes shrinkage of the thymus, the role of which is to produce new T-cells, and a marked reduction in native T-cells in people over 65 years of age (Mcmanus and Heneka, 2017). Many studies have also shown low grade chronic inflammation in older groups and an increase in the production of pro-inflammatory cytokines, which Franceschi and

colleagues were the first to term as immunosenesence 'inflammaging' (Franceschi *et al.*, 2000; Molteni and Rossetti, 2017). Interestingly, the incidence of bacterial and viral infections are higher in AD and PD patients than their healthy counterparts (Mcmanus and Heneka, 2017).

It was once thought that the brain was an 'immune privileged' site, meaning that it did not have strong immunological activity as it was well protected by the skull and the BBB from external and internal insults. The term was created following a study conducted by Medawar and colleagues who found that skin grafts implanted into the brain took longer to get rejected than skin grafts in the periphery, and the apparent lack of lymphatic drainage from the brain also suggested immune privilege (Medawar, 1947). However, it has now been discovered that there are lymphatic vessels within the dura mater that aid the drainage of CSF into deep cervical lymph nodes, and that there are many innate and adaptive immune cells contained within the meninges (Buckley and Mcgavern, 2022; Mapunda *et al.*, 2022). The meninges and choroid plexus (CP) are the two main immunological sites of the brain and waste matter from the brain parenchyma can pass through the lymphatic vessels to access the cervical lymph nodes and produce an immune response (Louveau *et al.*, 2017).

Microglia, a type of neuroglial cell, are the most dominant immune cells in the CNS and respond to stimuli by changing their conformation, or becoming 'activated', and initiating the release of pro-inflammatory cytokines (Wang *et al.*, 2015). Microglia are part of both the innate and adaptive immune response and their activation is triggered through various stimuli such as infection, trauma, brain lesions and ischemic attacks (Luca *et al.*, 2018). There are two subtypes of microglia: M1 and M2. The M1 type initiates the release of pro-inflammatory cytokines whilst the M2 type is involved in tissue repair through injury (Luca *et al.*, 2018). Macroglia are another type of neuroglial cell, with astrocytes as the main type. These are involved in a number of physiological processes including contributing to the immune response by expressing Major Histocompatibility Complex (MHC) Class II antigens and triggering an inflammatory cascade leading to apoptosis (Luca *et al.*, 2018).

A key feature of the innate immune response in the CNS involves pattern recognition receptors (PRR), which are expressed by microglial cells and oligodendrocytes and are found either as membrane bound (Toll-like receptors), or within the cell cytoplasm (Nod-like receptors (NLR)(Singhal *et al.*, 2014). These PRRs recognise certain pathogen specific proteins (PAMPs), or damage associated proteins (DAMPs) released in response to tissue damage (Singhal *et al.*, 2014). Once a PAMP or DAMP has been detected, an NLR will form a protein complex called an 'inflammasome' comprising the NLR, the proinflammatory caspase (caspase 1), and an adaptor protein (Zhou *et al.*, 2011). The proximity of these molecules in the inflammasome results in the activation of caspase-1, which in turn cleaves the precursors of the proinflammatory cytokines interleukin (IL)-1β and IL-18,

releasing their active forms (Singhal *et al.*, 2014). IL-1β is the primary pro-inflammatory cytokine involved in inflammatory processes (Strowig *et al.*, 2012; Freeman and P.-Y Ting, 2016). Many inflammasomes have now been identified, but NLRP3, NLRC4, AIM2, and NLRP6, have been well characterised and studied in various diseases (Strowig *et al.*, 2012; Freeman and P.-Y Ting, 2016). Immune cells of the meninges and CP detect the inflammatory cytokines released in the CNS and in healthy individuals, can mount a response to allow the brain to return to health (Schwartz and Cahalon, 2022).

Although required to correct immune deviations in the brain, microglial and macroglial activation can also have cytotoxic effects. For example, there is an increase of MHC Class II antigens in response to bacterial lipopolysaccharide (LPS), and upregulation of pro-inflammatory cytokines tumour necrosis factor α (TNFα) and monocyte chemoattractant protein-1 contribute to neuronal insult and neurodegenerative effects (Calabrese *et al.*, 2018; Spagnuolo *et al.*, 2018). It is thought that these toxic effects occur when there is prolonged activation of microglia and astrocytes (Schwartz and Cahalon, 2022). Downstream of these micro and macroglia, NLRP3 has already been implicated in the pathogenesis of AD and recently a number of studies have suggested that it could also be implicated in PD disease progression (Herrmann *et al.*, 2018; Holbrook *et al.*, 2021). For example, von Hermann and colleagues found elevated levels of NLRP3 in mesencephalic neurons of post-mortem PD brain tissue, suggesting that dopaminergic neurons (DA) could be the origin for inflammasome activity (Herrmann *et al.*, 2018). Subsequently, the group evaluated genetic variants of NLRP3 from the Parkinson's Progressive Markers Initiative and found a single nucleotide polymorphism, r7525979, was associated with downregulation of NLRP3 activity and reduced risk of PD (Herrmann *et al.*, 2018). Similarly, Zhou and colleagues found that mitochondrial impairment increased NLRP3 expression in mouse microglia that were exposed to lipopolysaccharide (LPS) and pesticide rotenone, which amplified neurodegeneration in DA neurons (Zhou *et al.*, 2011).

Other studies have found positive associations between NLRP3 activation and α-synuclein aggregation. For example, Chatterjee and colleagues took blood samples from PD patients and age-matched controls and found a significant linear positive correlation between phosphorylated α-synuclein and NLRP3, however these did not correlate with motor symptoms and severity of PD (Chatterjee *et al.*, 2020). Nevertheless, various studies have implicated a role for NLRP3 in PD progression and α-synuclein aggregation, which has led to the development of novel therapeutic strategies that target NLRP3 modulator or the IL-1 and IL-1β receptors, such as small-molecule inhibitors of NLRP3 (Haque *et al.*, 2020). However, more information on how NLRP3 can directly control DA loss is still to be elucidated, which has hampered the progression of discovering a

selective NLRP3 modulator, and some drugs that had gone onto phase 2 trials were withdrawn due to hepatotoxicity in participants (Haque *et al.*, 2020).

Non-steroidal anti-inflammatory drugs (NSAIDs), such as aspirin and ibuprofen, have also been hypothesised to reduce risk of AD and PD. NSAIDs have been shown to reduce degeneration of dopaminergic neurons in mice models of PD (Aubin *et al.*, 1998), and are commonly used to eliminate pain or swelling (Ren *et al.*, 2018). Chen and colleagues conducted a prospective cohort study on men and women and found that participants who reported regular use of NSAIDs had a lower risk of PD (Chen *et al.*, 2003). Further, a meta-analysis study by Ren and colleagues found that from 15 studies analysed, NSAID use was not associated with an increased risk of PD but that some studies had found slight association of use of NSAIDs and reduced risk of PD (Ren *et al.*, 2018). The immunological factors described in this section point to the increasing evidence of inflammation, through various causes, becoming cytotoxic and causing downstream effects, which in turn has been implicated in the development or progression of AD and PD. The NSAID studies described also highlight that anti-inflammatory agents could reduce risk of neurodegenerative effects by reducing inflammation (Ren *et al.*, 2018), however more research is still needed.

1.4.3 The Blood-Brain-Barrier and other routes of entry into the CNS

The brain is protected from the periphery by a physical and metabolic barrier, the BBB, which shields the brain from toxins, pathogens and other material in the blood (Persidsky *et al.*, 2006). The brain microvascular endothelial cells (BMVEC) of the BBB are much thinner than muscle endothelial cells and are held together by tight junctions, forming a physical barrier. Cellular transport systems within them regulate the movement of molecules between the blood and the brain (the metabolic barrier) (Daneman and Prat, 2015). In addition, the BMVECs contain adherens junctions, which also block the transport of a variety of molecules, reducing paracellular permeability. However, certain mechanisms such as passive diffusion still allow some solutes and macromolecules to pass (Dando *et al.*, 2014).

There are areas of the CNS that lack protection from the BBB, namely the circumventricular organs, which include the pineal gland, posterior lobe of the pituitary gland and the choroid plexus (CP) (Norsted *et al.*, 2008). Cerebral spinal fluid (CSF) is produced by the CP and fills the subarachnoid space and the ventricles of the brain providing mechanical support, maintaining chemical homeostasis and regulating ion composition (Dando *et al.*, 2014). The blood-cerebrospinal fluid barrier (BCSFB) also contains tight junctions like the BBB, however it has a lower electrical resistance and therefore it may be more vulnerable to the permeation of toxins and microbes (Dando *et al.*,

2014). Normal CSF contains minimal cell numbers (around 30-35 cells per ml) (Forrester *et al.*, 2018). However, during infections, lymphocytes and monocytes as well as bacteria can pass through CP epithelial cells and enter the brain. Bacterial pathogens are generally limited to the CSF, suggesting that the BBB is breached less frequently than the BCSFB (Forrester *et al.*, 2018).

There are three routes to crossing the BBB/BCSFB. Some pathogens such as *Streptococcus pneumoniae* are taken up by endothelial cells following binding to a host receptor, and cross into the brain by a transcellular route (Forrester *et al.*, 2018). Alternatively, pathogens may enter the CNS via the 'Trojan Horse' pathway, for example initially infecting phagocytes or leukocytes in the blood, which are then transported to the CNS. This pathway has been suggested for the bacterium *Listeria monocytogenes* (Drevets, 1999; Dando *et al.*, 2014). Other bacterial pathogens such as *Neisseria meningiditis* are able to disrupt the tight junctions of the BBB by specific host-pathogen interactions, making it leaky and entering the CNS via a paracellular route (Dando *et al.*, 2014). The dysregulation of selective transport systems across the BBB and/or the deterioration of its physical structure with ageing is known to be a factor in neurodegenerative diseases such as AD and PD (Delaney and Campbell, 2017).

BBB permeability studies in humans use brain imaging together with biochemical methods such as assessing the CSF/plasma albumin ratio (Popescu *et al.*, 2009). Several studies have found higher albumin release from the BBB in older compared to younger individuals and confirmed the degree of BBB permeability using computerised tomography (CT), magnetic resonance imaging (MRI), positron emission tomography (PET), as well as assessing IgG levels to determine immune activation in the CNS (Farrall and Wardlaw, 2009). Serum albumin is an established marker of BBB breakdown and in ageing individuals, BBB breakdown is strongly correlated with MCI (Senatorov Jr *et al.*, 2019). Montagne and colleagues (2015) quantified BBB permeability in different regions of the living brain using dynamic contrast-enhanced MRI (DCE-MRI) and analysis of biomarkers of BBB breakdown in the CSF. They found a significant increase in the CSF plasma/albumin ratio in individuals with MCI compared to age matched non-cognitively impaired (NCI) controls, while DCE-MRI confirmed that BBB breakdown was more pronounced in individuals with mild cognitive impairment (MCI) (Montagne *et al.*, 2015). In NCI individuals there was an age-dependent increase of BBB permeability in the hippocampus but no significant changes in other areas suggesting that BBB breakdown during ageing begins in the hippocampus, which is one of the brain regions first affected in AD (Montagne *et al.*, 2015).

CNS infection by viruses is relatively common and frequently caused by human cytomegalovirus. This virus can cause encephalitis and meningitis and uses a neuroinvasive route to gain entry to the brain

(Dando *et al.*, 2014; Forrester *et al.*, 2018). Neurons within the CNS contain axons whose role is to transmit action potential and signals from the cell body to the synapse, support glial cell functions and prevent neurodegeneration (Jha and Morrison, 2018). Organelles such as mitochondria are able to pass freely through the axon to provide energy needed for neuronal transmission and it is this axonal transport that viruses, such as herpes simplex virus 1 (HSV-1), often take advantage of to infect the CNS (Miranda-saksena *et al.*, 2018). Viruses can also infect the CNS by crossing the BBB transcellularly or paracellularly. Disruption of the tight junctions to diffuse across the BBB is aided through induced expression of pro-inflammatory cytokines such as IL-1β, in the cells of the BBB (microvascular endothelial cells, pericytes and astrocytes), causing permeability (Govic *et al.*, 2022).

The olfactory nerve is also a proposed route to the brain that viruses in particular can take advantage of, and which Braak and colleague proposed as an initiation pathway in their 'dual-hit' hypothesis in PD (Hawkes *et al.*, 2009). The nasal cavity and CNS are connected by the olfactory nerve, which is the shortest nerve connection between the external environment and the CNS (Riel *et al.*, 2015). Various mouse and human studies have shown evidence of antigens from viruses such as Influenza and herpes virus present on olfactory nerves and glial cells in the olfactory tract, suggesting that these viruses entered the CNS via the olfactory route. However, whilst many studies suggest this is a common pathway, the mechanisms of transport are poorly understood (Riel *et al.*, 2015).

1.4.4 Infections in the periphery, a risk factor for Parkinson's Disease?

Infections occurring in the periphery have also been suggested to be a risk factor for PD (Ferrari and Tarelli, 2011). Studies such as the case-control study of Dunn and colleagues have found a positive association between the number of episodes of prior infection and increased risk of developing dementia in elderly patients (Dunn *et al.*, 2005). Indeed, the elderly are more prone to developing infections especially of the urinary and respiratory tract, as well as experiencing higher levels of bacterial resistance. This increased infection risk is associated with mini-mental state examination (MMSE) scores of below 24 (Mcmanus and Heneka, 2017). Interestingly, the main causes of death in individuals with PD are pneumonia and respiratory infections (Beyer *et al.*, 2001). Inflammatory markers have also been found to be raised in plasma and the brain many years prior to dementia diagnosis (Engelhart *et al.*, 2004). It is thought that prolonged inflammation in the periphery could cause pro-inflammatory cytokines to cross the BBB and potentially contribute to cognitive decline (Wang *et al.*, 2015). In support of this, circulating TNFα, a pro-inflammatory cytokine, is known to cause permeability of the BBB (Shoemark and Allen-Birt, 2017).

The gut-brain-axis of bidirectional communication is now widely accepted, and several studies have shown dysbiosis of the gut microbiome in PD compared with controls (Scheperjans *et al.*, 2015). It is also well known that pathogenic α-synuclein is present in the gut and GI tract of PD patients and occurs in response to infection that activates the immune system (Stolzenberg *et al.*, 2017). Further evidence of the gut's involvement in the risk of developing PD was highlighted in Killinger and colleagues' study (2018), who investigated the role of the vermiform appendix by analysing two independent epidemiological datasets. The authors found in both datasets, which together covered 91 million person-years, that having an appendectomy was associated with lower risk of developing PD, and that if one occurred decades before PD diagnosis, this was associated with delayed age of onset (Killinger *et al.*, 2018).

In the laboratory, studies have indicated a potential microbial cause of PD that likely originates from an infection in the periphery (Pisa *et al.*, 2020), although most evidence for bacteria/bacterial metabolites in the brain comes from AD studies to date. Gram negative lipopolysaccharide (LPS), *E. coli* DNA and K99 pili protein were shown to be raised in AD post-mortem brain compared with controls (Zhan *et al.*, 2017). In addition, Pisa and colleagues investigated polymicrobial infections in entorhinal cortex/hippocampus regions of AD brain tissue using immunohistochemistry and polymerase chain reaction (PCR) and found fungal and yeast like structures as well as several bacterial species such as *Burkholderia spp* and *Streptococcus* in AD samples (Pisa *et al.*, 2017). A study by Emery and colleagues also looked at post-mortem AD tissues Next Generation Sequencing (NGS) and PCR primers that were designed to cover the widest possible taxonomic spectrum (Emery *et al.*, 2017). The authors found considerably higher bacterial reads in AD as compared to control brains, with the highest operational taxonomic unit (OTU) reads being *Propionibacterium acnes* (*P. acnes* now designated as *Cutibacterium (C. acnes*)), which they suggested contributed to neuroinflammation as it is well documented that *C. acnes* can stimulate the innate immune system (Emery *et al.*, 2017). *C. acnes* is a commensal of skin and hair follicles, which in dysbiosis has been linked with skin diseases such as acne vulgaris (Leheste *et al.*, 2017).

In a study by Lu and colleagues, an in vitro cell culture BBB model was developed and when this was cocultured with *C. acnes,* high concentrations invaded the BBB via the transcellular traversal pathway (Lu *et al.*, 2019). This was not the first time that *C. acnes* had been implicated in the infection of non-skin sites; it had also been found to be able to invade prostate epithelial cells and induce a prolonged immune response (Mak *et al.*, 2012). These authors also found that vimentin, a filament protein found in cells of many tissues, was key for *C. acnes* invasion (Mak *et al.*, 2012). Interestingly, during pro-inflammatory states, vimentin is released by macrophages and other

immune cells as well as endothelial cells, and has been found to induce macrophage superoxide production, which increases the ability of the cells to kill bacteria (Yu *et al.*, 2018).

Further to their post-mortem brain AD study, Pisa and colleagues subsequently investigated six post-mortem PD samples and found the same yeast-like cells and hyphal structures as well as chitin (a component of fungal cells walls) supporting the existence of fungal infection in PD brain (Pisa *et al.*, 2020). PD brain tissue was also stained to look for bacterial peptidoglycan, followed by nested PCR to confirm the existence of bacteria, and similar to the AD study, *C. acnes* was detected (Pisa *et al.*, 2020). Using NGS, it was shown that some bacteria were more common in PD brain tissue than in other neurodegenerative brain diseases such as AD or amyotrophic lateral sclerosis (ALS), such as the genera *Streptococcus* and *Actinobacter* in certain brain regions (Pisa *et al.*, 2020). A viral cause of PD has also been investigated, as PD symptoms are similar to those caused by Japanese encephalitic virus (Ogata *et al.*, 1997), and subsequent studies have provided evidence for an association of PD with Influenza A virus (Chiara *et al.*, 2012).

There is now emerging evidence of a link between periodontal (gum) diseases and neurodegeneration (Scannapieco, 2013). Periodontal diseases have been implicated in a number of systemic diseases such as cardiovascular disease, diabetes, rheumatoid arthritis, adverse pregnancy outcomes and dementia, to name a few (Hajishengallis, 2015; Emery *et al.*, 2017). Interestingly, several pathogens implicated in periodontitis have been found to dampen and/or evade the immune response, and the DNA and/or antibodies of these pathogens have been found in extra-oral sites such as atherosclerotic plaques and synovial fluid in patients with rheumatoid arthritis (Ogrendik, 2013; Hussain *et al.*, 2015).

1.4.5 Periodontitis and Parkinson's Disease

1.4.5.1 Periodontal disease in the population

Periodontitis (gum disease) is an infection of the tissues supporting the teeth (the periodontium) which is composed of the gingiva, connective tissue, and ligament between cementum and alveolar bone (Könönen *et al.*, 2019). It is a common and prevalent disease affecting up to 50% of the population worldwide (Nazir *et al.*, 2020). In the most recent Adult Dental Health Survey (2009), the largest epidemiological survey of adult dental health in the UK, 45% of the surveyed adults had evidence of periodontitis while only 17% of adults had healthy periodontal tissue (The NHS Information Centre Dental and Eye Care Team, 2009). More recent surveys conducted in general dental practice similarly report high prevalence figures for periodontal disease; a cross-sectional study in NHS practices in South West England found 28% of participants had evidence of

periodontitis (Midwood *et al.*, 2019) and an oral health survey conducted by Public Health England found that 52.9% of participants had some form of gingival bleeding (Public Health England, 2020). Severe periodontitis, a major cause of tooth loss, affects around 11% of adults and is a major public health concern (Chapple *et al.*, 2015). Periodontitis becomes more prevalent with age, in particular severe periodontitis (Könönen *et al.*, 2019).

Although common, periodontitis is, in the majority, a preventable disease and its development is mainly dependent on lifestyle factors such as poor oral hygiene and smoking. However, it also is partly dependent on genetics (Chapple *et al.*, 2015). Gingivitis precedes periodontitis, and although not all individuals who suffer from gingivitis will develop periodontitis, prevention of inflammation of the gingivae through excellent self-directed daily oral hygiene and behaviour modification will prevent periodontitis in most people (Kinane and Attström, 2005; Chapple *et al.*, 2015).

Why is a disease that is highly preventable and eminently treatable if detected at an early stage be so prevalent globally? Unfortunately, evidence has shown that the majority of the population do not clean their teeth and gums adequately or regularly enough to prevent biofilm (plaque) accumulation (Claydon, 2008). Individuals often are not aware of the symptoms of gum disease such as bleeding gums or do not recognise this as a problem, which consequently impacts on seeking dental treatment early enough (Midwood *et al.*, 2019). In addition, many patients seek treatment too late as they are able to live with these diseases (gingivitis and periodontitis) with few or no symptoms at all until teeth have become loose, hence why it is often regarded as a 'silent' disease (Buset *et al.*, 2016). Lack of awareness and underreporting of symptoms of periodontal diseases by patients has been studied and data supports this view of periodontal diseases as 'silent'. For example, Midwood and colleagues found a significant disparity between the percentage of patients who self-reported gingival bleeding and clinical bleeding on probing scores (29% and 75% respectively) (Midwood *et al.*, 2019). Thus, the condition is able to persist in a large proportion of the population giving rise to the high prevalence figures for periodontitis seen globally (Nazir *et al.*, 2020).

1.4.5.2 The oral microbiome and oral disease

The oral cavity is a habitat for a diverse range of microorganisms such as bacteria, viruses and archaea, and together they form part of a community that adhere to tooth structures and form a well ordered biofilm that exists in harmony with the host in health (Marsh and Zaura, 2017). However, if the biofilm is not regularly disrupted through tooth brushing, for example, it grows thicker, there is more interaction with the gingival surfaces and it becomes more difficult to disrupt from oral surfaces (Meyle and Chapple, 2015). As a result of this, deep in the biofilm at the

tooth/gum surface, contact with saliva and oxygen decreases and acid released by bacterial metabolism increases as the distance to the biofilm surface in the oral cavity grows, conditions that begin to favour species such as *Fusobacterium nucleatum* (Meyle and Chapple, 2015). *F. nucleatum* is able to sense and influences its environment leading to gingival inflammation that favours more pathogenic bacterial species such as *Porphyromonas gingivalis* (Meyle and Chapple, 2015). Gingivitis, a reversible condition and the precursor to periodontitis, is the body's first response to an increase of biofilm near the gingiva and is initially characterised by gingival inflammation in response to bacterial toxins (Abusleme *et al.*, 2021). If the biofilm persists, pro-inflammatory molecules such as IL-1 and TNF-α continue to be produced and gingival bleeding occurs (Abusleme *et al.*, 2021). However, as indicated above, not all patients with gingivitis will proceed to periodontitis and the dynamics of the progression from gingivitis to periodontitis is not fully understood (Abusleme *et al.*, 2021). Although it is recognised that the biofilm alone is not sufficient to cause progression to periodontitis, importantly, the host immune response to the biofilm and the complex interactions between them account for around 80% of the tissue damage seen in periodontal patients (Meyle and Chapple, 2015; Kilian *et al.*, 2016).

The composition of the microbiome in the oral cavity in health and disease has been studied extensively more recently using new genomic technologies such as NGS. As a consequence, the bacteria that are implicated and specific to periodontitis are well known (Kilian *et al.*, 2016). Using 16S rRNA sequencing, studies have found that there are over 700 microbial species in the oral cavity (Peterson *et al.*, 2013). Certain bacteria have been long associated with periodontitis, such as the anaerobic species *Porphyromonas gingivalis, Tannerella forsythia,* and the spirochete *Treponema denticola.* However, with advancements in sequencing techniques, many more bacterial species have now been associated with biofilms in the oral cavity and with periodontal inflammation (Scannapieco, 2013). It has been shown that there is a highly diverse oral bacterial population in periodontal disease including anaerobic bacteria from the phyla Firmicutes, Proteobacteria, and Bacteroidetes, and the dysbiotic environment alongside their virulence factors help the biofilm adapt in a challenging and inflammatory environment (Hajishengallis, 2015).

1.4.5.3 The oral microbiome and systemic disease

There are a plethora of studies showing associations between periodontitis and systemic diseases such as diabetes, cardiovascular disease and rheumatoid arthritis (Otomo-Corgel *et al.*, 2012), and many more are finding periodontal pathogens outside of their normal environment. Several studies have reported evidence of increased continuous presence of periodontal pathogens in the blood

(bacteraemia) after toothbrushing and periodontal procedures (Tomás *et al.*, 2012). As indicated above, oral biofilms commonly exist on either teeth or gingival surfaces such as periodontal pockets (Parahitiyawa *et al.*, 2009). Gingival bleeding in response to persistent plaque occurs as the tissue that lines the periodontal pockets is not protected by a keratinised layer such as that which forms the outer layers of skin, and it is highly vascularised (Parahitiyawa *et al.*, 2009). In periodontitis, the gingival inflammatory response leads to an increase in vasculature and vessels also dilate creating a large surface area that microbes can take advantage of to gain entry to the bloodstream (Parahitiyawa *et al.*, 2009). Bacteraemia of periodontal source is proposed to be a significant contributing factor to cardiovascular disease (Sanz *et al.*, 2020), and a study by Emery and colleagues found that 50% of bacterial species in blood from patients with periodontitis were of oral origin (Emery *et al.*, 2021). Furthermore, the techniques used indicated that the bacteria were viable at the time of sample collection (Emery *et al.*, 2021). Thus it appears that oral bacteria can evade the host immune system, and pathogenic oral bacteria implicated in periodontitis such as *P. gingivalis and T. denticola* have been and continue to be investigated at depth to understand the mechanisms by which they evade the host immune response and may contribute to systemic diseases such as rheumatoid arthritis (Hajishengallis, 2015).

In light of the evidence of periodontal pathogens translocating out of their natural habitats, evading host immune responses and having implications in systemic disease, there has been a surge of cohort, in-vitro and in vivo studies to examine if they are associated with neurodegenerative diseases. Tooth loss is considered one of the significant risk factors in the development of dementia (Mucci *et al.*, 2004; Gatz *et al.*, 2006; Stein *et al.*, 2007). Patients with PD have been reported to have fewer natural teeth and poorer oral health than patients without PD; the former also tended to have lower mini-mental state examination scores than their healthy counterparts (Hanaoka and Kashihara, 2009). This raises the question: could poor oral health initiate or exacerbate PD and could improving oral health in PD patients improve their symptoms?

There have been a number of clinical studies conducted that have recruited PD patients and determined their periodontal health compared with controls. Schwarz and colleagues gathered oral health data on 70 PD patients and 85 aged-matched controls using the 'Community Periodontal Index for Treatment Needs' (CPITN), and found significantly higher (poorer) scores in PD patients (Schwarz *et al.*, 2006). In another study, Hanaoka and colleagues compared the oral health of patients with PD with that of two control groups, those with mild neurological impairment but no motor impairment and in-patients with acute ischemic stroke with no previous motor or cognitive impairments (Hanaoka and Kashihara, 2009). They found a significantly higher percentage of untreated caries, which tended to increase with Hoehn and Yahr stage score, as well as fewer

remaining teeth and deeper periodontal pockets in patients with PD (Hanaoka and Kashihara, 2009). A later cross-sectional study also examined dental caries, missing teeth, and measured periodontal deep pockets and found a significantly higher number of missing teeth and more periodontal disease in patients with PD than controls (Cicciu *et al.*, 2012). These findings were supported by a 2015 study by Pradeep *et al* that investigated similar parameters (Pradeep *et al.*, 2015). In these latter two studies it was concluded that more effort was needed to encourage PD patients with no cognitive impairment to use plaque control methods. However, it was acknowledged that increased motor impairment affects self-oral care, and other behavioural changes such as apathy and depression affect the patient's ability to notice or try to address any dental problems (Cicciu *et al.*, 2012; Pradeep *et al.*, 2015).

In a recent cross-sectional study conducted by Lyra and colleagues (Lyra *et al.*, 2020), severe tremor and rigidity of upper extremities of PD patients was associated with increased plaque and gum bleeding, a finding that also corroborates the previous studies described above.

This data indicates that there are links between periodontitis and PD. However, whether the cause of periodontitis is due to the patient's deteriorating dexterity and therefore less effective oral hygiene habits, or whether periodontitis is the instigator to systemic inflammation causing or exacerbating PD cannot be determined from these studies. No prospective longitudinal studies to determine whether periodontitis might be causal or accelerate PD have been undertaken to date. However, there are some retrospective studies that have utilised a national database and reported on the associations between PD and periodontal disease over time. Using a Taiwanese database, Liu and colleagues demonstrated that individuals with chronic periodontitis had a significantly higher risk of PD as compared to individuals with good oral health after a five year follow up (Liu *et al.*, 2013). Similarly, using a South Korean database and following individuals for 8 years, Jeong and colleagues demonstrated that there was an association between PD and periodontitis, and that the risk of PD increased in those who needed more than one dental treatment (Jeong *et al.*, 2021). Overall, this data is indicative that periodontitis elevates PD risk, but further controlled trials are needed to confirm this.

1.5 Justification and aims

There is now quite substantial evidence of a microbial presence in AD post-mortem brains (Emery *et al.*, 2017). Differences in bacterial populations in PD post-mortem brains have also been reported (Pisa *et al.*, 2020), and there is now evidence to suggest that α-synuclein has an antimicrobial role similar to that of Aβ in AD (Barbut *et al.*, 2019). This indicates that bacteria may play a role in PD, however more research is needed to confirm this.

Braak et al (2003) described a staging system for postmortem brain that characterised disease progression, and if bacteria are present in PD brain, determining where they are in the brain may shed some light on their association with disease stage.

1.5.1 Aim

To determine if bacteria might play a role in PD progression, this study will investigate bacteria presence and levels in post-mortem PD brains compared with control brains.

1.5.2 Specific objectives

- To quantify the numbers of bacteria in control as compared to PD post-mortem brain
- To determine in which areas of the brain bacteria are found and whether there are differences in bacterial composition between brain areas and also between control and PD post-mortem brain
- To determine the original source of infections (e.g mouth).

To correlate α-synuclein levels with bacterial levels found in brain tissue to determine whether there is any association.

Chapter 2 Materials and Methods

2.1 Tissue cohort

Human brain tissue taken post-mortem from donors was obtained from the South West Dementia Brain Bank, (SWDBB), HTA Licence no 12273, with ethical approval for the pilot project described here under the SWDBB approval ITA134 and ITA135. Brain donations are prepared by technicians at SWDBB. After removal of the cerebellum first, the left and right hemispheres are separated by cutting the corpus callosum; the left hemisphere is sliced into 1 cm equal thickness coronal sections and stored at -80^{o}C. It is from these sections that the samples were taken for this project. The right hemisphere is fixed in formalin and paraffin embedded tissue sections taken for diagnostic purposes. Additionally, cerebrospinal fluid (CSF) samples are available from some donors. All donors are anonymised, and details are tabulated on the Medical Research Council (MRC) database (https://brainbanknetwork.ac.uk/)

Parkinson's Disease (PD) cases (n=10) were chosen that had previously been diagnosed clinically and then confirmed by the presence of PD pathological changes. Where possible, samples with post-mortem intervals (PMI) of less than 40 h were selected. Sample selection was also based on cause of death (C.O.D.). Additionally, age matched controls (n=10) were chosen alongside for the comparative study of appropriate brain regions.

Brain tissue (approximately 400 mg) cut from frozen brain was supplied; this included cortical areas: BA34 (anterior entorhinal cortex, associated with the olfactory cortex), BA11 (prefrontal lateral, part of the orbitofrontal cortex), BA38 (anterior lateral temporal lobe, or temporal lobe). Additionally, brain stem areas included the midbrain SN (substantia nigra) and pons, locus coeruleus (LC) and the area adjacent to the vagus nerve. Samples of the choroid plexus (CP) were also available for 17 individuals. CP samples were 200 mg, and since the area containing the SN is usually shrunken in PD cases due to neurodegeneration, samples averaged around 200 mg. Cerebral spinal fluid (CSF) samples from the same 20 individuals were also requested. However, it was only possible to obtain 16 CSF samples from these donors with a volume of approximately 1ml. These samples were immediately frozen at -80^{o}C for subsequent processing.

Each donor was assigned a 'brain bank' (BB) number for identification and this number is used to identify samples in this thesis. Table 2.1 shows mean age and post-mortem delay with standard

deviations given. Further details, including pathology diagnosis and the brain areas obtained for each donor, are shown in Table 2.2.

Areas were taken from both control and PD where available:

Cortex: BA34 (medial: entorhinal cortex), BA11 (lateral: lower frontal), BA38 (anterior temporal). Midbrain: Pons: Locus coeruleus, LC; Midbrain: Substantia nigra, SN; Brain stem: BS; Vagus or motor nucleus or region between as available, Choroid Plexus, (CP).

Table 2.1: Summary of cohorts

	Number	Age	Post-mortem interval (PMI)	Tissues with APOE genotyping at postmortem
Control (C)	10	82.7 ± 8.5 yrs	42.9 ± 10.0 hrs	N= 5
PD (PD)	9	81.4 ± 9.5 yrs	38.9 ± 20.6 hrs	N= 3
PD (AD)*	1	81	79hrs	N= 1
* Clinically diagnosed as AD. At post-mortem diagnosed as PD-LB and AD. This sample was included in the analysis but was not incorporated into NGS2.				

Table 2.2: Cohort characteristics

BB#	Age at Death (years)	Post-mortem delay (hours)	Clinical diagnosis	Cause of Death	Pathology	Gender (Male/Female)	APOE Genotype	Brain area availability
31	94	41	PD	UK	PD/LB	M	2/4	BA34/CP
82	78	19	PD	UK	PD/LB	M	4/4	BA34/CP
181	89	81	PD	UK	PD/LB	F	3/3	B34/CP/CSF
313	81	79	AD, unspecified	UK	AD - Braak Tangle stage III, PD- LB	F	3/3	BA34/CP
766	92	34.25	C	Acute cardiac failure, left ventricular hypertrophy, hypertension	Moderate non-amyloid SVD Braak tangle stage II CERAD sparse neuritic plaques	M	3/4	BA34/SN
781	87	24	C	Acute renal failure, myeloma	Mild non-amyloid small vessel disease, Mild arteriolar CAA Braak tangle stage II no plaques	M	3/3	BA34/BA11/BA38/BS/LC/SN/CSF
785	94	40	C	Debility of old age	No AD or other neurodegenerative disease. Infarct/s Moderate non-amyloid SVD Mild arteriolar CAA Braak tangle stage II CERAD no plaques	M	2/2	BA34/SN/CP/CSF
801	82	30.5	PD	Haemopericardium, type A dissection of thoracic aorta	Moderate CVD	F	3/3	BA34/SN/CP/CSF
805	80	41	PD	Intestinal ischaemia, PD	PD with neocortical LB Moderate non-amyloid SVD Mild arteriolar CAA Braak tangle stage II CERAD sparse neuritic plaques	F	-	BA34/CP/CSF

826	86	32	C	colon cancer	Moderate non-amyloid SVD Moderate arteriolar CAA Braak tangle stage II CERAD no plaques	F	3/4	BA34/SN/CSF
877	82	67	C	Cerebrovascular event, metastatic prostate cancer, end stage renal failure	No abnormality detected Mild non-amyloid SVD Braak tangle stage II CERAD no plaques Very mild arteriosclerotic SVD with occasional microinfarct	M	-	BA34/SN/CP/CSF
880	67	24	PD + dementia	PD and unspecified dementia	PD – dementia Severe CAA Mild to moderate AD changes (CERAD 'possible AD')	M	3/3	BA34/SN/CP/CSF
894	74	57.5	C	Disseminated metastatic cancer	Mild non-amyloid SVD Braak tangle stage 0 CERAD no plaques Argyrophilic grain disease	M	-	All
897	74	27.5	C	Metastatic cancer	Argyrophilic grain disease Severe CAA Mild to moderate arteriosclerotic CVD	F	-	All
902	79	48	C	Metastatic pulmonary adenocarcinoma	No abnormality detected Mild non-amyloid SVD Braak tangle stage II CERAD no plaques	F	2/3	BA34/SN/CP/CSF
937	96	31.75	PD	Bronchopneumonia, congestive cardiac failure, PD	PD, Braak LB stage 5, Braak tangle stage II CERAD no plaques Moderate non-amyloid SVD Lacunar infarct/s in cerebral cortex Moderate/severe arteriosclerosis in occipital white matter	M	2/3	All

938	69	54.25	PD	Myocardial infarction, PD	Braak LB stage 4 Braak tangle stage II CERAD no plaques Moderate atherosclerosis of basal arteries Microinfarct in temporal neocortex	M	3/3	All
949	69	31.25	C	Non-small cell lung cancer	No plaques, Braak tangle stage II, LB stage 0, mild argyrophilic grain disease	M	-	BA34/SN/CP/CSF
971	90	67.25	C	Metastatic cancer of bladder	Control: Mild non-amyloid SVD, sparse plaques /Braak tangle stage I, Braak LB stage 0	F	3/4	BA34/SN/CP/CSF
1000	78	13	PD	Myocardial infarction, ischemic heart disease, PD	PD, Braak LB stage 5, no plaques, Braak tangle stage I, Mild non-amyloid SVD	M	3/3	BA34/SN/LC/BS/CP/CSF

All indicates BA34, BA11, BA38, SN, LC, BS, CP, CSF are present
Cortex: BA34 (medial: entorhinal cortex), BA11 (lateral: basal frontal), BA38 (lateral basal temporal). Midbrain: Locus coeruleus; LC, Substantia nigra; SN, Brain stem; BS, Vagus or motor nucleus or region between as available, CP: Choroid Plexus
CERAD: Consortium to Establish a Registry for Alzheimer's Disease, SVD: Small Vessel Disease, CVD: Cardiovascular Disease CAA: Cerebral Amyloid Angiopathy

2.2 Materials

Plastic consumables and standard reagents were obtained from Sigma Aldrich (St. Louis, Missouri, USA). for molecular techniques, unless otherwise stated, reagents and equipment were obtained from Thermo Fisher (Waltham, MA, USA).

All oligonucleotide primers and probes were manufactured by Eurofins Genomics (Ebersberg, Germany).

2.3 DNA

2.3.1 DNA extraction

In a Labculture Class II laminar flow cabinet (ESCO Lifesciences Group, Singapore), to obtain sufficient DNA content from the sample, a piece weighing approximately 100 mg was cut from the brain tissue stocks and placed into a sterile 1.5 ml Eppendorf. Over dry ice, the frozen tissue was homogenised using a sterile plastic pipette tip, refrozen and then homogenised a second time. The tissue was then resuspended in 0.5 ml TE buffer (10 mM Tris.Cl pH8, 1 mM EDTA) and then an equal volume of phenol:chloroform:isoamyl alcohol (25:24:1, equilibrated in TE pH 8), was added to the homogenised sample. The samples were then vortexed and spun down (9,447 g, 3 ^{o}C, 10 min).

Following centrifugation, the supernatant was transferred to another sterile 1.5 ml Eppendorf tube and 100% (v/v) ethanol was added at 2.5x the volume of supernatant in the presence of 0.2 M sodium chloride (NaCl). The samples were then vortexed and stored in a -20 ^{o}C freezer overnight to precipitate. Precipitated samples were spun down (9,447 g, 3 ^{o}C, 10 min) and the supernatant was carefully poured off leaving the DNA pellet in place. 500 µl of 70% (v/v) ethanol was then used to wash DNA pellets of impurities and carefully poured off immediately leaving the DNA pellet in the Eppendorf. With the lids left open the DNA pellets were then left to air-dry in a sterile cell culture laminar flow hood. Once dry, 50 µl of TE buffer (pH 7.5) was added to each pellet, vortexed, and then left in the fridge for at least an hour to dissolve before use. DNA concentration was determined using the Quantifluor® double-stranded (ds)DNA assay described below.

2.3.2 Quantification of DNA

To detect the concentration of dsDNA in brain tissue samples, the A260/A280 absorption was measured initially using a Nanodrop spectrophotometer (ThermoFisher Scientific, Waltham,

Massachusetts, USA). Samples with an A260/A280 ratio of between 1.8 and 2 were then quantified by their fluorescence using the QuantiFluor® dsDNA system (Promega, Madison, Wisconsin, USA) used according to the manufacturer's instructions. The QuantiFluor® dsDNA Dye supplied was already dissolved in 100% dimethylsulfoxide (DMSO) and stored frozen at 2 °C. The supplied 20X TE buffer pH 7.5 was diluted to a working solution of 1X using DNase free water. The QuantiFluor® dsDNA dye protected from light was then thawed and the required quantity diluted to a working concentration of 1:400 (in 1X TE pH 7.5). Using a 100 µg/ml dsDNA standard diluted in 1X TE, a standard curve of 300, 200,100, 30, 20 and 10 ng/µl was prepared and dispensed in duplicate wells into a black flat-bottom 96-well plate. The standards were prepared with these concentrations so that there was a wide enough range to be able to accurately detect when there were small amounts of dsDNA in the samples.

The prepared dsDNA dye (200 µl) was added to two wells of the 96-well plate as a blank, and 1 µl of each sample of unknown concentration was added in duplicate to the remaining wells. Finally, 199 µl of the prepared dsDNA dye was also added to each well, containing either 1 µl of standard or 1 µl of sample. The plate was incubated at room temperature for 5 min protected from light and then using a FLUOstar Optima fluorometer (BMG Lab Tech, Offenburg, Germany), the DNA concentration of standards and samples was measured at 504 nm; the fluorometer subtracted the blank from the results automatically. The multivariate adaptive regression spline (MARS) Data Analysis Software (BMG Lab Tech, Offenburg, Germany) was used to perform linear regression on standards and interpolate the values of the samples.

2.3.3. Quantifying bacteria in human tissue by qPCR of 16S rRNA

Quantitative PCR (qPCR) utilises the monitoring of fluorescence to detect amplification of DNA, where fluorescence intensity mirrors the amount of DNA present in that sample at a particular point in a cycle (Kralik and Ricchi, 2017).

This technique was used to measure the amount of bacterial DNA (all bacteria) present in human brain tissue using *Escherichia coli* standards as controls. To detect the broadest possible spectrum of bacterial species, the universal primers designed by Nadkarni *et al* (Nadkarni *et al.*, 2002) were used. To identify these primers, Nadkarni and colleagues assessed hypervariable regions within 16S rRNA to determine which sequences, that might also allow taxonomic classification, were universally present in bacteria by aligning rRNA sequences that represented most bacterial groups described in *Bergey's Manual of Determinative Bacteriology* (Holt *et al.*, 1994; Nadkarni *et al.*, 2002). The optimal

primer sequences were identified as the universal rRNA hypervariable region V3-V4 primers (Figure 2.1), which can identify sequences of 16S regions of rRNA that are conserved across bacterial species and allow classification to specific taxonomic levels, which may be down to species (Nadkarni *et al.*, 2002).

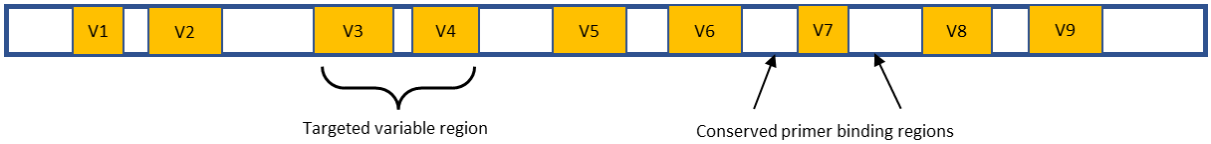

Figure 2.1: Hypervariable regions within 16S rRNA

The sequences of the V3-V4 primers and the probe used to emit the fluorescence, are shown in Table 2.3.

Table 2.3: V3-V4 primer sequences for 16S rRNA

	Sequence 5' – 3'	Tm (°C)	Base Pair
V3 Forward	TCCTACGGGAGGCAGCAGCAGT	59±4	22
V4 Reverse	GGACTACCAGGGTATCTAATCCTGTT	58±1	26
Fluorogenic Probe	5'-(6-FAM)-CGTATTACCGCGGCTGCTGGCAC-(TAMRA)-3'	69±9	23

6-FAM: 6-carboxyfluorescein, TAMRA: 6-carboxy-tetramethylrhodamine

For all PCR reactions (both the qPCR described here and the PCR for amplicon generation described below), sample and reagent preparation were undertaken in a Labculture Class II laminar flow cabinet (ESCO Lifesciences Group, Singapore), using disposable sterile pipette tips and gloves to prevent contamination. Gilson pipettes were disinfected before use and were solely used for PCR set up to avoid cross contamination.

2.3.3.1 Bacterial genomic DNA standards

To be able to quantify the amount of bacteria in the human brain samples, it was necessary to generate a standard curve of bacterial DNA of known concentration that could be amplified in parallel. Bacterial genomic DNA was supplied for this that had been extracted from an *E. coli* strain DHα1B (K12-derived). *E. coli* was chosen to use as a standard as it is easy to grow on culture and extract DNA from. In the laboratory the DNA was quantified by Quantifluor Analysis and used to generate a standard curve (serial dilution from 100-100,000,000 ng/ml), which was included in each PCR plate and amplified at the same time as the bacteria in the brain samples using the same PCR

primers (Nadkarni *et al.*, 2002). Following qPCR, the standard curve was used to estimate bacterial level and adjusted for 16S gene copy number to determine bacterial cell numbers in each brain sample.

2.3.3.2 Human genomic DNA standards

The goal was to include approximately 150 ng of total template brain tissue in each qPCR reaction. To measure and normalise the amount of human brain tissue in each sample so that bacterial counts in each could be compared, the human housekeeping gene betaglobin (BG) was used as a control. Betaglobin is one of the common housekeeping genes used in genomic studies to normalise the amount of template, as it is considered to be the most stably expressed gene (not altered or impacted in different conditions) in cells and under experimental conditions (Yang *et al.*, 2015). Prostate cancer cells (PC3) that had been cultured under sterile conditions were donated by Dr C. Perks, Bristol Medical School and were used for the BG qPCR. The concentration of genomic DNA that had been extracted from the prostate cells was determined using the Quantifluor® assay, and a standard curve of BG standards of 25, 50, 75, 100, 125, 150 and 175 ng/ml was prepared which was included in each PCR plate so that brain tissue amounts could be quantified.

The sequences of the betaglobin primers and probes are shown in Table 2.4:

Table 2.4: Primer sequences for betaglobin

	Sequence 5' - 3'	**Base Pair**
Forward Primer	GTGCACCTGACTCCTGAGGAGA	22
Reverse Primer	CCTTGATACCAACCTGCCCAG	21
BG Fluorogenic Probe	(HEX)-AAGGTGAACGTGGATGAAGTTGGTGG-(BHQ®1)	26

HEX: BHQ®1: Black Hole Quencher 1

2.3.3.3 qPCR reactions- conditions and cycle parameters

The qPCR reactions for the amplification of 16S RNA using the V3-V4 primers were undertaken based on the conditions of Nadkarni and colleagues (Nadkarni *et al.*, 2002) and were also used for the amplification of BG. Approximately 150 ng template DNA or 2 µl of standards in duplicate were pipetted into the wells of a MicroAmp® Fast 96-well Reaction Plate, and DNase free water added to 8.5 µl. To each well 11.5 µl qPCR mix was added so that each 20 µl reaction contained forward and reverse primers at a final concentration of 500 nM together with 100 nM fluorogenic probe and 1X

TaqPath qPCR mastermix. Standard curve data was always generated on the same PCR plate as sample data and from the same mastermix. For bacterial amplification, a negative control was included substituting the 150 ng of brain tissue with 150 ng of PC3 DNA.

The PCR cycle included a 'hot start', such that the Thermal Cycler was warmed up before the reaction started, with 5 min at 95 °C. Hot start was followed by 40 cycles: 30 s at 95 °C the 40 s at 60 °C. PCR was performed in an Applied Biosystems StepOne Plus® Real-Time PCR system using StepOne software v2.3.

16S levels were expressed with reference to the amount of human genomic DNA present as determined from the BG standard curve.

2.3.4 Preparation of amplicon libraries by PCR for Next Generation Sequencing (NGS)

To generate amplicon libraries, PCR was undertaken with the same universal forward and reverse 5'-3' primers V3-V4 described in 2.3.3, adapted by the addition of 'bar code' adapter sequences to generate indexed primers for use on the Illumina platform (Illumina Inc. San Diego, California USA). The full indexed primer sequences are shown in Table 2.5.

Table 2.5: V3-V4 indexed primer sequences for 16S rRNA with illumina adapter sequences shown in blue

	Sequence 5' – 3'	Tm (°C)
V3 Forward	ACACTCTTTCCCTACACGACGCTCTTCCGATCTTCCTACGGGAGGCAGCAGT	59±4
V4 Reverse	GACTGGAGTTCAGACGTGTGCTCTTCCGATCTGGACTACCAGGGTATCTAATCCTGTT	58±1

Purified DNA template concentrations of 150-200 ng of brain tissue as determined by Quantifluor analysis were used for each reaction, diluted in DNase free water. Similar to the qPCR described above, a Mastermix for all samples was made up but for a 50 µl final volume. The Mastermix contained final concentrations as follows: 1 µM each of the indexed forward and reverse primers, 200 nM each of dNTPs (dATP, dCTP, dGTP, dTTG), 2.5 Units of GoTaq® DNA polymerase (Promega, Madison, Wisconsin, USA) and 1 x GoTaq® green reaction buffer (which included gel loading dye). The negative control initially contained 150 ng ds genomic PC3 DNA diluted in DNase free water in place of brain tissue template. However, as the bacterial content was so low, no product was generated as the presence of human tissue inhibits the PCR, so there was nothing from this reaction

that could be sent as a negative control for NGS. Initially, as there was no product or insufficient to be processed by Novogene a control was not available for comparison with the brain samples. As the first round of NGS where no control was available appeared to show contamination (although this could not be proved (see results)), a different approach to generate a negative control was adopted in which the PCR reaction was undertaken in the absence of human DNA template using sterile water in its place as a no template control (NTC).

The PCR reaction was carried out using the Applied Biosystems® 2720 Thermal Cycler and was again a 'hot start' reaction, 95 ^{o}C for 5 min, followed by 38 cycles as follows: denaturing 94 ^{o}C for 30 seconds, annealing 65 ^{o}C for 30 seconds, extension 72 ^{o}C for 45 seconds. A final extension 72 ^{o}C for 7 min was added to the final cycle after which the reaction was held at 4 ^{o}C. The aim was to generate a PCR product of minimum 50 ng/µl concentration, as this was the sample requirement for NGS.

2.3.5 Agarose gels for visualising and purifying PCR products.

Agarose gels (1%) were prepared by adding Agarose Superstrength (Melford Biolaboratories Ltd, Ipswich, Suffolk, UK) to distilled H_2O, and heating in a microwave for 5 min with removal and swirling until dissolved, followed by the addition of 50X Tris-Acetate-EDTA (TAE) to a final concentration of 40 mM Tris-acetate, 1 mM EDTA. The hot gel mix was poured smoothly into a gel casting tray to avoid bubbles and a comb inserted to create loading wells.

Once set, the gel was placed into a gel tank (BioRad®, Watford, Hertfordshire, UK) connected to a BioRad® Power Pac 300 (BioRad®, Watford, Hertfordshire, UK), and covered with 1X TAE buffer (final concentration 40 mM Tris-acetate, 1 mM EDTA). A 100 bp ladder (4 µl, New England Biolabs®, Ipswich, Massachusetts, USA) was loaded in the far right well and then 7 µl of each PCR product added to each consecutive loading well. Loading dye was already included in the 5X PCR buffer used in the PCR reaction. The gel was then run at 120 volts for approximately 40 min and then visualised and the image captured using ultra-violet light using ChemiDoc MP Imaging system by BioLabs® with Image Lab™ software. PCR products that showed a clear single band on the gel at the size of 16S rRNA were identified for NGS and aliquoted into 1.5 ml Eppendorfs and wrapped in plastic film to prevent spillages for dispatch for sequencing.

2.3.6 Next Generation Sequencing (NGS)

Microbial *de novo* sequencing was performed out of house by Novogene (HK) Company Ltd (Hong Kong), or by Eurofins Scientific SE (Luxembourg), with additional data processing and statistical analysis undertaken by Novogene. Sequencing was performed using Illumina HiSeq PE15- platform. Initially, at the NGS facility, samples were tested for quality as follows: Nanodrop was used to determine DNA purity (260/280 ratio), agarose gel electrophoresis was used to determine if there was DNA degradation or potential contamination, then a Qubit Fluorometer (ThermoFisher Scientific) was used to precisely quantify the DNA concentration. DNA libraries were then generated on a paired-end Illumina platform on those samples that passed quality control.

The barcodes or 'indexed primers' allowed all samples to be pooled and sequenced simultaneously, increasing the number of samples analysed without increasing run cost and time. These reads were then identified and sorted computationally based on the indexes and then aligned together for data analysis. This method creates short read lengths and generates 250 base pair (bp) paired-end reads.

2.3.6.1 NGS sequence data processing

At the NGS facility, after standard Illumina chastity filtering, reads were demultiplexed based on their index sequences so that paired-end (PE) reads were assigned to samples. Only PE reads where both the expected forward and reverse primer had been found and there were no mismatches in primer sequences were carried forward. The index and primer sequences were then clipped away leaving just the amplified sequence. Where the ends of forward and reverse PE reads overlapped, sequences were merged to form one longer read using FLASH (v2.2.00) (Magoc and Salzberg, 2011) and then merged reads were assessed to determine if their length was expected from the target region. Only those close to the expected length were retained. All reads with ambiguous bases or that were chimeric as detected by the UCHIME algorithm (Edgar *et al.*, 2011) were removed.

2.3.6.2 NGS assignment of taxa

Eurofins: The high-quality PE reads remaining were processed using minimum entropy decomposition (MED) (Eren *et al.*, 2013, 2015) and DC-MEGABLAST was used to assign taxonomic information to each operational taxonomic unit (OTU), with further processing and assignment undertaken using QIIME (v1.9.1, http://qiime.org). To improve estimates of abundance of taxonomic

units, lineage-specific copy numbers of relevant marker genes were used for normalisation (Angly *et al.*, 2014).

Novogene: Sequence analysis was carried out using UPARSE software (v7.0.1001) (Edgar, 2013) and those sequences with similarity of 97% or more were assigned to the same OTU. For each sequence represented, Mothur (Schloss *et al.*, 2009) was used with the SILVA SSU rRNA database (Wang *et al.*, 2007) to allow annotation at each taxonomic rank (Threshold: 0.8~1)(Quast *et al.*, 2013). To determine the phylogenetic relationship of all OTU sequences represented, the multiple sequence alignment tool (MUSCLE, v3.8.31) (Edgar, 2004) was used. To normalise samples, subsampling was carried out using a standard sequence number that corresponded to the sample with the least sequences. This output data was analysed for alpha and beta diversity as well as phylogenetic tree construction and used for statistical analysis.

2.3.6.3. NGS alpha and beta diversity, and statistical analysis

Assessment of alpha and beta diversity and the associated statistical analysis was carried out by Novogene. Alpha diversity was determined by the Chao, Shannon and Simpson indices, and statistical differences between brain tissue groups were calculated using the Wilcoxon nonparametric test.

For beta diversity, dissimilarity coefficients between pairwise brain tissue samples were determined using weighted and unweighted Unifrac distance as calculated by QIIME software (v1.7.0). Principal component analysis (PCA) reduced the dimension of the original variables using the FactoMineR package and ggplot2 package in R software (v2.15.3), reducing the complexity of the data and making it more likely that patterns and trends could be seen. Principal Co-ordinate Analysis (PCoA) allowed the visualisation of how close brain groups, and the samples within them, were and is displayed by weighted gene co-expression network analysis (WGCNA), stat and ggplot2 in R software package (v2.15.3). Unweighted Pair-group Method with Arithmetic Means (UPGMA) clustering was performed as a type of hierarchical clustering method to interpret the distance matrix using average linkage and was conducted by QIIME software (v1.7.0). Differences between bacterial community structure between brain tissue groups were analysed by four non-parametric tests: the Analysis of Similarity (ANOSIM), the Multi-response Permutation Procedure (MRPP), the nonparametric multivariate test ADONIS and AMOVA calculated by Mothur (http://www.mothur.org/wiki/Amova), were conducted with R software.

Differences in abundance of taxa were also examined by T test with correction for false discovery rate (q-values) and Metastat (R software) and linear discriminant analysis (LDA) with effect size (LEfSe) (LEfSe software).

2.3.6.4 BLASTn

BLASTn is a programme used for large scale DNA analysis that can allow for identification of bacteria (Belshaw and Katzourakis, 2005).

Any uncharacterised sequences performed by Eurofins or Novogene were imported into BLASTn to determine bacterial species in samples.

2.4 Protein

2.4.1 Protein extraction

Soluble proteins were extracted from approximately 100 mg of brain tissue placed in an Eppendorf tube. Following the addition of 1% (v/v) reconstituted protease inhibitor cocktail (Sigma) (diluted 1 tablet in 10 ml ddH_2O) in RIPA (Radio Immuno Precipitation Assay) lysis buffer (10 mM Tris-HCl pH 8; 50 mM sodium chloride; 5 mM EDTA; 15 mM sodium pyrophosphate; 50 mM sodium fluoride; 1% (v/v) Triton X-100; 100 µM sodium orthovanadate), 200 µl RIPA buffer was added to the Eppendorf tubes containing brain tissue and the tissue left to lyse for 10 min over ice.

The Eppendorf's were then spun for 20 min (9,447x g, at 3 ^{o}C). The supernatant containing soluble proteins was removed, and the pellets were washed with a further 100 µl of RIPA lysis buffer and re-spun for 20 min.

The insoluble pellets were washed with RIPA buffer (without the protease inhibitor cocktail) and spun (9,447x g, 3 ^{o}C) for 20 min and the supernatant discarded; this was repeated three times to make sure any traces of soluble protein were removed. Depending on the size of the pellet, around 200 µl of 8 M guanidine hydrochloride solution (Sigma) was added (or 100 µl for smaller pellets) and the pellets left at room temperature for 30 min to dissolve before the Eppendorf tubes were placed in the fridge for storage until ready for use.

2.4.2 Protein assay to determine protein concentration

The Thermo Scientific Pierce™ (Bicinchoninic Acid) (BCA) Protein Assay kit (Thermo Fisher). was used to determine total protein content of the protein extractions.

Bovine serum albumin (BSA) standards of 25, 125, 250, 500, 750, 1000, 1500 and 2000 µg /ml, diluted according to the manufacturer's instructions, were prepared. Sufficient BCA working reagent buffer for all the samples to be assayed was also prepared by mixing BCA reagent A with BCA reagent B at a ratio of 50:1 respectively (A:B).

One aliquot of each protein sample was thawed on ice and then duplicate wells of a Thermo Scientific Pierce™ microwell plate were loaded with 5 µl of standard or sample followed by 200 µl of buffer AB (1:1). The microwell plate was covered and incubated in the dark at room temperature for 30 min. The absorbance was then measured at a wavelength of 570 nm on a BioRad iMark™ Microplate reader using software Microplate Manager 6.

2.4.3. ELISA

Enzyme-linked Immunosorbent assay (ELISA) was used to measure recombinant human alpha-synuclein (α-Synuclein) in brain tissue using the (Bio-techne®) Human α-Synuclein DuoSet ELISA Kit (R&D Systems, Abingdon, Oxfordshire, UK) according to the manufacturer's instructions. Reagents supplied in the assay kit were brought to room temperature and prepared to their working concentrations according to the manufacturer's instructions before use. Sufficient capture antibody for a 96-well plate was diluted to its working concentration of 4 µg/ml in phosphate buffered saline (PBS), and 100 µl was immediately pipetted into each well, sealed with a cover and left overnight at room temperature.

The following day, to wash the wells, each was aspirated and filled (400 µl) with 1X wash buffer (diluted from concentrate in dd H_2O), a total of three times for three washes. The plate was then inverted and blotted against clean paper towels to ensure complete removal of liquid. The plate was then blocked by adding 300 µl of 1X diluent reagent to each well and incubated at room temperature for a minimum of 1 hour.

Samples and a standard curve were prepared as follows: the insoluble protein samples, where the presence of phosphorylated α-synuclein is found, were diluted 1:20 in 1X diluent reagent. Standards were prepared from the Recombinant Human α-Synuclein Standard (supplied at 195 ng), reconstituted with 0.5 ml of diluent reagent, and dilution of the standard in diluent reagent was

undertaken to create the following standards: 20, 10, 5, 2.5, 1.25, 0.625 and 0.313 ng/ml. 100 µl of reagent diluent was used as the blank. Following three washes of the plate, as described above, to remove the blocking agent, duplicate prepared samples, standards and the blank were added to the plate at 100 µl/ well, and the plate covered with an adhesive strip and incubated for 2 hours at room temperature.

Sufficient detection antibody for the 96 well plate was reconstituted to its working concentration of 25.0 ng/ml in reagent diluent. Following a further three washes of the plate, 100 µl of detection antibody was added to each well, covered with adhesive strip and incubated at room temperature for 2 hours. Next, sufficient Streptavidin-HRP for the 96 well plate, diluted 1:40 in reagent diluent, was reconstituted. Following a further three washes of the plate, 100 µl of reconstituted Streptavidin-HRP was added to each well, the plate covered with adhesive strip and incubated in the dark at room temperature for 20 min. Whilst the plate was incubating in the dark, the substrate solution was prepared by mixing 1:1 of Colour Reagent A (H_2O_2) and Colour Reagent B (Tetramethylbenzidine), then 50 µl of this was added to the Streptavidin-HRP in the wells and the plate gently tapped to ensure a good mix. Finally, 50 µl of stop solution supplied (2 M H_2SO_4) was added to each plate and gently tapped to mix. The optical density was read on absorbance microplate reader BMG Labtech set at 450 nm.

2.4.4 Haemoglobin assay

The haemoglobin assay was kindly undertaken on my behalf during the pandemic as I was unable to get to the laboratory. This assay was relevant to this study and a parallel study of AD brain.

Haemoglobin content within soluble protein samples was measured using a Haemoglobin Colorimetric Assay Kit (Cayman, Ann Arbor, Michigan, USA).

Chapter 3 Results

Tissue stocks for the planned experiments were limited. Brain tissues were used for optimisation and various downstream molecular experiments as well as two Next Generation Sequencing cycles. It was not possible to obtain further brain tissues from the same donors therefore the results highlighted in this study do not reflect all brain tissue samples stated in the Materials and Methods chapter.

3.1 Quantification of bacterial levels by qPCR

3.1.1 Betaglobin as a standard

An example of a standard curve generated from known betaglobin concentrations by qPCR, as used to normalise brain samples so that each well contained equivalent concentrations, is shown in Figure 3.1.

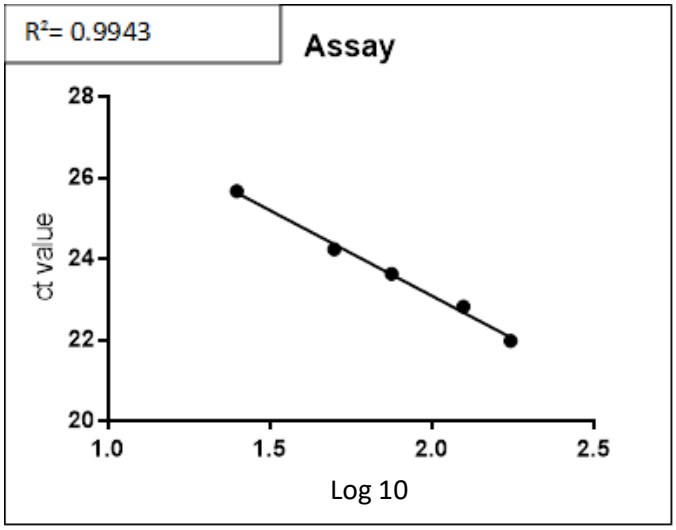

ng	Average
175	21.98
125	22.83
75	23.64
50	24.25
25	25.68

p value = <0.001

Figure 3.1: Standard curve of betaglobin and the associated Ct values

The graph was generated in GraphPad Prism 8.4.2.679 where ng was converted to log of 10 on the X axis and plotted against the Ct value, which refers to the number of amplification cycles in the qPCR reactions; the lower the Ct value the higher concentration the of betaglobin.

Only standard curves with an R^2 value of 0.955 or higher were accepted for sample normalisation.

3.1.2 Bacterial standards for calculating 16S copies/100 ng brain template

An example of a standard curve generated from known concentrations of *E. coli* DNA by qPCR and used to quantify bacteria in the brain samples is shown in Figure 3.2.

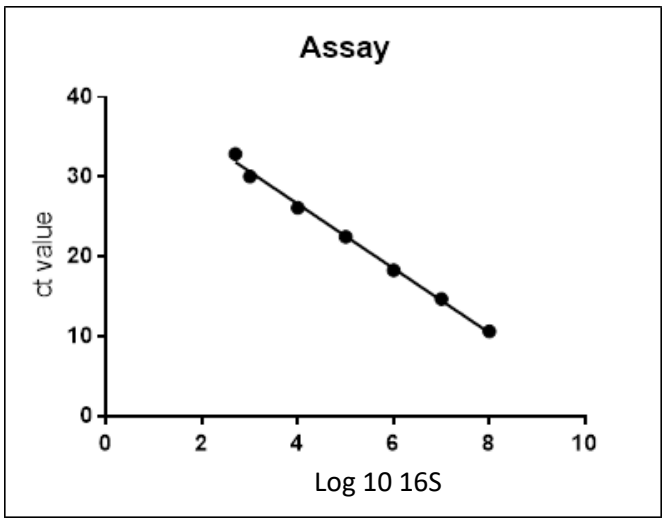

16S/100 ng	Dilution	Average
100000000	10^3	10.63
10000000	10^4	14.69
1000000	10^5	18.28
100000	10^6	22.47
10000	10^7	26.12
1000	10^8	30.06
500	10^9	32.89

R^2= 0.9955
P value= <0.001

Figure 3.2: *E. coli* standard curve and associated Ct values

The graph was generated in GraphPad Prism 9.4.1 where ng was converted to log of 10 on the X axis and plotted against the Ct value, which refers to the number of amplification cycles in the qPCR reactions; the lower the Ct value the higher the number of 16S molecules.

Only qPCR reactions with *E. coli* standard curves with an R^2 value of 0.955 or higher were accepted for calculation of sample 16S levels.

Bacterial 16S levels within brain tissue samples as determined from the *E. coli* standard curve are depicted as bar charts with standard deviations in Figure 3.3 (A) - (F).

A)

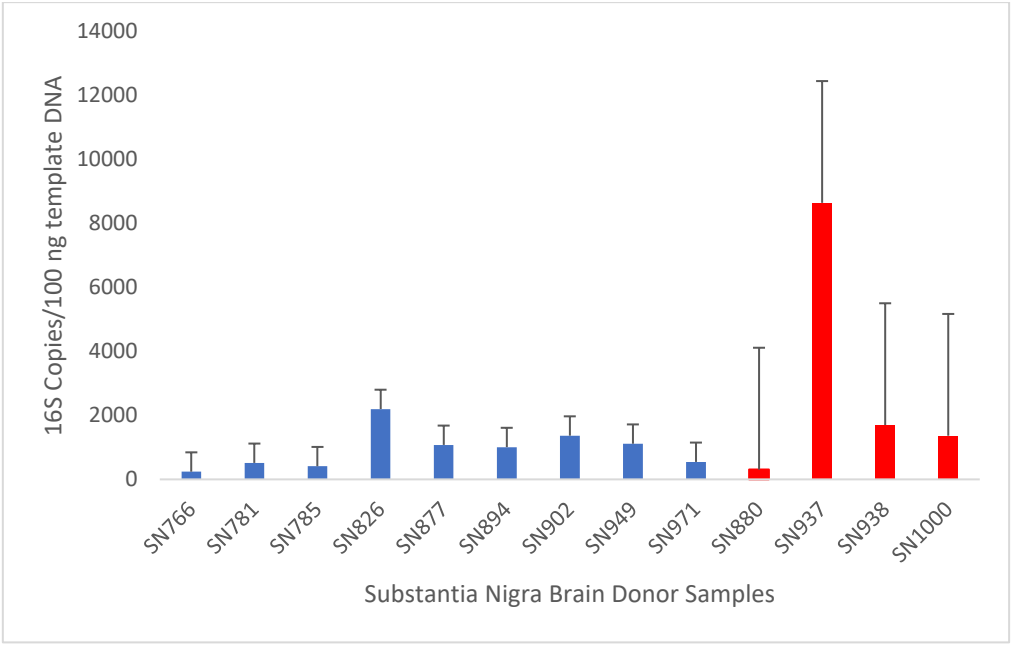
14000
12000
10000
8000
6000
4000
2000
0
16S Copies/100 ng template DNA
SN766
SN781
SN785
SN826
SN877
SN894
SN902
SN949
SN971
SN880
SN937
SN938
SN1000
Substantia Nigra Brain Donor Samples

B)

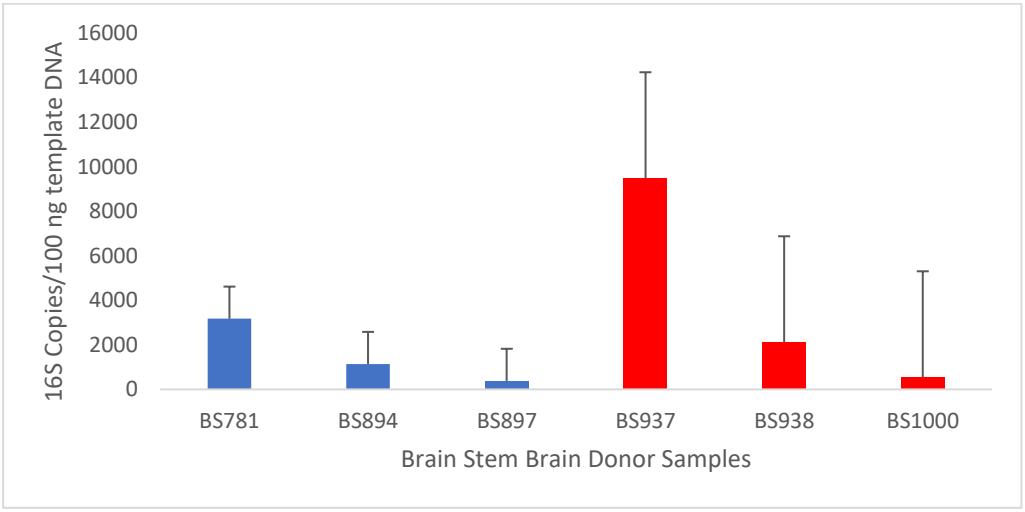
16000
14000
12000
10000
8000
6000
4000
2000
0
16S Copies/100 ng template DNA
BS781
BS894
BS897
BS937
BS938
BS1000
Brain Stem Brain Donor Samples

C)

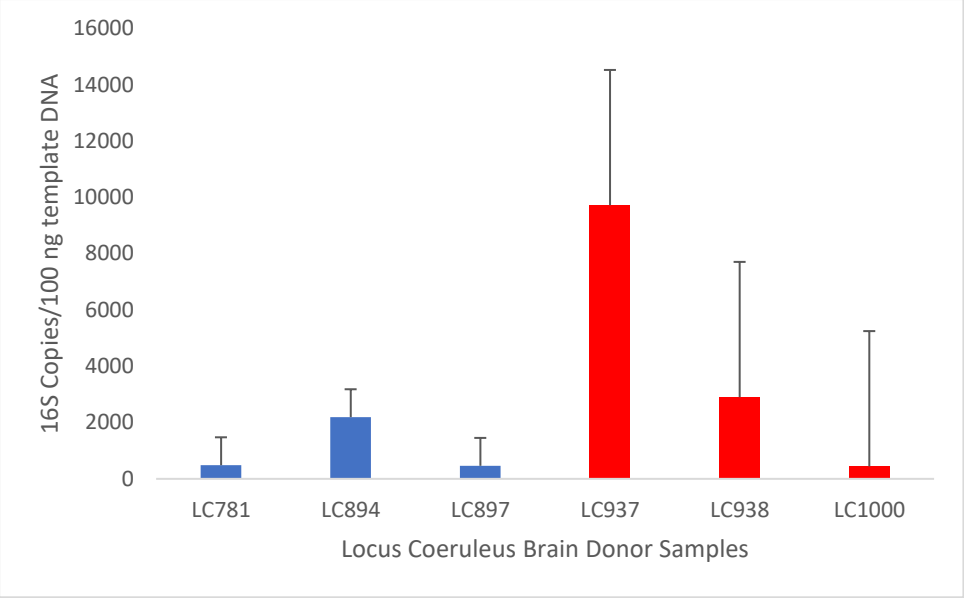
16000
14000
12000
10000
8000
6000
4000
2000
0
16S Copies/100 ng template DNA
LC781
LC894
LC897
LC937
LC938
LC1000
Locus Coeruleus Brain Donor Samples

D)

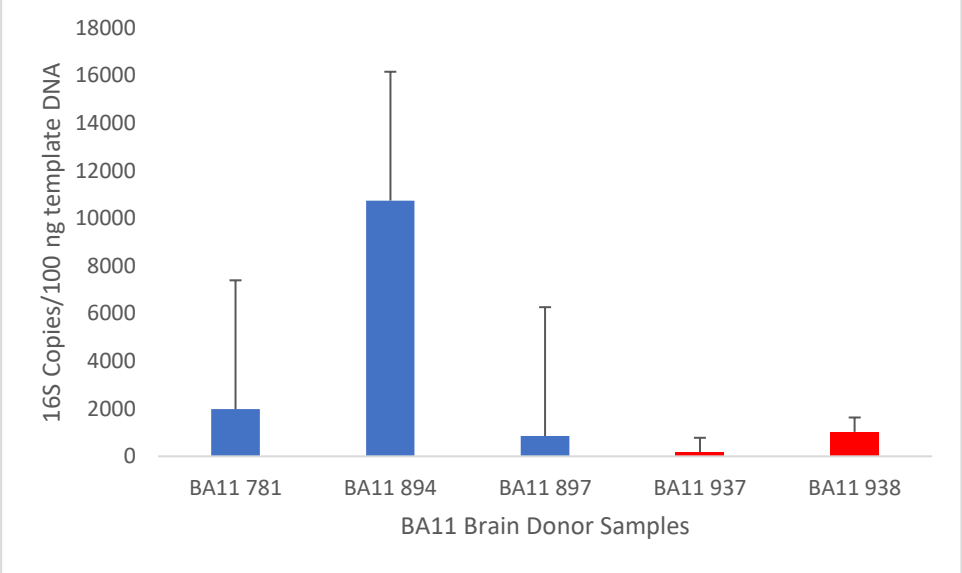
18000
16000
14000
12000
10000
8000
6000
4000
2000
0
16S Copies/100 ng template DNA
BA11 781
BA11 894
BA11 897
BA11 937
BA11 938
BA11 Brain Donor Samples

E)

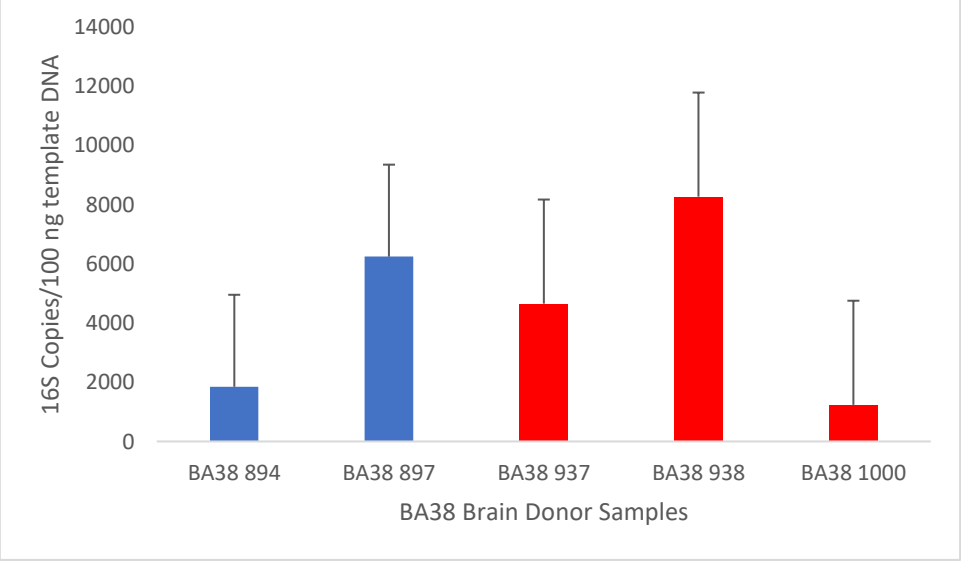
14000
12000
10000
8000
6000
4000
2000
0
16S Copies/100 ng template DNA
BA38 894
BA38 897
BA38 937
BA38 938
BA38 1000
BA38 Brain Donor Samples

F)

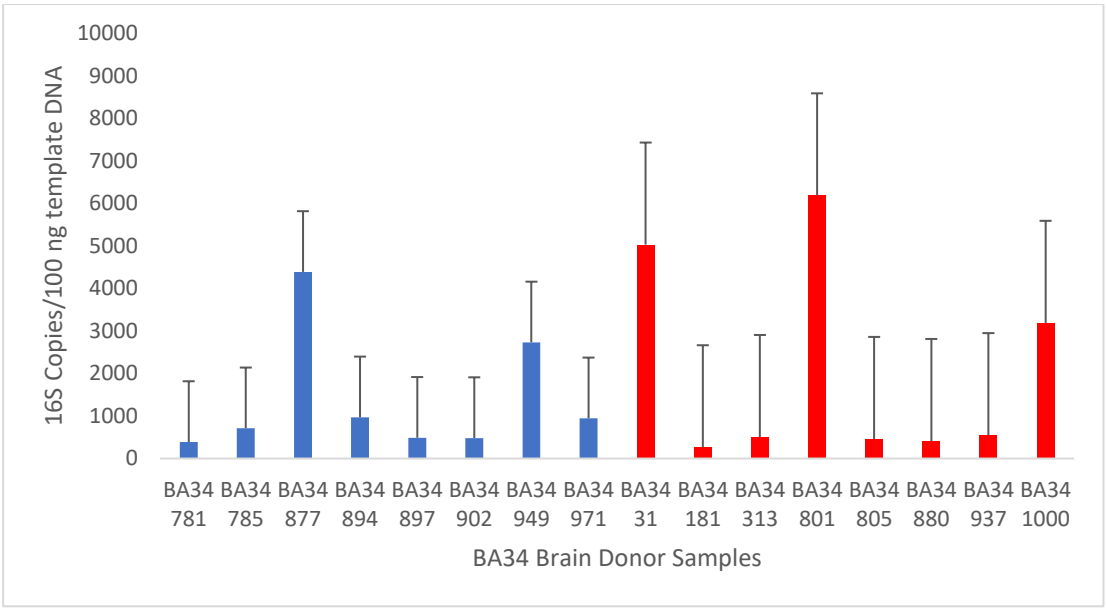

Figure 3.3: A – F: Bar charts of total 16S bacterial DNA molecules per 100 ng genomic DNA brain template and standard deviation grouped by brain area

The six bar charts depict the 16S levels quantified by qPCR and their standard deviations for each brain area. The blue colour bars depicts the control brain samples and the red bars depicts the PD samples.

Bacterial 16S copies in different brain areas in control and PD samples are depicted in Figure 3.4.

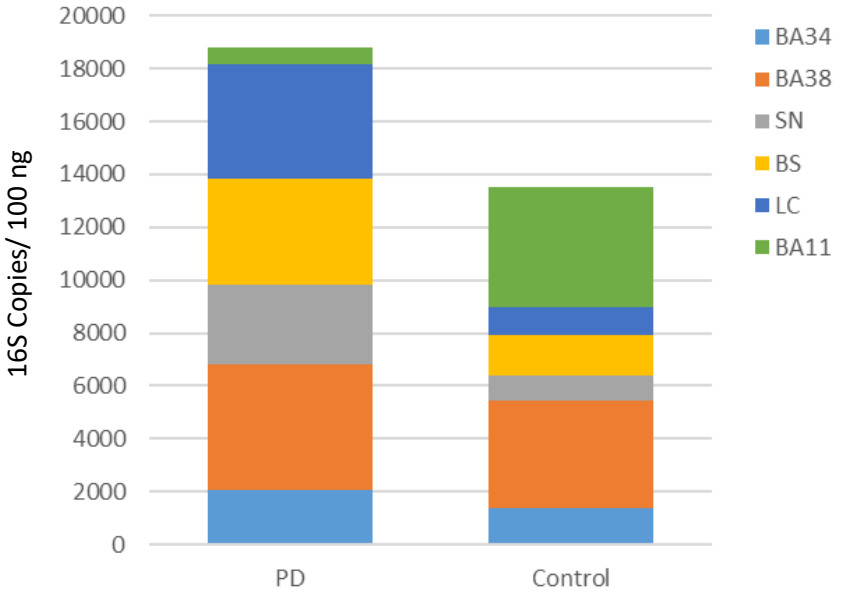

Figure 3.4: Comparison of 16S copies/100 ng brain template overall and by brain area between PD and C samples

Bacterial levels of 16S per 100 ng brain template DNA from each brain area from PD samples and all control samples are combined and shown in two separate bars.

Figure 3.4 shows cumulatively the number of 16S copies/100 ng brain template were higher in PD brain than in control, in particular, the midbrain areas of SN, LC and BS had a higher levels of 16S in PD than in control. In contrast, BA11 16S copies per 100 ng brain template was higher in control samples.

The mean values of 16 copies/100 ng brain template in PD and control, in tabular format, with the number of samples included for each brain area are shown in Table 3.1.

Table 3.1: Mean and standard error of 16S copies/100 ng template for each brain area

Brain area (n)		Mean		Standard Error of Mean	
BA11 PD (2)	BA11 C (3)	602.955	4525.80	426.17	3125.84
BA38 PD (3)	BA38 C (2)	4720.73	4045.01	1172.31	1554.29
BA34 PD (8)	BA34 C (8)	2075.32	1389.22	300.14	178.48
BS PD (3)	BS C (3)	4034.30	1563.52	1590.13	481.13
LC PD (3)	LC C (3)	4354.18	1046.22	1601.96	330.56
SN PD (4)	SN C (9)	3003.38	940.96	951.59	67.17

3.1.3 Statistical analysis comparison of 16S copies in PD and control

A non-parametric Mann-Whitney U Test was performed to determine whether 16S copies/100 ng brain template in PD and control were significantly different (Table 3.2).

Table 3.2: Non-parametric Mann-Whitney U statistical analysis

Tissue	Number of tissues	Mean Rank	Sum of ranks
Control	23	24.39	683.00
PD	28	27.96	643.00
Mann-Whitney U	277.000		
Wilcoxon W	683.000		
Z	-0.852		
Asymp. Sig. (2-tailed)	0.394		

The Mann-Whitney analysis showed that there was no significant difference in 16S copies/100 ng brain template between PD and control samples.

To rule out any influence of contamination on levels of 16S, the Post-Mortem Delay (PMD) (time between death and the time at which the brain tissue was frozen in hours) was plotted against 16S copies/100 ng Figure 3.5.

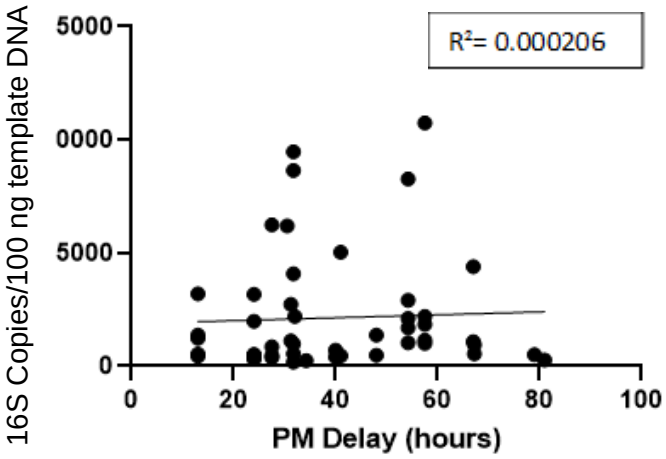

Figure 3.5: Scatter plot graph of PMD against 16S copies/100 ng brain template
All samples that were analysed by qPCR (PD and control combined) are shown here plotted against PM Delay.

To formally confirm if there was any correlation between PMD and the number of 16S copies/100 ng brain template, a Spearman rank correlation was undertaken (Table 3.3).

Table 3.3: Spearman two-sided analysis to determine correlation between PMD and 16S copies/100 ng template

Spearman r	Result
r	0.1319
95% Confidence Interval	-0.1572 to 0.4003
P value (two-tailed)	0.3561
Significant (alpha 0.05)	No

The Spearman rank correlation indicated that there was no significant association between PMD and the number of copies of 16S/100 ng template.

To further investigate whether there was an effect of PMD when the delay was long compared to shorter PMD times, 16S copies/100 ng brain template in samples with PMDs of below or over 40 hours were compared (Figure 3.6).

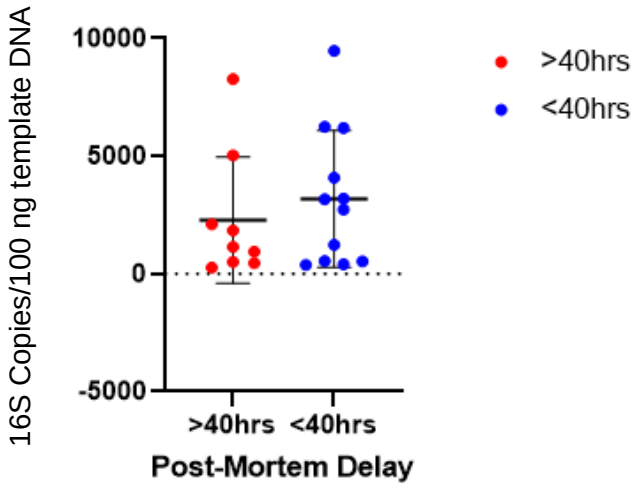

Figure 3.6: Grouped comparison of 16S copies/100 ng brain template in brain tissue with PMDs of < and > 40 hours
All samples that were analysed by qPCR (PD and control combined) are shown here.

Mann-Whitney analysis of the difference in 16S levels between the below 40 hour and above 40-hour PMD samples indicated that there was no significant difference p = 0.4221.

3.2 Conventional PCR for NGS

For successful NGS, a high-quality PCR product of 50 ng/µl was needed. PCR products generated for NGS were visualised by agarose gel electrophoresis to determine if they were the desired size and in sufficient quantity, as indicated by a clear thick band in the correct position (just less than 500 bp) by the DNA ladder/marker.

During optimisation of the PCR, different buffers and numbers of cycles were tested to determine the best parameters to obtain at least the minimum DNA concentration and purity required for NGS.

Figures 3.7 to 3.9 show gels of PCR products generated testing the difference between a colourless buffer, and one with a loading dye already incorporated, and PCRs conducted at 35 and 38 cycles.

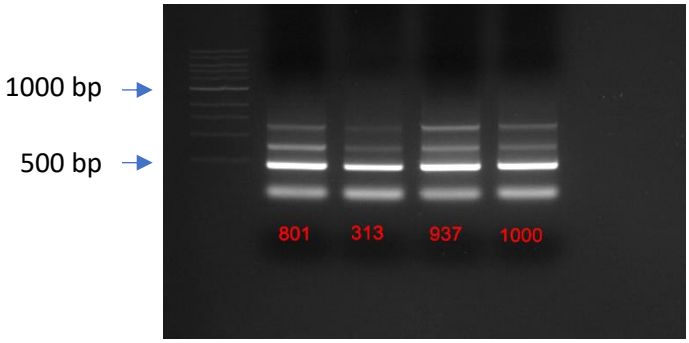

Figure 3.7: Agarose gel showing a PCR of 35 cycles
The DNA ladder (left, with 500 and 1000 bp indicated) and four PD brain samples that were amplified under for 35 cycles are shown. The bright band at ~500 bp is the sized predicted for the PCR product. The smaller bands are primer-dimers**.**

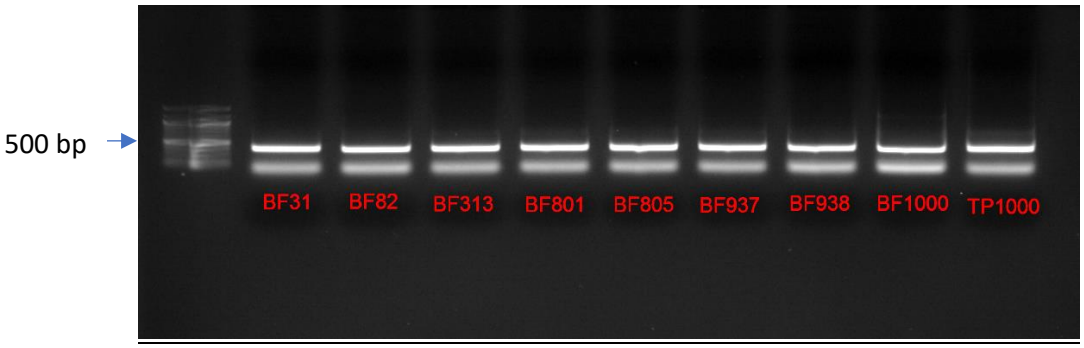

Figure 3.8: Agarose gel showing a PCR of 38 cycles
Nine PD brain samples that were amplified for 38 cycles are shown. BF = BA11, TP = BA38. One clear band at ~500 bp is visible for each sample together with the primer-dimers.

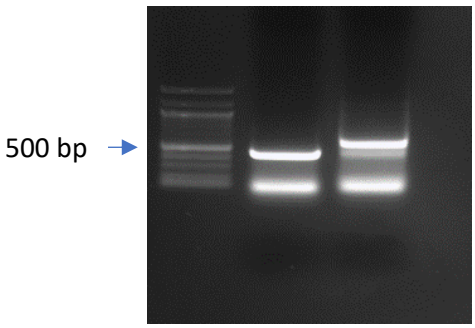

Figure 3.9: Agarose gel of a brain sample PCR of 38 cycles using two different buffers
A clear buffer solution (right band), and a buffer solution with loading dye (left band). Three bands can be seen in the product amplified using the clear buffer solution.

These agarose gels indicated that 35 cycles of PCR were too few as additional bands heavier than the band at 500 bp were also amplified. Therefore, NGS PCR was carried out using 38 cycles. The gel in Figure 3.9 also shows that the buffer solution with loading dye on the left amplified a product of 500 bp whereas the main product amplified using the clear buffer solution was between 600-700. Therefore, the preloaded buffer solution was selected for NGS PCR.

3.3 NGS 1

PD samples from this study and AD post-mortem samples from a separate study were processed together by Novogene and therefore the sequencing analysis statistics depict both PD and AD samples.

3.3.1 Processing statistics

Out of 98 samples processed, 49 were brain samples (PD or control) for this study. Figure 3.10 shows all the observed species (operational taxonomic units, or OTUs) across all 98 samples processed, and depicts the species diversity across the samples as well as the adequacy of the sample size. The rise of the curve indicates the large number of species found in the samples, whilst the box plots flattening at the top of the curve indicate that as further samples were sequenced the number of additional species added was minimal.

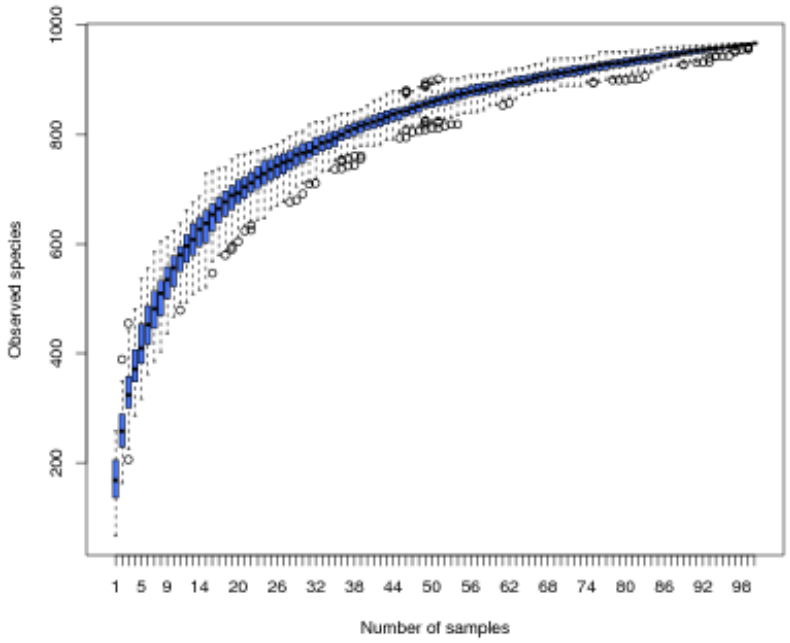

Figure 3.10: Species accumulation box plot of all samples processed for sequencing

In total, 971 OTUs were identified from the taxon tags (sequence reads). During identification, reads with 97% DNA sequence similarity were grouped into single OTUs as they were considered to be homologous in species (97% clustering). Table 3.4 and Figure 3.11 show the number of OTU reads for each sample.

Table 3.4: Number of effective tags (sequence reads) and OTUs per sample

Sample	Effective tags	OTUs		Sample	Effective tags	OTUs		Sample	Effective tags	OTUs
BA34-766C	201430	135		BS-894C	283920	121		CP-785C	304654	217
BA34-781C	201127	200		BS-897C	229689	139		CP-877C	146900	223
BA34-826C	254404	93		BS-937P	247971	173		CP-894C	231410	200
BA34-877C	247874	89		BS-938P	122122	214		CP-897C	232984	252
BA34-894C	301610	196		LC-781C	272683	180		CP-949C	177746	221
BA34-897C	296420	124		LC-894C	418981	206		CP-971C	337478	201
BA34-902C	267153	116		LC-897C	152622	180		CP-31P	355558	216
BA34-971C	218062	195		LC-937P	180286	170		CP-82P	316208	180
BA34-949C	228588	179		LC-938P	146712	130		CP-801P	273527	229
BA34-805P	183374	127		LC-1000P	186178	206		CP-880P	226921	216
BA34-313P	221662	137		SN-781C	153099	114		CP-937P	182296	192
BA34-880P	268839	175		SN-785C	227751	157		CP-938P	266458	186
BA34-937P	239492	156		SN-894C	199848	163		CP-1000P	177615	171
BA34-1000P	130918	108		SN-937P	197631	105		CSF-949P	297526	198
BA38-781C	250450	129		SN-938P	236711	85		Average	231318	169
BA38-937P	167235	214		SN-880P	241298	89				
BA38-938P	162646	149		SN-1000P	147547	185				
BA38-1000P	316071	220								

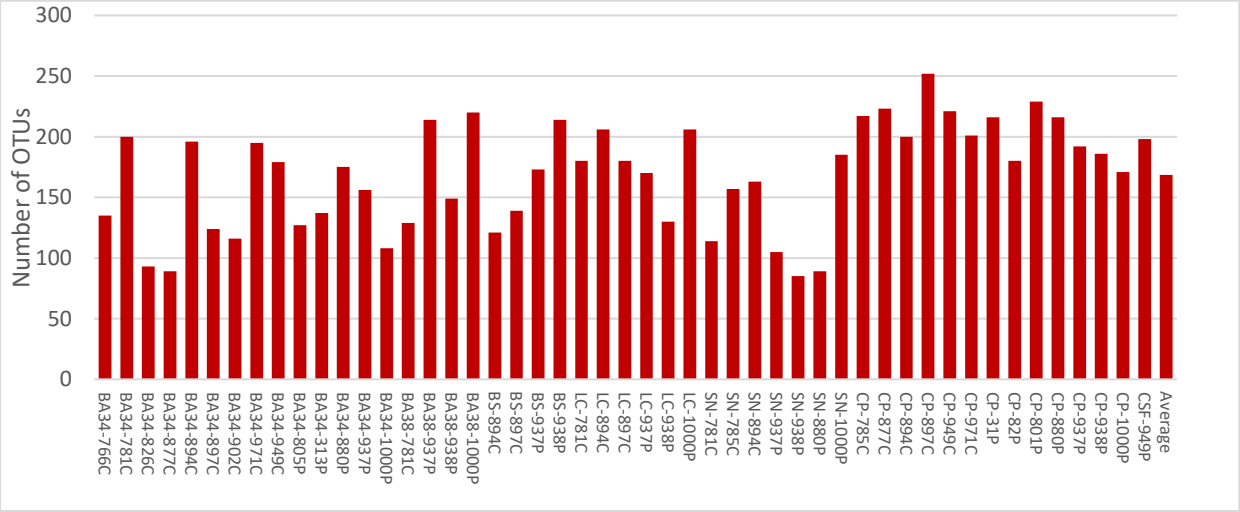

Figure 3.11: The number of OTUs found in each sample

PD and control samples varied in respect of the numbers of OTUs they contained, the highest being 252 in CP-897C, with an average of 169 across all samples.

Novogene assigned taxa to the OTUs and provided data on bacterial taxa abundance.

3.3.2. Relative abundance of taxa

The relative abundance of bacterial taxa at the phylum level found in brain samples is shown in Figure 3.12.

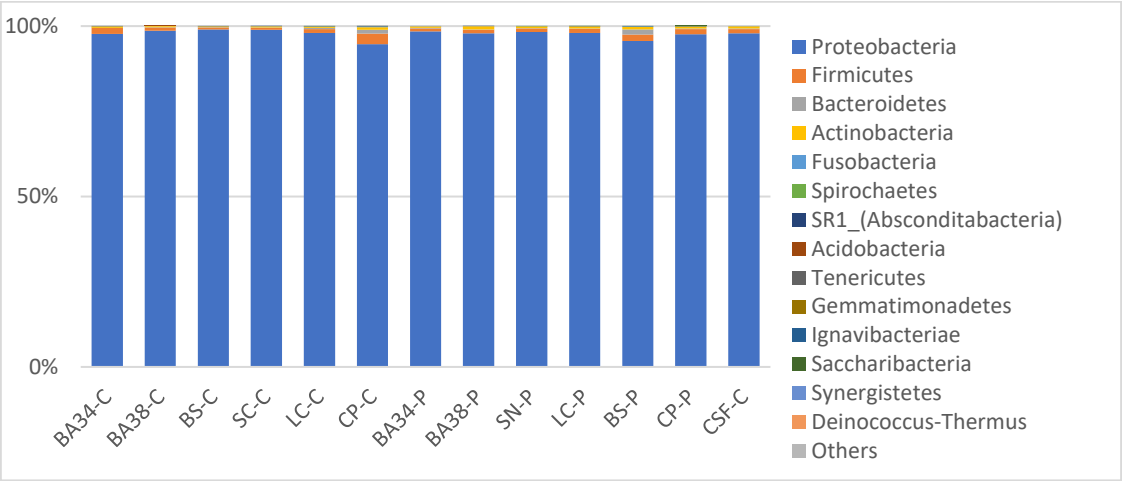

Figure 3.12: Relative abundance of bacterial taxa at the phylum level for each brain sample group
Samples of all donors are grouped by brain area and by disease status where PD = 'P' and Control = 'C'.

A very high proportion (>90%) of bacterial taxa in each brain area and in both PD and C was identified as Proteobacteria. Figure 3.13 depicts the relative abundance for the same brain areas grouped by disease status but at genus level. *Escherichia-Shigella* was the most abundant of the Proteobacteria present.

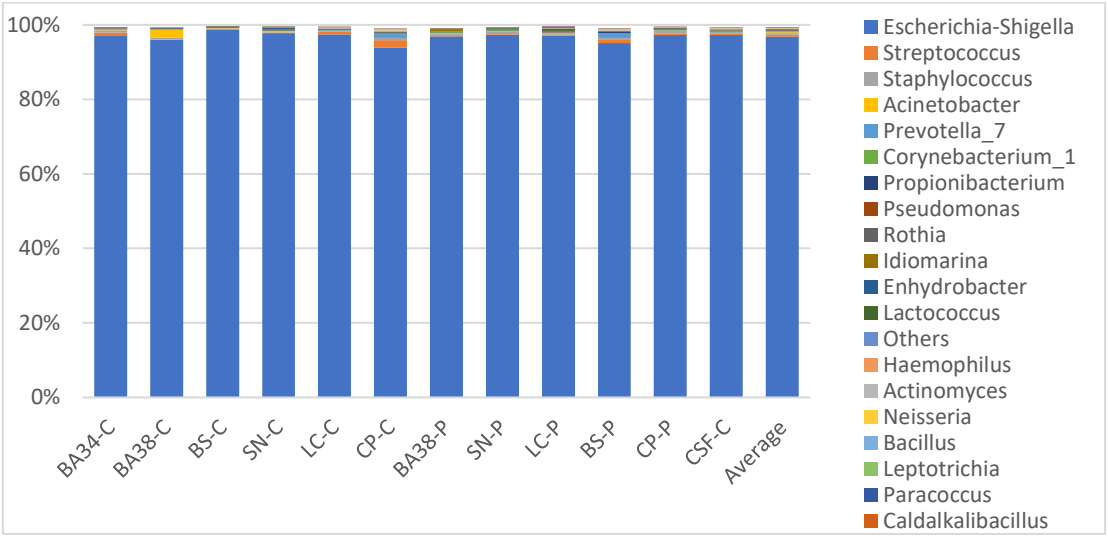

Figure 3.13: Relative abundance of bacteria at the genus level for each brain area
Samples are grouped by area as P (PD) or C (Control).

As the phylum Proteobacteria was found to have such a high relative abundance compared to all other phyla present, it was removed from the data to better visualise the proportion of the other phyla present in each brain area (Figure 3.14). These phyla represented <6% of those identified, with the second most abundant phylum shown to be Firmicutes.

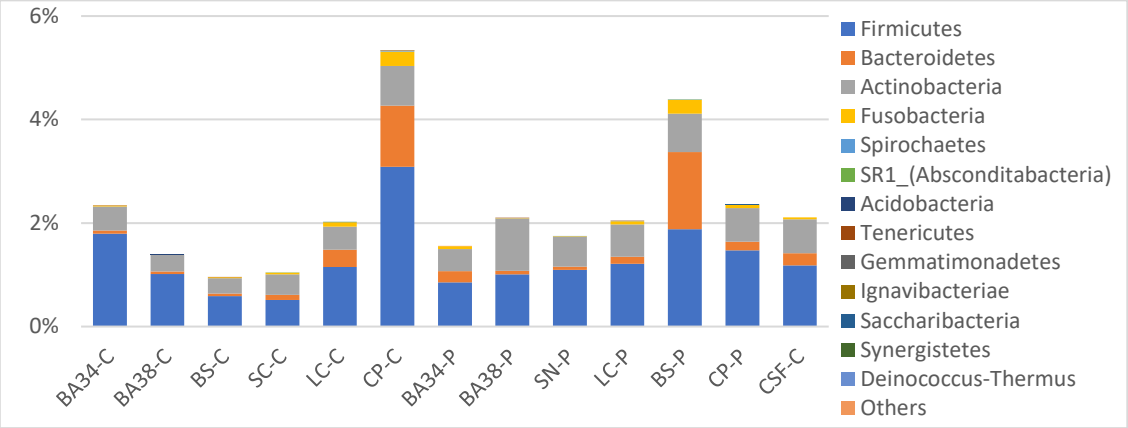

Figure 3.14: Relative abundance of taxa at phylum level with Proteobacteria removed from the data
Samples grouped as health (control – C) or disease (PD – P) per brain area.

Similarly, to better visualise the other genera, *Escherichia-Shigella* was removed from the genus level data (Figure 3.15).

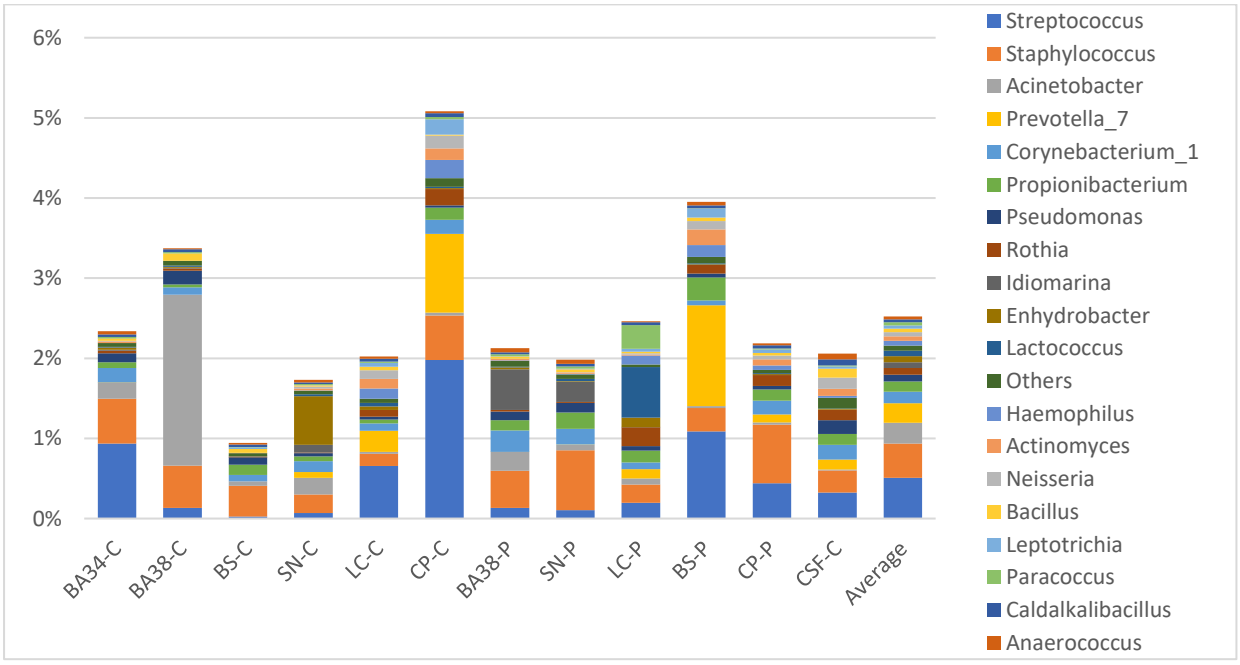

Figure 3.15: Relative abundance of taxa at genus level with *Escherichia-Shigella* removed
Samples grouped as health (control – C) or disease (PD – P) per brain area

The remaining genera accounted for <6% of relative abundance. After *Escherichia-Shigella*, the most abundant genera differed depending on the brain area with, for example, *Streptococcus* common in a number of groups and the most common genus in BA34-C and CP-C, and *Staphylococcus* relatively abundant in all groups, and the most common genus in CP-P (PD), SN-P (PD) and BS-C. *Prevotella*, of which some species have been implicated in periodontal disease, was the most abundant genus in the brain stem PD tissue.

3.4 NGS 2

A second round of NGS was performed using newly generated PCR samples from the same brain tissue donors where sufficient tissue remained. The rationale for this was that in NGS1 *Escherichia-Shigella* was ubiquitous and highly abundant in all samples and is a known common contaminant. A negative control could unfortunately not be processed along with the NGS1 samples as the quantity of the control PCR product, amplified from an unrelated human source (a prostate cancer cell line), was insufficient due to the suppression of bacterial amplification by the genomic DNA of the cell line. Therefore, although contamination was suspected in NGS1, sample profiles could not be compared with a control to confirm this. In the repeat NGS2, a no template control (NTC) generated with medical grade water and no human material was included.

At this time (Dec 2019), the COVID-19 pandemic had stalled routine NGS processing at Novogene (Hong Kong), therefore NGS2 was conducted by Eurofins, which were operating normally. However, as Eurofins do not provide statistical analysis, this was conducted at a later date by Novogene.

3.4.1 Processing statistics

High quality out reads were processed using Minimum Entropy Decomposition (MED), which is a more efficient computational way of separating marker genes into OTUs, effectively obtaining 99% OTU clustering compared with Novogene's 97%. This gives rise to greater taxonomic resolution.

In total 2786 OTUs were identified and assigned to Taxa by Eurofins (Table 3.5, Figure 3.16).

Table 3.5: Number of reads assigned to OTUs and OTUs/brain sample

Sample	Sequences assigned to OTUs	Number of OTUs
BA34-766C	60015	164
BA34-781C	54045	167
BA34-949C	543966	171
LC-897C	30926	107
LC-937PD	42123	242
BA11-781C	39303	162
BA11-897C	41585	210
BA11-937PD	36716	247
BA11-1000PD	37585	103
BA38-897C	41679	96
BA38-1000PD	29481	148
SN-766C	41445	115
SN-781C	27121	115
SN-826C	35756	105
SN-949C	40125	114
SN-801PD	275370	120
SN-880PD	28973	164
SN-937PD	30562	143
NTC	51674	197

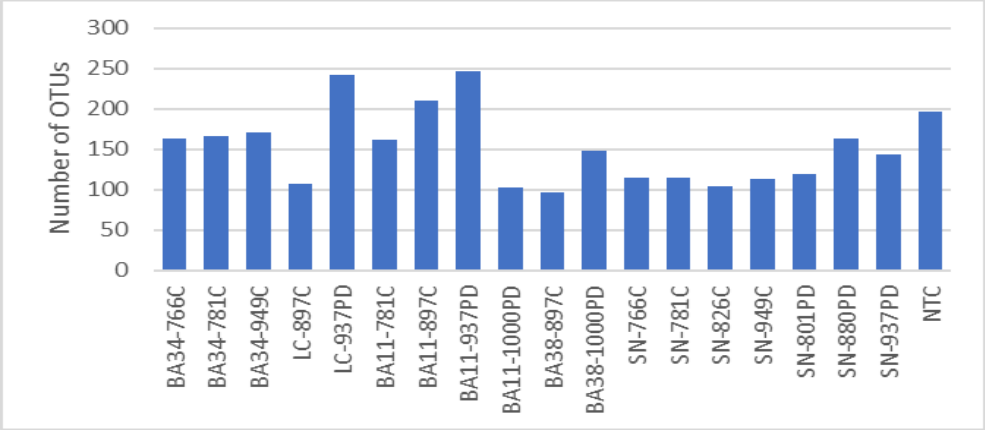

Figure 3.16: The number of OTUs per sample (Eurofins)

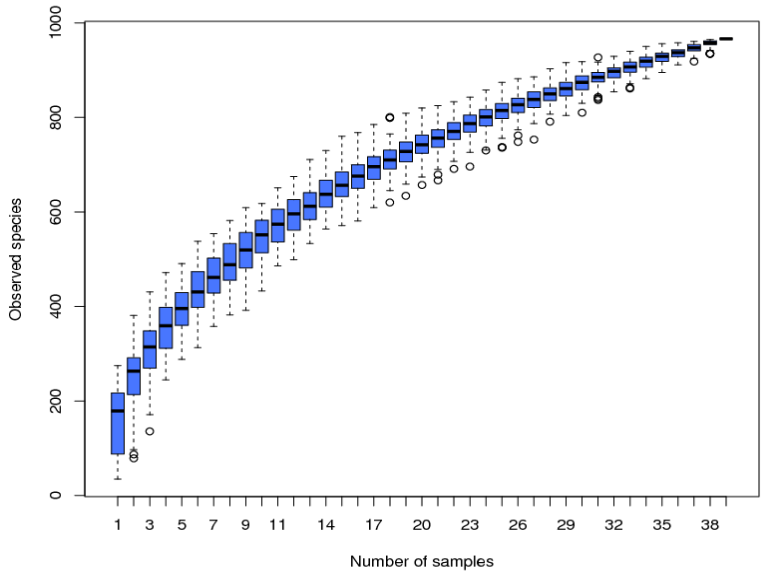

Figure 3.17: Species accumulation box plot of all samples processed for sequencing
The sample set processed included some obtained from AD brains for a separate study**.**

The accumulation plot shown in Figure 3.17 indicated that the sequencing was adequate capturing the diversity and majority of sequences present.

When sent for analysis, Novogene identified 976 OTUs from the NGS library (Figure 3.18) using Uparse software and assigning taxa using the SSUrRNA SILVA database. The number of OTUs was less than identified by Eurofins due to the different methods of clustering; Eurofins use a method that separates by single nucleotide differences and provides higher taxonomic resolution.

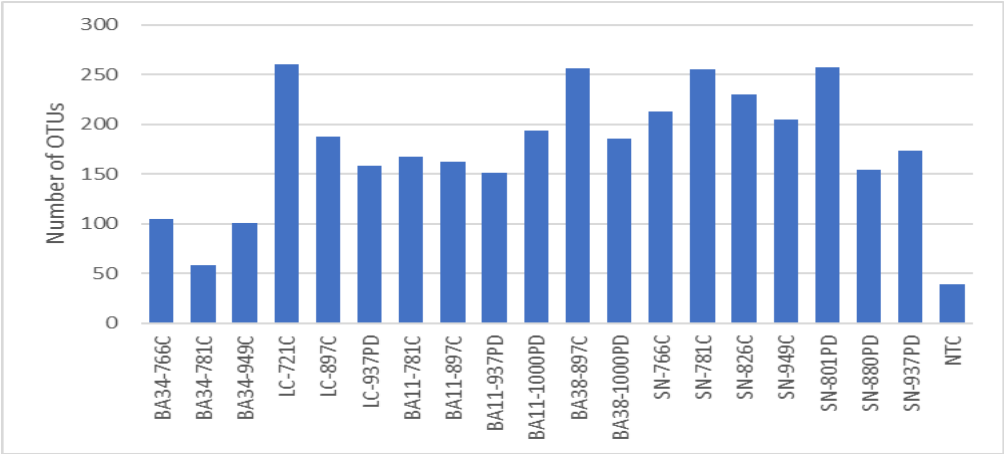

Figure 3.18: The number of OTUs per sample (Novogene)

There were a range of OTU reads across all samples, with the lowest number of OTUs identified in the NTC.

3.4.2 Relative abundance of taxa

The relative abundance of taxa down to the genus level is shown in Figures 3.19A (Eurofins) and 3.19B (Novogene)

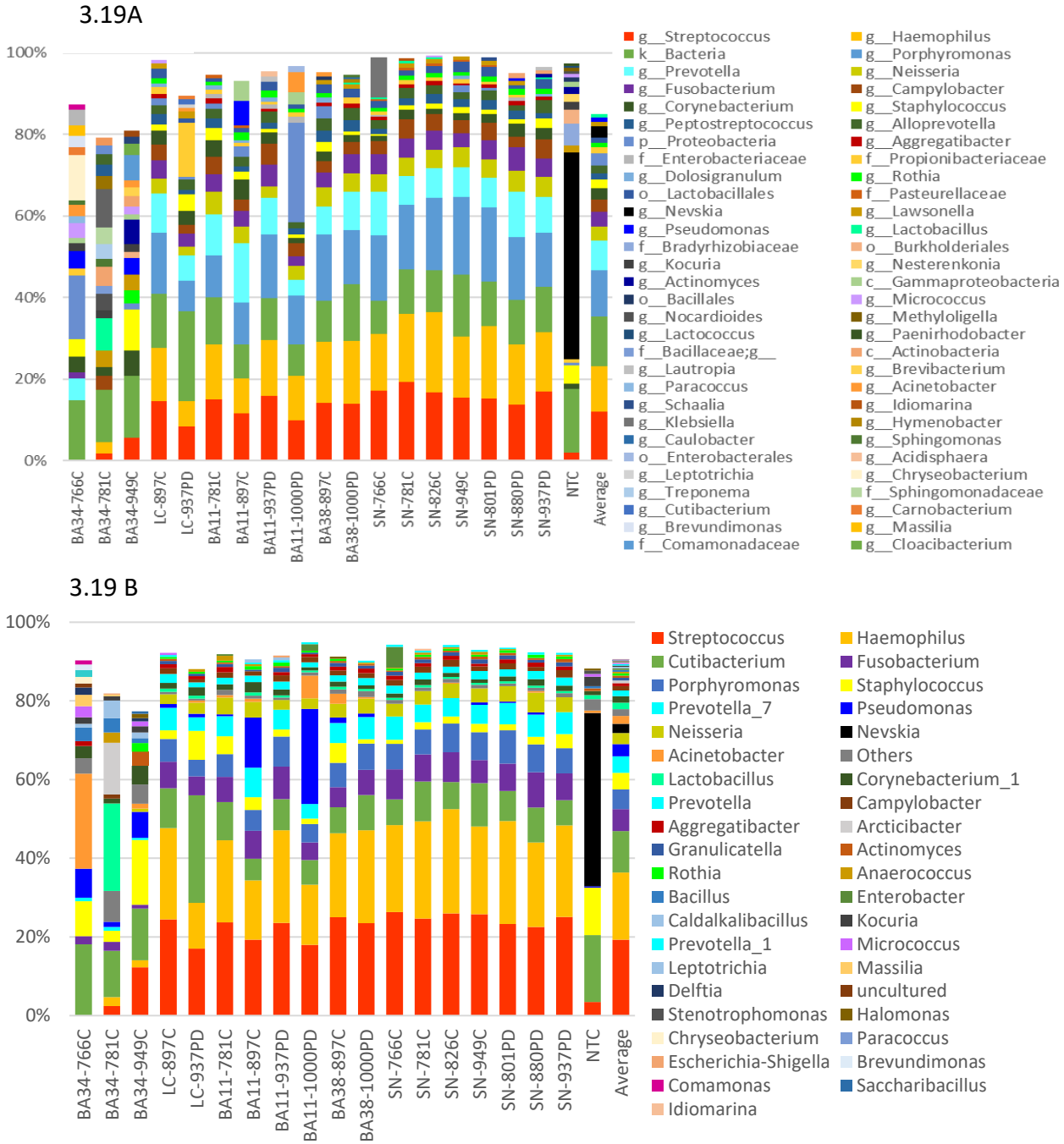

Figure 3.19: A & B: Relative abundance of bacterial taxa down to the genus level
Each bar represents the top 20 bacterial taxa found in a particular brain group, therefore there are more than 20 bacterial taxa depicted on the graphs. Average is the average abundance across all samples.

Overall, the pattern of abundance of taxa was similar irrespective of whether the samples had been processed by Eurofins or Novogene, with the NTC showing a different spectrum and abundance of taxa compared to brain tissue samples. Finding bacteria in the NTC indicates that there was some contamination of the PCR, however as explained the patterns of taxa were different from those seen in brain tissue. In both Figure 3.19A and B, *Streptococcus* and *Haemophilus*, were the most abundant taxa generally in most samples. The OTU assigned 'Kingdom bacteria' by Eurofins (3rd most abundant taxa overall) was run through a BLASTn search engine, which returned it with 99% certainty as *Cutibacterim acnes*. and *Cutibacterium* was also the 3rd most abundant genus overall as identified by Novogene.

The abundance of bacteria in brain area BA34 was visibly different compared to the other brain areas, as depicted with the different colours and height of the bands.

Out of the top 10 genera in the groups that showed a similar profile, 8 were those that are found in oral mucosal surfaces in health and disease.

The NGS2 data was compared to that obtained in NGS1, but with the potential contaminant, (*Escherichia-Shigella*) removed from the NGS1 data. For this comparison, only groups that were processed for both NGS runs are shown.

NTC is not included in Figure 3.20 as there was no NTC processed for NGS1, therefore a comparison could not be made. There were 11 genera plus ‘others’ common to both the NGS1 and NGS2 top 20 taxa, implying that these samples were not all that dissimilar once *Escherichia-Shigella* was removed. A major difference was in the relative abundance of *Staphyloccocus,* which was much less overall in NGS2 than in NGS1, whereas *Streptococcus* was more abundant in NGS2 than in NGS1. Despite the relative similarity of these profiles, subsequent analysis was limited to that of NGS2, as the effects of the dominance of *Escherichia-Shigella* in NGS1 were unknown.

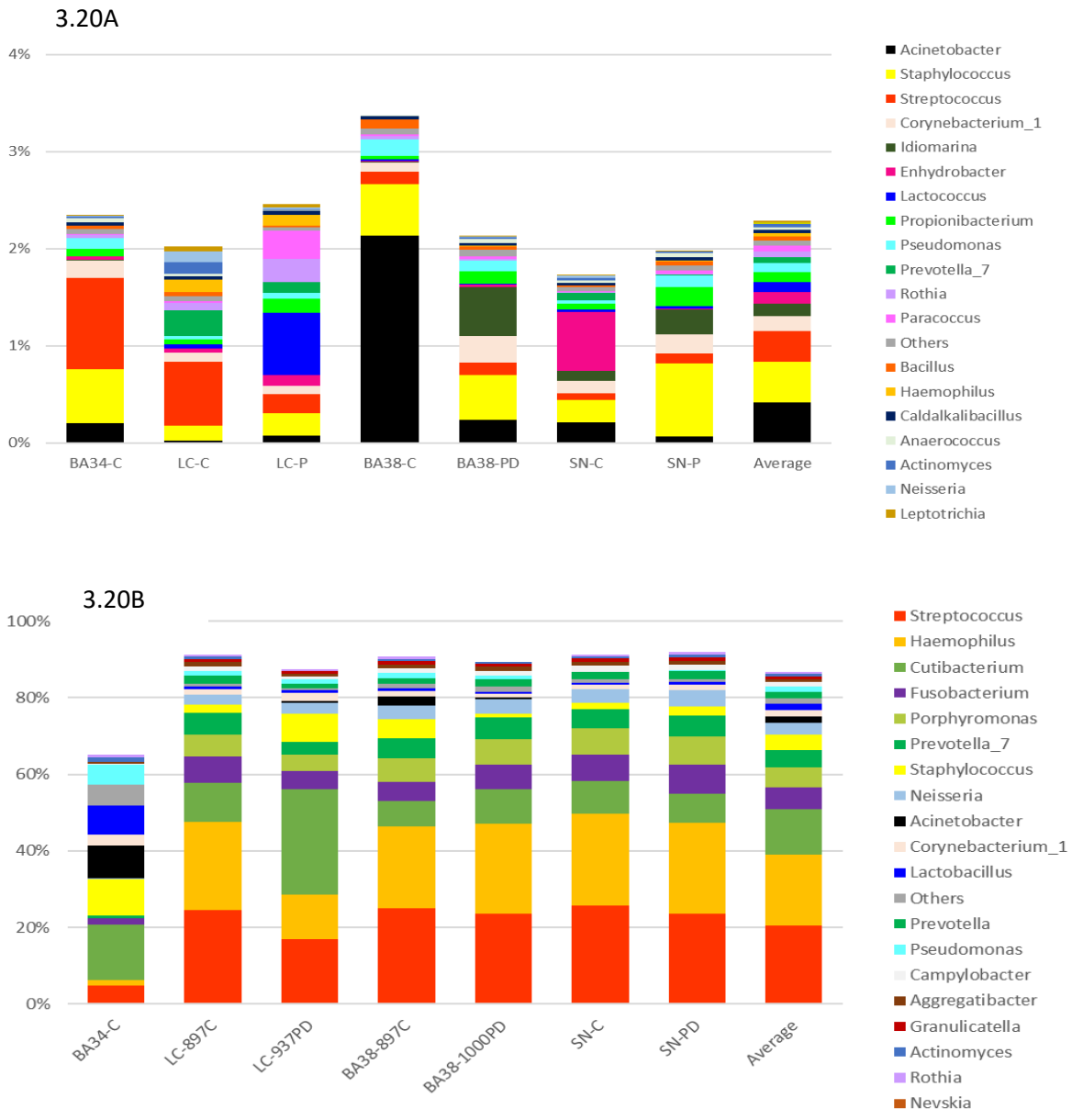

Figure 3.20: A & B: Relative abundance of top 20 genera (%) for (A) NGS1 (no *Escherichia-Shigella*) and (B) NGS2

NGS2 is Eurofins. The average abundance of genera across all groups was determined, and genera in the top 20 are depicted for each group. Samples are grouped by brain area and disease status.

NGS2 data was also compared with that obtained from blood samples processed using the same technique (Figure 3.21). This figure shows the relative abundance of the top 20 genera averaged across brain samples, blood, and NTC and demonstrates that the abundance pattern of taxa in blood and NTC is different to that found in the brain samples, suggesting that the genera seen in the brain have not come from contamination or a blood source.

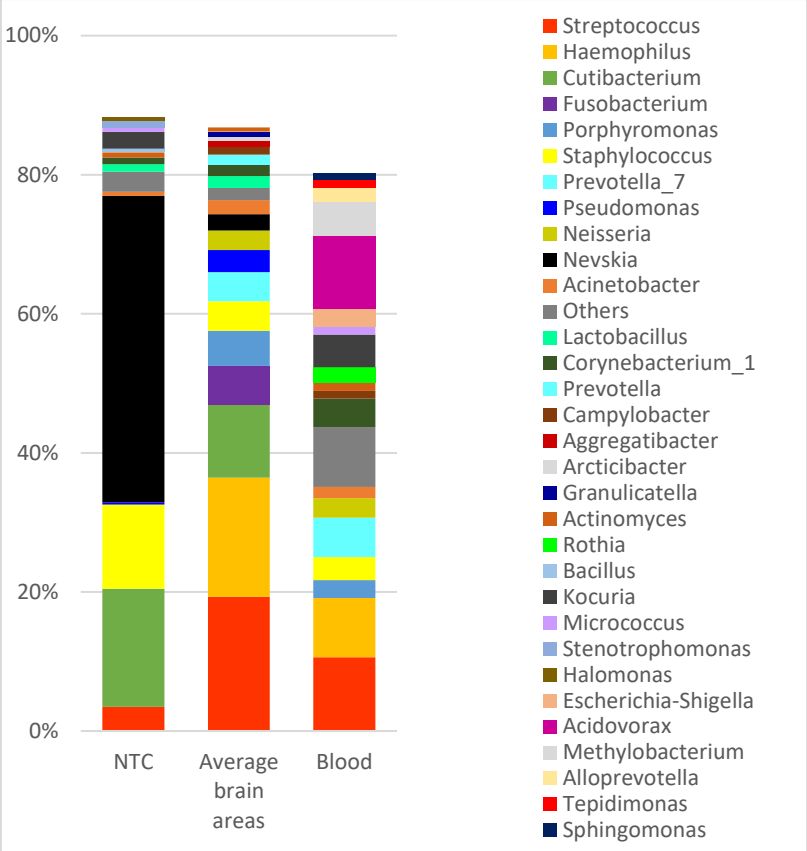

Figure 3.21: Relative abundance of top 20 genera in blood, NTC and brain
Blood data is the average of four samples from a related study (Emery *et al.*, 2021), and brain data is the average of all the brain samples from NGS2. NTC is from NGS2.

3.4.3 Alpha diversity

Alpha diversity indices attempt to describe the microbial diversity within each sample/sample group. Figure 3.22 shows the comparison of alpha diversity between samples grouped by disease and brain area assessed by three community richness indices: Chao1, Shannon, and Simpson. Each alpha diversity index uses slightly different assumptions to determine richness, so using three different ones gives a good overall picture of differences in diversity between groups.

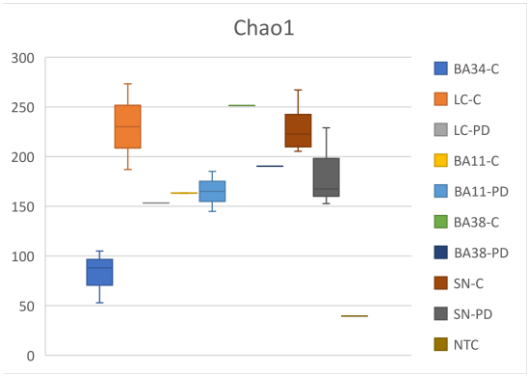

	Difference	pvalue sig	LCL	UCL
BA34-C v LC-C	-21.33	0.00866	-36.71	-5.96
BA34-C v BA38- 897C	-26.33	0.0101	-45.78	-6.88
BA34-C v SN-C	-22.33	0.0015	-35.2	-9.47
LC-C v NTC	27.00	0.0125	6.37	47.63
LC-897C v NTC	32.00	0.0106	8.18	55.82
NTC v SN-C	32.00	0.0106	8.18	55.82

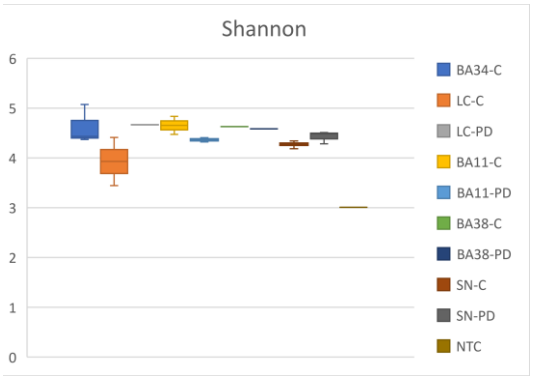

	Difference	pvalue sig	LCL	UCL
BA34-C v NTC	20.67	0.0399	1.03	40.3
BA34-C v SN-C	13.67	0.0400	0.68	26.65
LC-937PD v NTC	25.00	0.0422	0.95	49.05
BA11-C v NTC	23.00	0.0318	2.18	43.82
BA11-C v SN-C	16.00	0.0344	1.27	30.73

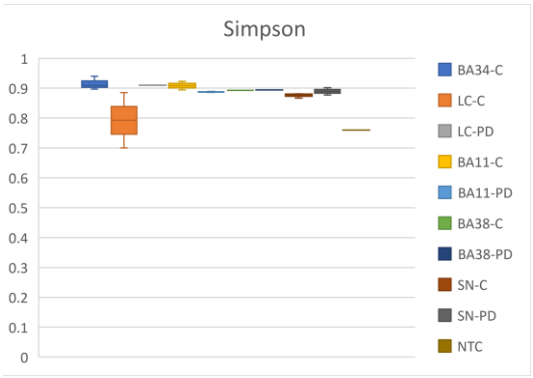

	Difference	pvalue sig	LCL	UCL
BA34-C v LC-C	21.58	0.0058	6.89	36.28
BA34-C v BA11-PD	15.08	0.0447	0.39	29.78
BA34-C v NTC	0.01	0.011	6.25	43.42
BA34-C v SN-C	21.33	0.0015	9.04	33.63
BA34-C v SN-PD	13.50	0.0445	0.36	26.64
LC-937PD v LC-C	22.75	0.0255	3.04	42.46
LC-937PD v NTC	26.00	0.0269	3.24	48.76
LC-937PD v SN-C	22.50	0.0164	4.50	40.50
LC-C v BA11-C	-19.00	0.0226	-35.10	-2.90
BA11-C v NTC	22.25	0.0286	2.54	41.96
BA11-C v SN-C	18.75	0.0105	4.81	32.69

Figure 3.22: Shannon, Simpson and Chao1 alpha diversity indices across each sample group
Tables showing significant differences between groups as calculated by Wilcoxon test are set alongside the relevant index.

The tables indicate statistical differences between sample pairs as determined by the particular index. All comparisons shown are those for which there was a significant difference in alpha diversity (microbial richness) by the index ($p < 0.05$). Differences in alpha diversity were seen between most groups by at least one measure, with the most consistent difference being between BA34-C and SN-C, which was significant as determine by Wilcoxon test for each index.,

3.4.4 Beta diversity

Beta diversity compares differences in microbial composition between collections of samples (compared to alpha diversity that compares within a single sample/group). There are several indices used to analyse beta diversity. the visuals below use unweighted UniFrac (based on phylogenetic sequence distances), and weighted UniFrac (weighted by relative abundances) indices.

Figure 3.23 shows Weighted UniFrac distances plotted on a beta-diversity heatmap.

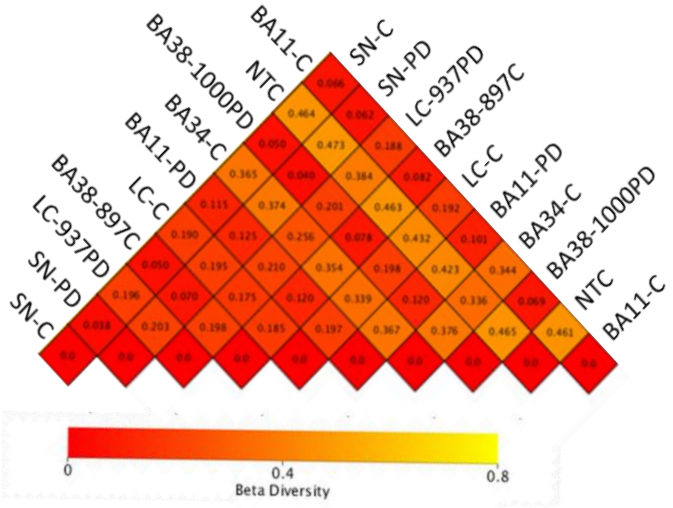

Figure 3.23 : Beta diversity heatmap based on Weighted Unifrac distances
Each grid value represents the dissimilarity coefficient between a pair of samples. The darker the colour, the more similar the pairs of samples are in microbial composition.

It can be seen from the lighter coloured grids, that NTC and BA34-C are less similar to the other groups.

A comparison of brain group beta diversity is shown in Figure 3.24, where box plots of groups containing a minimum of three samples are presented. The differences between these groups were analysed by Wilcoxon test (Table 3.6) to determine whether the differences observed were significant.

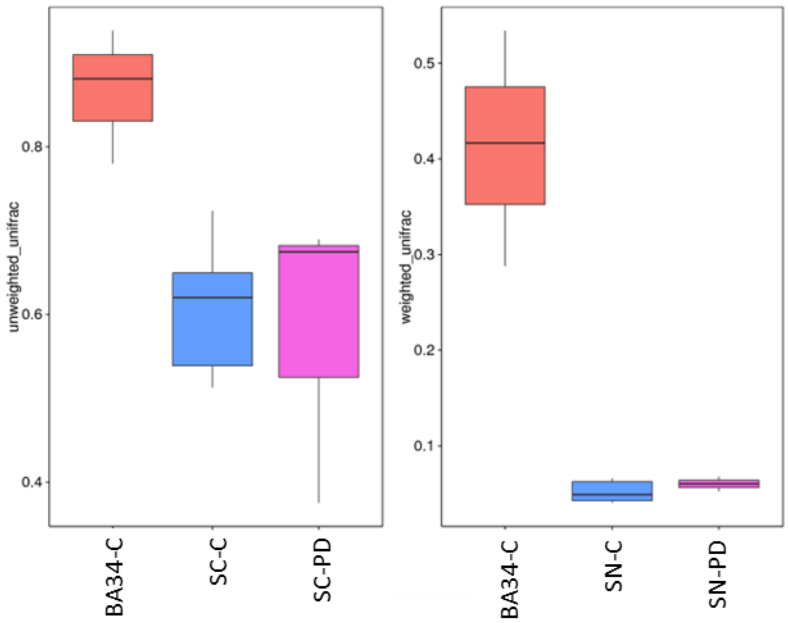

Figure 3.24: Unweighted and Weighted beta diversity box plots
Box plots compare the three sample groups that contain three samples or more.

Table 3.6: Wilcoxon test of beta diversity differences between 3 sample groups

Comparison	Unifrac (p-value)	
	Unweighted	Weighted
BA34-C v SN-C	0.001	<0.001
SN-C v SN-PD	0.813	0.676
BA34-C v SN-PD	0.006	<0.001

The box plots in Figure 3.24 visually show differences in Weighted and UnWeighted beta diversity between BA34-C, SN-C and SN-PD sample groups. The bacterial composition of BA34-C appears different to that of the other two groups a finding that was confirmed by the Wilcoxon test (Table 3.6).

Figure 3.25 shows beta diversity depicted by a Non-Metric Multi-Dimensional Scaling (NMDS) analysis graph, which uses OTUs to rank microbial differences between individual samples. NMDS plots are an ordination technique used for non-linear biological data sets such as this one.

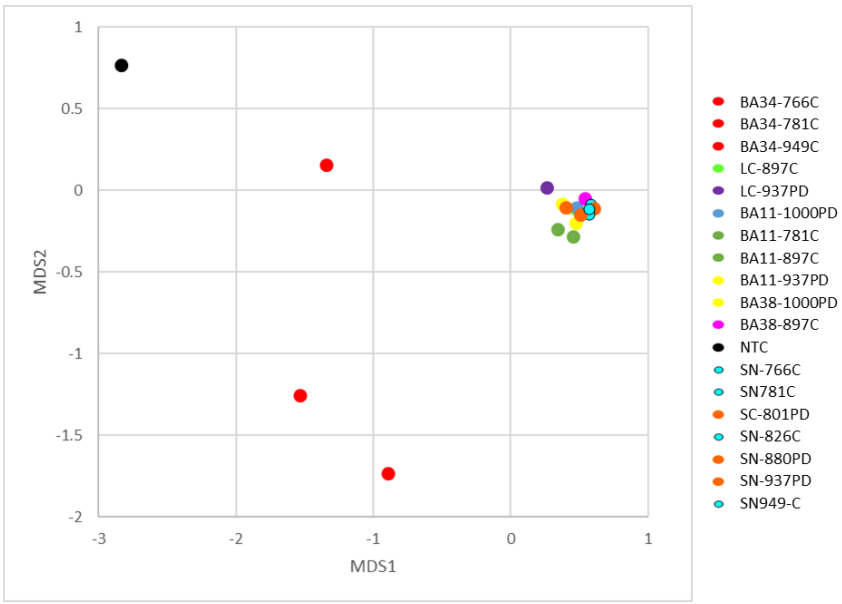

Figure 3.25: NMDS plot of dissimilarity between samples

The NMDS plot shows the BA34-C samples separate to other brain samples that have clustered together, indicating the microbial composition of the BA34-C samples is different to that of the other sample groups (as also shown by the other diversity measures above). The No Template Control (NTC) is plotted further away from all samples indicating, along with other analyses shown here, that it has a distinct composition suggesting it is likely that there has been no contamination.

Principal coordinate analysis (PCoA) is another beta diversity dissimilarity matrix that tries to order samples/data along axes of principal coordinates to explain variance using phylogenetic distances. Figure 3.26 shows the Weighted UniFrac PCoA, which was analysed with samples from another study.

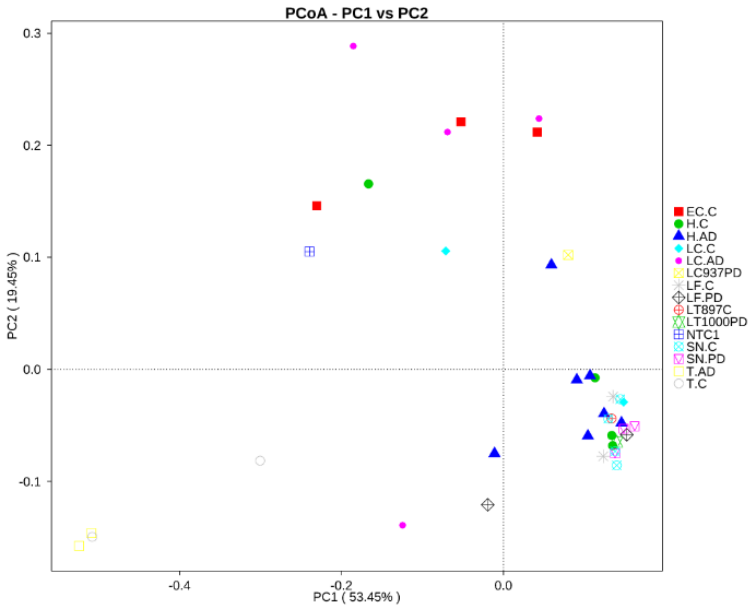

Figure 3.26: Principal Coordinate Analysis (PCoA) showing dissimilarity between samples
LF relates to BA11 brain area, LT relates to BA38, and EC relates to BA34. H-C, H-AD, LC-AD, T-C and T-AD relate to another study.

As in the NMDS plot, the PCoA plot depicts BA34-C (EC-C) separate to other samples from this study, indicating that they are dissimilar or their composition is at a greater phylogenetic distance to the that of the other brain samples.

3.4.5 Species variance statistics

Novogene conducted species variance statistics on brain groups that comprised at least 3 samples, to find taxa that were represented differently in these groups. T-tests demonstrated that there were taxa that differed in abundance between PD and C groups of the SN brain area. This is the brain area most affected by neurodegeneration in PD. No species variation was seen between the other pairs of groups that could be analysed. T-tests that demonstrated significance at each taxonomic rank are shown in Figure 3.27.

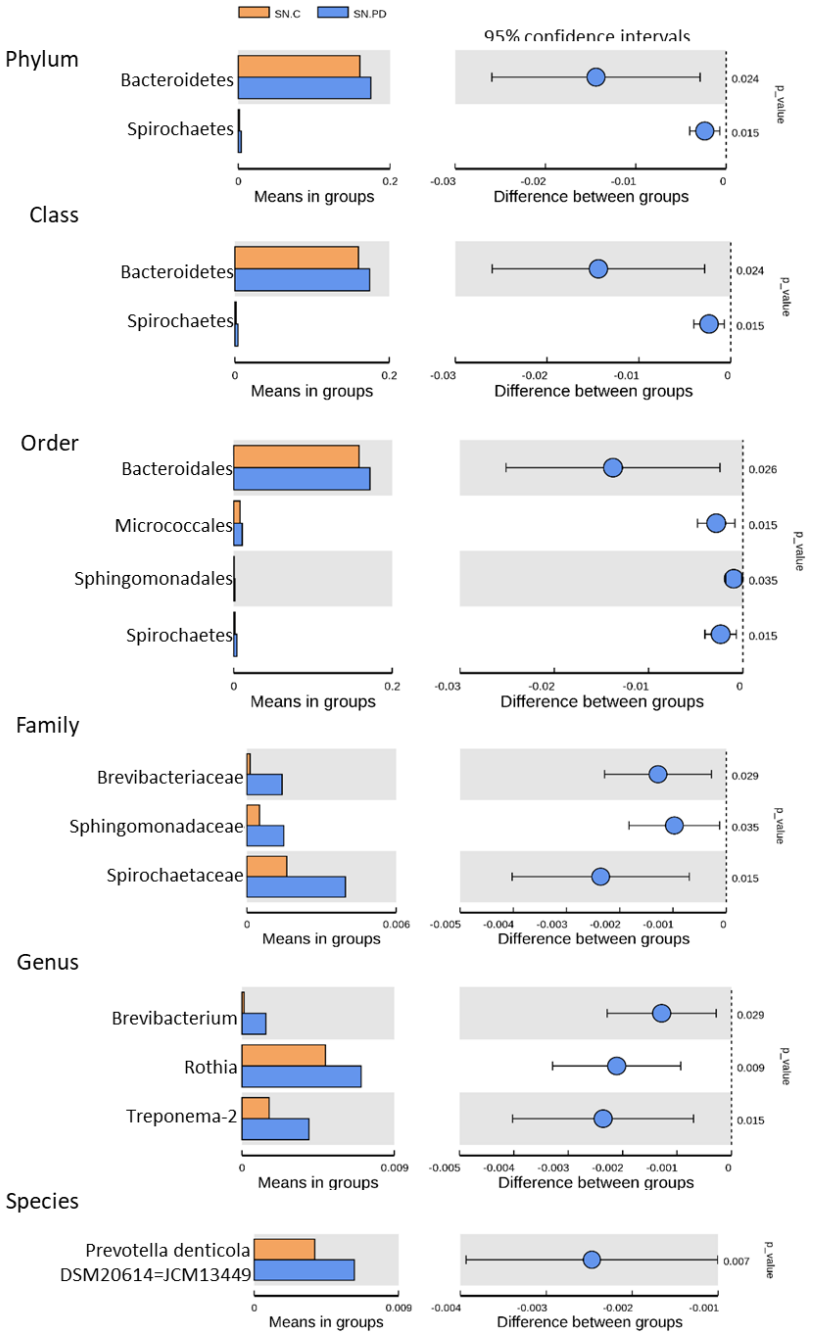

Figure 3.27: T-tests showing differences in taxa between PD and C in SN brain area, with p value

At the species level, *Prevotella denticola,* a periodontal pathogen, was found to be the most differentially represented species between control and PD SN samples, with it being represented significantly more in PD samples ($p < 0.01$). This difference was also reflected at higher orders of taxa (p_Bacteroidetes, C_Bacteriodetes, O_Bacteroidales). At the genus level, significant differences in the presence of *Brevibacterium* and *Rothia* (p_Actinobacteria), and *Treponema-2* (p_Spirochaetes) were also identified, with more in PD than control samples of the SN.

Linear discriminant analysis (LDA) Effect size (LEfSE) analysis was undertaken to identify species that were characteristic of brain groups and could potentially distinguish between them.

LEfSe identified a potential bacterial signature for only one pair of groups, SN-C as compared to SN-PD (Figure 3.28).

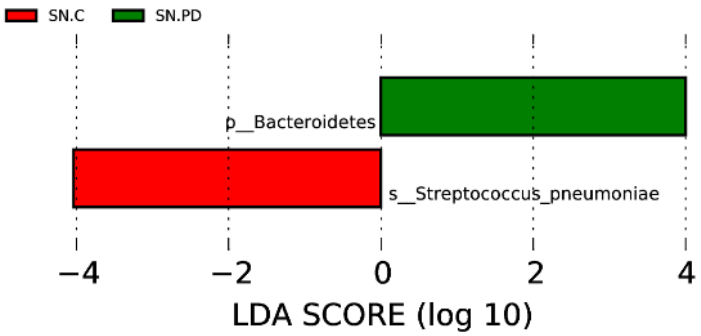

Figure 3.28: LefSe analysis showing differences between SN-C and SN-PD

The bacterial taxa that characterised SN-PD were p_Bacteroidetes, of which *P. denticola* is a species, while SN-C were characterised by *S. pneumoniae*.

There were no differences between any groups as analysed by Metastat analysis, which identifies taxa with significant intra-group variation.

3.5 α-synuclein levels and bacterial load

Total insoluble (aggregate) α-synuclein levels are tabulated alongside the 16S copies/100 ng template for their corresponding brain sample. There were three samples where it was not possible to obtain data for 16S copies for this comparison (Table 3.7).

Table 3.7: Total insoluble α-synuclein and bacterial concentrations by brain area

Brain area (sample #)	Total α-synuclein (µg)	qPCR (16S/100 ng)
BA34		
31- PD	9.49	5031.54
82- PD	15.35	
181- PD	35.76	263.71
313- PD	15.90	505.83
766- C	1.98	
785- C	5.46	712.41
801- PD	3.93	6189.37
805- PD	17.90	459.79
880- PD	9.58	411.97
937- PD	3.66	549.62
938- PD	3.90	
971- C	4.33	946.57
1000- PD	2.62	3190.74
BA11		
781- C	4.98	1980.93
897- C	7.34	853.01
938- PD	3.74	1029.12
BS		
937- PD	1.71	9467.44
LC		
938- PD	14.07	2900.61
SN		
1000- PD	2.02	1364.26
938- PD	42.79	1697.71
BA38		
1000- PD	17.55	1236.93
938- PD	7.02	8269.87
937- PD	29.39	4087.22

Total insoluble α-synuclein (µg) were calculated for each sample from the α-synuclein concentration and the volume (ml) it was suspended in. A comparison of levels of insoluble α-synuclein in C and PD samples is shown in Figure 3.29.

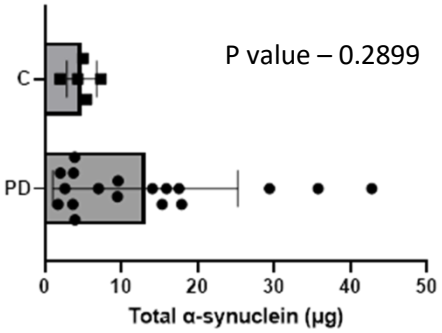

Figure 3.29: Bar chart with total insoluble α-synuclein in diseased or control states
Analysed by Mann Whitney U test.

Figure 3.29 above clearly shows that none of the C samples contained high levels of α-synuclein. By contrast, there was a wide range of α-synuclein levels in PD tissue samples, with low levels similar to that of C seen in around half of the samples. The other samples showed levels that were 2 – 10 times as high. However, there was no significance between the two sample groups.

Figure 3.30 below shows all samples for which both total α-synuclein and 16S copies/100 ng template were available and compared to reveal if there was any correlation.

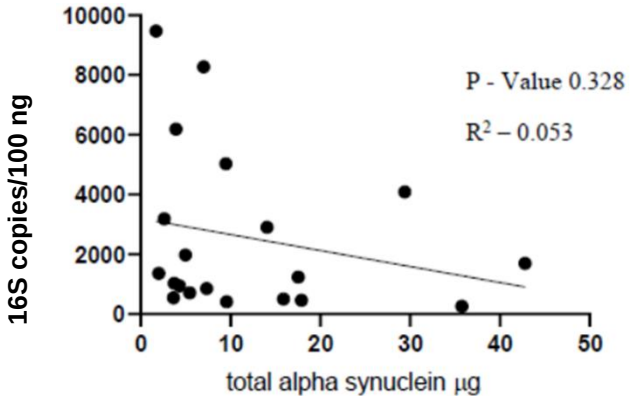

Figure 3.30: Total α-synuclein plotted against 16S copies/100 ng brain template (all PD and C samples)

Figure 3.30 shows that there was no correlation between levels of total α-synuclein and the number of 16S copies. The p value depicts no significance.

To determine if there was any correlation between number of 16S copies/100 ng brain template and α-synuclein levels in PD or C samples when these were considered separately, each was plotted against α-synuclein as shown in Figure 3.31.

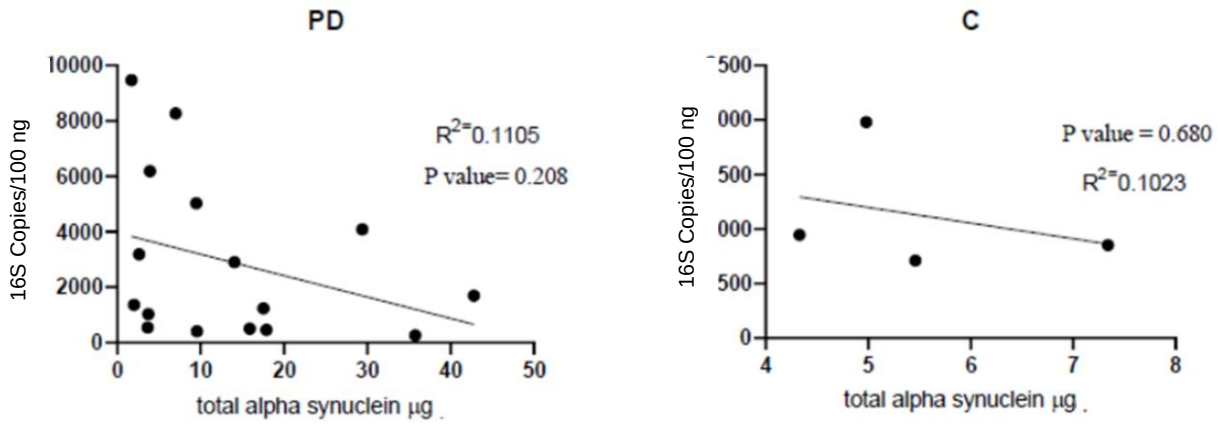

Figure 3.31: Total α-synuclein plotted against 16S copies/100 ng brain template in PD and C

There was a negative trend i.e., the higher the number of 16S copies/100 ng template, the lower the total α-synuclein level. However, this was not significant either when samples were considered together or split by health and disease.

Chapter 4 Discussion

The primary aim of this study was to establish if there were any differences in microbial levels or composition in PD as compared to C brain tissue, both overall and by brain area. To observe a noticeable and statistical difference indicating either higher levels of bacteria in PD brain or differences in relative abundance of taxa in PD as compared to C samples, may suggest a microbial origin to PD. Differences in patterns between areas might support Braak staging (Braak *et al.*, 2004). Correlation of bacterial load with α-synuclein levels would augment the hypothesis of microbial involvement in PD further.

Several experiments were conducted to investigate this hypothesis, with NGS and subsequent analyses undertaken by external parties to compare bacterial composition using various indices and diversity analyses as described in Chapter 3.

4.1 Bacterial levels found in brain tissue

Overall, bacterial load as indicated by the number of copies of 16S/100 ng brain template determined by qPCR was higher in samples of PD than C brain collectively, however this was not statistically significant with a t-test. In addition, the mean 16S copies in the LC was four times greater for PD than control, was three times greater than control in the SN and 2.5 times greater than control in the BS regions. Although not statistically significant, the finding that levels of 16S in BS, LC, and SN, which are areas involved in early PD (Braak stages 1-3), were higher than controls suggests a possible role in disease (Braak *et al.*, 2003). This is not the first study to show bacteria present in diseased brain tissue (Branton *et al.*, 2013; Pisa *et al.*, 2017, 2020). However, very few have attempted to quantify and analyse the abundance of a wide range of bacteria (rather than specific species) in post-mortem brain tissue in disease (Emery *et al.*, 2017; Pisa *et al.*, 2020). Similar to the present study, Emery *et al* (2017) found higher levels of bacterial sequencing reads in diseased (AD) brain tissue than in controls. Hardly any studies have examined bacterial levels either overall or as individual species in PD brain. However, one study by Pisa and colleagues (Pisa *et al.*, 2020) has reported on polymicrobial infections in PD-CNS. In this study the authors looked at specific CNS areas in PD brain samples, using immunohistochemistry and also NGS against fungal and bacterial strains. A broad range of bacteria were identified, mostly from the phyla Actinobacteria and Proteobacteria (Pisa *et al.*, 2020), supporting the theory of polymicrobial infections in PD. The Pisa study supports the findings in this research study of a possible microbial involvement in PD.

The qPCR study described here was designed to assess microbial load in specific regions of the brain affected by PD and described in Braak staging, using universal primers to detect a wide range of bacteria. The olfactory bulb, which is impacted by Lewy nitrites in Braak stage 1, is located in both hemispheres at the base of the forebrain, and has orders of neurons of which the second-order neurons project into the mesial temporal lobe, which includes the entorhinal cortex or BA34 (Lie *et al.*, 2021). In the present study in the BA34 region, PD brain was found to have almost twice as high levels of 16S/100 ng template than C brain, which could be an indicator of the microbial involvement described by Braak and colleagues in their dual-hit hypothesis, suggesting the oral-nasal route as one potential routes of entry by a pathogen (Hawkes *et al.*, 2007). In addition, copies of 16S/100 ng template in the BS (Braak stage 2), which includes the vagus nerve region, were twice as high in PD as compared to C brain, potentially indicating the gut as another route of bacterial entry (Dong *et al.*, 2022). Levels of 16S copies were similarly higher in PD as compared to C brain in both the Braak stage 3 regions LC and SN (Braak *et al.*, 2003). By contrast, in BA11, which Braak staging indicates becomes involved a little later in PD progression, the number of copies of 16S were higher in C as compared to PD brain. More work would need to be done, for example a bigger sample size, to determine if this area is an exception to the pattern, and if the pattern is truly consistent, as none of the differences in 16S levels reached significance.

The spread of α-synuclein pathology (LB) and neurodegeneration proposed by Braak and colleagues describes it moving from a caudal to rostral pattern, with the higher cortex areas affected last (Braak *et al.*, 2003). If α-synuclein were a response to infection, one might expect to find early-stage midbrain areas such as BS and LC with higher levels of bacteria than the cortex areas. However, this would also depend on the age of the patient at PD-onset and age at death. The longer the patient was alive with PD, the more likely it would be that you would see bacteria and increased LB in the midbrain and in the cortex. Consideration would also have to be given to familial PD diagnosis, as the progress of symptoms and dementia is faster than in sporadic PD (Guo *et al.*, 2022). It has also been proposed that there are distinct pathways of cellular dysfunction between familial PD and sporadic PD that can affect α-synuclein toxicity (Wong and Krainc, 2017). Further work would involve use of donor medical records to consider age of PD on-set and diagnoses, and any genetic factors, as these would not be stated in brain bank records. If possible, donors would be selected for whom there were a complete set of brain areas, allowing a comparison of bacterial loads without donor-to-donor confounders.

This study found control brains also had bacteria present, albeit at lower levels (with exception of BA11). This could indicate some early bacterial involvement without the patient exhibiting any

symptoms before death, as some C samples had Braak tangles identified post-mortem (such as donor 766), or it could indicate the existence of a brain microbiome. The brain has long been thought to be a privileged sterile site, with onset of disease such as brain abscess only arising if specific microbes breach the brain's physical and immunological barriers (Link, 2021). However, there have been some studies suggesting the presence of a brain microbiome (Branton *et al.*, 2013), which would not be unsurprising considering new evidence of microbiomes in other sites once thought to be sterile such as blood (Castillo *et al.*, 2019) and the lungs (Miriam and William, 2017).

All control samples were found to have different levels of 16S, which could also suggest a brain microbiome in individuals without overt disease. As the BBB is known to breakdown with age, this could explain differing levels in the different regions. However, as Link points out in his paper, it would be beneficial to study brain areas from donors across all ages to investigate the brain microbiome hypothesis further (Link, 2021).

4.2 α-synuclein and bacterial load

Total insoluble α-synuclein was determined in the brain samples that were available; 18 PD and 5 C. Most samples were from the BA34 brain region, with only 1 PD sample available for BS and LC, and 2 PD samples for SN. In addition, there were samples from 5 brain areas for only one PD donor (938), and from 3 areas for only a further 2 PD donors, limiting the ability to decipher patterns of α-synuclein spread that followed Braak's staging in individual donors. For donor 938, 2 midbrain samples (SN and LC) had high total α-synuclein levels, with lower levels detected in brain areas BA38, BA11, and BA34. This follows the α-synuclein trajectory, however, at post-mortem the patient was diagnosed at Braak LB stage 4. This would involve the temporal mesocortex (the entorhinal region and prefrontal cortex), and levels of α-synuclein in BA34 were lower than would be expected from this diagnosis. This patient was also found to have had a microinfarct (small stroke) in the temporal neocortex at post-mortem. It is known that ischemic stroke creates a disruption in homeostasis in the cell, leading to apoptosis and resulting in degradation and cross-linking of proteins (Radak *et al.*, 2017). This apoptotic process has been suggested to be implicated in neurodegenerative diseases (Ong *et al.*, 2017). This may explain low levels of α-synuclein in BA38 region due to cell degradation. However, it is unknown whether the infarct occurred in or close to the BA38 area.

Interestingly, all 5 C brain samples had low levels of insoluble α-synuclein, which is consistent with no diagnosis of PD when alive. Three C samples were diagnosed with Braak tangle stage 2 post-mortem, of which 2 had no plaques and 1 had sparse neuritic plaques. One donor was diagnosed

with Braak tangle stage 1 post-mortem, and the fifth (donor 897) had argyrophilic grain disease, which is common in the elderly and is a sporadic neurodegenerative disease, with hyperphosphorylated tau the major component of the lesions (Rodriguez and Grinberg, 2015). The fact that these C donors had evidence of neurofibrillary tangles or plaques post-mortem may explain the low levels of insoluble α-synuclein detected in their brain tissue, as it is sometimes found with other proteins in LB and LN such as tau or ubiquitin (Moussaud *et al.*, 2014). The presence of some insoluble α-synuclein may be more common than thought in elderly people. Indeed it has been shown that aggregates of α-synuclein are found post mortem in 8-15% of patients who do not exhibit any motor symptoms, and could represent normal ageing or the prodromal phase of PD before the patient died (Kasen *et al.*, 2022).

The site of origin of LB pathology has been debated as an alternative to Braak staging, as not all patients follow the Braak staging scheme consistently. This model suggests two different patterns of propagation of α-synuclein: a caudo-rostral (body) and an amygdala (brain) centred pattern (Borghammer *et al.*, 2021). This 'body-first' or the 'brain-first' model suggests that in some individuals with PD, LB pathology starts in the body, such as in the ENS, spreading to the brainstem with a relatively faster disease progression; in others it originates in the CNS (amygdala), before spreading to the brain stem and then to the peripheral autonomic nervous system with an overall slower progression (Borghammer *et al.*, 2021). The presence of these two potential pathways could help explain the differences in levels of insoluble α-synuclein found across the different brain areas in this study.

As α-synuclein has been found to have AMP properties like Aβ (Park et al, 2016), demonstrating a correlation between total α-synuclein levels and bacterial levels would cement this hypothesis further. In studies of other diseases such as West Nile Virus, which can cause encephalitis, it has been found that in areas of infection there were increased levels of native α-synuclein in brain grey matter (Beatman *et al.*, 2016). Similarly, Stolzenberg and colleagues found monomeric and oligomeric α-synuclein levels positively correlated with the degree of inflammation in endoscopic biopsies from children with norovirus infection (Stolzenberg *et al.*, 2017). In addition, they showed that both forms of α-synuclein had chemoattractant activity, suggesting that α-synuclein played a part in inflammation and that GI infection could be implicated in PD (Stolzenberg *et al.*, 2017).

By contrast in this PD study no significant correlation between α-synuclein levels and copies of 16S/100 ng template was found when all brain samples were plotted together. However, there were far more PD samples than controls, and for some samples with α-synuclein data there was no corresponding bacterial qPCR, making it difficult to draw definitive conclusions. Analysis of more PC

and C brain samples for an association between insoluble α-synuclein and bacterial levels would be required, and if one of the roles of native α-synuclein is as an antimicrobial peptide, then it would be prudent to examine the correlation with soluble α-synuclein levels as well in the future.

4.3 Next Generation Sequencing analysis

Samples were sequenced and taxonomy assigned by different means using two companies, Novogene and Eurofins, due to the Covid-19 pandemic.

4.3.1 Potential confounding factors

Data from the first round of sequencing (NGS1) is only referenced here briefly due to the consistently high levels of *E. coli* in all samples, indicative of possible contamination. *E. coli* is ubiquitous in nature, can cross-contaminate and is also a common contaminant in some reagent kits (Salter *et al.*, 2014). Extracting bacteria from low biomass samples can be difficult and since the onset and rapid rise of the use of NGS, the potential for contaminants to cause misleading results has been recognised (Lusk, 2014; Salter *et al.*, 2014). It is important to identify if any contaminants are present so that these can be excluded from overall findings (Glassing *et al.*, 2016). This is usually achieved by comparison with a NTC. However, in NGS1, insufficient PCR product meant that an NTC could not be analysed in the sample set, therefore it could not be compared to confirm if the *E. coli* detected was indeed a contaminant. It should be noted that other research groups have isolated *E. coli* (in particular K99, which has been found to promote formation of amyloid-like plaques in animal models), in AD brain, suggesting a role in AD pathology (Zhan *et al.*, 2017). However, other studies did not detect *E. coli* in AD brain (Pisa *et al.*, 2017), and the consistent dominance of *E. coli* in all samples of the NGS1 dataset strongly suggested it as a contaminant in the present study.

In NGS2, where there was an NTC for comparison, the relative abundance figure that compared the top 20 genera in blood, brain and NTC showed they had different compositions. Finding taxa in the NTC indicated that there was some contamination, however, it is unlikely that this impacted the brain tissue data as in NGS1 where the PCR no brain template control included sterile prostate cancer cells which did not generate sufficient amplicon for NGS. Due to the inhibitory effect of genomic DNA on bacterial PCR amplification, any contaminants amplified in brain tissue are likely to be very low level. As consistency of patterns of abundance is indicative of contamination (Hu *et al.*,

2021), the differences in composition observed provided confidence that the bacteria identified in the second sequencing analyses were not contaminants. In a parallel study of the same brain samples undertaken in our laboratory, blood content was analysed using a haemoglobin assay to indicate to what extent the bacteria found could have come from the circulation. It was shown that brain samples had only around 3.7% blood content. Together with the NGS2 analysis, which indicated that while around half of genera found were seen in both blood and brain groups, the relative abundance patterns were starkly different this data suggests that a large proportion of the bacteria identified in brain had not come from the blood.

Another potential source of contamination is that which can occur in the time between death and post-mortem, with the longer the PMD, the higher the chance of post-mortem contamination. In the present study, analysis of PMD against levels of 16S/100 ng brain template showed no correlation between them, suggesting there was no association between PMD and contamination in these samples. A similar lack of correlation between PMD and 16S rRNA gene copies has been found in a previous study (Bedarf *et al.*, 2021), suggesting that while this should always be considered, samples with a long PMD should not be excluded on this basis without confirmation of likely contamination.

Based on the evidence above, the second sequencing result (NGS2) was unlikely to contain contamination, and the source of a large proportion of the bacteria detected was likely derived from the brain tissue. One further consideration when analysing the data, however, is that it is unknown whether the bacteria found in post-mortem brain tissue in the present study were viable. Using a different DNA extraction method such as the MolYsis® system, which has been shown to isolate intact bacterial cells from oral tissue samples and blood (Horz *et al.*, 2008; Emery *et al.*, 2021), alongside NGS, would assist isolating viable bacteria. This would be an important consideration because human tissues undergo metabolic and microbiome changes after death, and certain bacteria have been found to be increased depending on cause of death and age of patient (Lutz *et al.*, 2020). It is also common for brain tissue from patients with neurodegenerative disease to be fixed and frozen promptly for autopsy, whilst control tissues are processed more slowly as no cause of death is required. This results in a clear time difference in PMD between disease and control tissues, which could impact on studies such as this present one (Blair *et al.*, 2016). However, in the present study, the comparison of samples with a PMD of below and above 40 hours showed no statistical difference in 16S copies/100 ng. However, to allow consideration for changes in bacterial composition due to different decomposition rates, MolYsis® could be used for future extractions. If abundance profiles altered as PMD increased, then tissues above a certain PMD, as determined by the degree of the changes, could be eliminated from the study. There remain other confounding

factors and limitations when considering PMD, such as temperature and pH of the brain, and variations in its collection and storage (Blair *et al.*, 2016), which can impact on microbiome abundance. However, this study could not examine the effects of all of these. The effect of PMD continues to be an important element of investigation in microbiome studies.

4.3.2 Relative abundance of taxa

Comparing the Eurofins and Novogene abundance data, the relative abundance pattern of genera for the second sequencing analysis (NGS2) was similar by both methods of assigning taxa. There were 8 genera in the average top 10 taxa across the groups that were shared across both analyses, these were: *Streptococcus, Haemophilus, Cutibacterium* (a BLASTn search on Eurofins 'Kingdom_Bacteria' identified *Cutibacterium* as OTU1, the main component of this assignment), *Porphyromonas, Fusobacterium, Prevotella*, *Staphylococcus,* and *Neisseria. Campylobacter* and *Corynebacterium* in the Eurofins top 10 were in the Novogene top 20, pushed down the order in part by the Novogene sub-division of *Prevotella* into different genera, and in part by the 'others' assignment by Novogene. However, these genera were of similar relative abundance overall by both methods. *Pseudomonas* and *Nevskia* in the Novogene top 10 were in the Eurofins top 25. Some OTUs were only assigned at phylum level as Proteobacteria by Eurofins. These are likely *Pseudomonas* (see BA11-1000PD), while the lower rank of *Nevskia* is likely due to more taxa being identified by Eurofins, where 97% clustering was not used. However, these two genera also had similar relative abundance profiles overall by both methods. The similarity of the relative abundance profiles suggests that sequence processing and taxonomic assignment was robust.

In the top 10 genera of both analyses, a high proportion of the taxa were those commonly found in the oral cavity in health and disease: *Streptococcus, Porphyromonas, Prevotella, Neisseria, Fusobacterium, Corynebacterium* and *Haemophilus*. The list of oral genera also included *Lactobacillus, Aggregatibacter, Rothia,* and *Actinomyces* when the top 20 taxa were reviewed (Brown *et al.*, 2019). The oral microbiome consists of bacteria, fungi, archaea and protozoa; the bacterial phyla dominating the oral cavity being Firmicutes, Proteobacteria, Actinobacteria, Spirochaetes, and Fusobacteria (Wade, 2013). Using a 16S rRNA gene sequencing approach, the web-accessible Human Oral Microbiome Database (HOMD) was created by Dewhirst and colleagues (2010), and it is now known that there are around 700 bacterial species present in the oral cavity. However, most people only have between 100 and 200 species, with diversity seen between individuals (Dewhirst *et al.*, 2010; Brown *et al.*, 2019). Although the genera identified in the top 10

relative abundance profiles here are not exclusively those that are pathogenic, all have the potential to cause inflammation and are thus capable of causing neurodegeneration (Sharon *et al.*, 2016).

There have been several studies that have investigated whether there are any obvious differences in abundance of oral bacteria taxa in oral samples obtained from PD patients as compared to controls. Pereira and colleagues used Illumina MiSeq sequencing and found an increase in *Prevotella, Lactobacillaceae,* and *Coriobacteriaceae*, and a decrease in *Rothia, Actinomyces, Haemophilus, Neisseria,* and *Corynebacterium* in oral swabs from patients with PD as compared to those from controls (Pereira *et al.*, 2017). In another study by Jo and colleagues that used shotgun sequencing of 16S rRNA, these findings were supported as consistently higher levels of oral *Lactobacillus* were found in oral swabs obtained from PD patients as compared to controls (Jo *et al.*, 2022). A study of saliva samples by Mihaila and colleagues also found higher abundance of *Lactobacillus* and *Bifidobacterium* in the saliva of PD patients as compared to controls (Mihaila *et al.*, 2018). Similarly, in an older study using culture methods, lactobacilli levels were higher in plaque samples from PD groups than controls (Kennedy *et al.*, 1994). PD patients have also been found to have higher numbers of oral Gram-negative bacteria (commonly found in oral disease) compared with controls, which was suggested to be due to the impairment of swallowing (Gosney *et al.*, 2003). However, this study was performed using culturing techniques rather than sequencing, so non-culturable bacteria were not captured. When interpreting these studies, it must be remembered that the decline in motor skills in PD patients mean that they are often unable to clean their teeth and gums well, and so any increase in the prevalence of periodontal pathogens may be a result of poor oral hygiene as a result of PD symptoms (Nakayama *et al.*, 2004).

Interestingly, in the present study, six of the top 10 genera (both analyses) were also identified in the top 10 genera in both PD and control oral swabs by Pereira *et al.* (Pereira *et al.*, 2017), and the top 5 phyla matched those identified by Jo *et al* (Jo *et al.*, 2022) in control and PD oral swabs. Although there are differences in the relative abundances between the studies, this indicates that the most common bacteria in the oral cavity of older individuals (average age 65) (Pereira *et al.*, 2017; Jo *et al.*, 2022) are those oral microbes that were found with the greatest abundance in the brain in the study described here. In addition, *Lactobacillus* was among the top 20 genera present across Novogene and Eurofins analysis. However, no differences in *Lactobacillus* levels between PD and control for any brain area were seen.

The mechanisms by which commensals and pathogens can translocate to the brain and then move to colonise other areas remain poorly understood. However, there have been *in vitro* and mouse studies that have attempted to study bacterial entry into the CNS. In a mouse study, Audshasai and

colleagues found *S. pneumoniae* applied to the nose was recovered from dissected brain tissue within 72 hours, providing evidence of horizontal transmission from the nose through the cribriform plate, invading the dura mata (Audshasai *et al.*, 2022). In another study, oral application of *P. gingivalis* resulted in neurodegeneration and amyloid plaque formation in the brains of wild type mice (Ilievski *et al.*, 2018).

Another potential route of entry into the CNS is via transient bacteraemia. In the oral cavity, gingival tissue is highly vascularised. Vessels become dilated in response to plaque bacteria, and it has been reported that oral bacteria, particularly those found in sub-gingival plaque, can gain access to the blood stream (Parahitiyawa *et al.*, 2009). In addition, studies have investigated whether dental treatment, including periodontal procedures, can result in transient bacteraemia of periodontal pathogens (Li *et al.*, 1999; Horliana *et al.*, 2014; Emery *et al.*, 2021). A systematic review confirmed bacteraemia in 50% of patients undergoing periodontal treatment, but data was insufficient to determine its extent or duration (Horliana *et al.*, 2014). Recently, NGS analyses of bacteria found in the blood of patients with periodontal disease and age-matched controls showed that 52% of species identified were those found on oral surfaces, and were commensal and oral species of the subgingival biofilm (Emery *et al.*, 2021). In this NGS study of whole blood from periodontitis patients and controls, Firmicutes, consisting of *S. mitis* and *S. epidermidis,* was the predominant oral taxon in both periodontitis and control blood. In a separate study that investigated if the bacterial composition in blood was different in PD patients and controls, 29 taxa with differential abundances between the two groups were found with LeFSe analysis, indicating genera *Myroides, Isoptericola, Microbacterium, Cloacibacterium* and *Enhydrobacter* were at higher levels in the PD group (Qian *et al.*, 2018). Both NGS studies used primers for the V3-V4 region on the 16S rRNA gene. However, Qian's group also used genus specific primers to study genera with differential abundance by NGS further, and found correlation between higher levels of *Cloacibacterium* and *Isoptericola* and PD disease duration and severity (Qian *et al.*, 2018; Emery *et al.*, 2021). Differences in the bacterial content of blood between the two studies likely reflects differences in DNA extraction. Qian *et al* (Qian *et al.*, 2018) extracted DNA from leukocytes using a standard phenol/chloroform method, while Emery *et al.,* (Emery *et al.*, 2021) extracted DNA from whole blood using MolYsis®. Comparing the Emery blood study with the present one shows that *Streptococcus* were quite high in abundance across both blood and brain tissue. However, the abundance of taxa were largely different, suggesting that the majority of taxa identified in the brain did not come from blood (Emery *et al.*, 2021).

In the only other similar PD brain study, Pisa and colleagues looked at CNS regions. Their sequencing analysis identified differences in bacterial composition in different areas and showed that although the genera *Acinetobacter* was present in all PD regions investigated, *Streptococcus* was more abundant in the motor cortex (Pisa *et al.*, 2020). At phylum level, Proteobacteria was the most abundant in the medulla region and Actinobacteria was the most abundant in the midbrain and cortex (Pisa *et al.*, 2020). In addition, PCA analysis clearly demonstrated a separation between PD CNS bacterial taxa and controls. However, the paper does not state which bacteria were found in the controls. Similar to Pisa *et al.* (Pisa *et al.*, 2020), in the present study, Proteobacteria was the most abundant phylum, with the other abundant phyla being Actinobacteria, Firmicutes and Bacteroidetes. However, no differences between C and PD were observed. Bacterial species detected by the same group using nested PCR, identified *C. acnes* and oral bacteria *R. dentocariosa* and *S. oralis* in PD samples (Pisa *et al.*, 2020).This also supports the present study findings, in which *C. acnes,* oral bacteria and the genus *Streptococcus* were abundant in most groups. Further, *C. acnes* has previously been found to be elevated in AD tissue (Emery *et al.*, 2017).

The similarities between the findings across these two PD studies using NGS to look at bacterial load in low biomass samples corroborates the robustness of the present study and supports the findings in similar AD brain studies, that microbial presence in brains exists (Emery *et al.*, 2017; Pisa *et al.*, 2017, 2020). Whilst this present study used only the V3-V4 hypervariable region of the 16S rRNA gene for amplification, Pisa and colleagues additionally used the interspacer region between the 16S and 23S genes when undertaking their nested PCR, and also looked for the presence of fungi, finding evidence of polymicrobial infections in PD brain tissue. Both studies examined differences in microbial profiles between regions in midbrain areas, with Pisa and colleagues also investigating the motor cortex (Pisa *et al.*, 2020). Although there are some slight differences in the approaches of the studies, there are similarities with bacteria identified and the demonstration of differences in abundance between brain areas and/or between disease and control, which strengthens the theory of microbial involvement in PD.

4.3.3 Differences between the BA34-C and other brain regions

In the present study, noticeably by both analyses (Novogene and Eurofins), the BA34 control group showed different relative abundance composition compared to other groups. In particular, there were fewer oral genera in this region, although oral bacteria still made up nearly a third of the content. Unfortunately, as the NGS had to be repeated, there were no BA34-PD areas for direct

comparison of taxa abundance either between BA34-C and BA34-PD, or BA34-PD and other groups. BA34 acts as an interface between the neocortex and hippocampus, and is impacted by LP in PD in stages 3-4 (Braak *et al.*, 2003; Dickson, 2018). It would therefore be important to investigate this region in PD in further studies, as any bacterial composition in BA34-PD might be hypothesised to be different to midbrain areas. In addition to the BA34-C group having a different profile to the other groups, the relative abundance profiles of the samples in the groups were also diverse. The predominant bacteria, for example, at phylum level in BA34-766C was Proteobacteria in Eurofins and Acinetobacter at genus level in Novogene. There were considerable differences between the two analyses, however *Cutibacterium* is the only genus to be consistently in the top three with abundance over 10% in both analyses. *Cutibacterium* was also in top three genera of BA34-781C and BA34-949C. All three donors had Braak tangle stage II at autopsy but different causes of death: acute cardiac failure (766), acute renal failure and myeloma (781), and non-small cell lung cancer (949). They all also had a similar PMD of 34.25, 24, and 31.25 hours respectively, were male, with one being of a relatively younger age of 69 years old (949). It is difficult to suggest why there were marked differences in the relative abundance profiles of the samples taken from this area, but it could perhaps be due to cause of death (Lutz *et al.*, 2020).

BA34-C was also the group that was most frequently different to the other groups by measures of alpha and beta diversity. The richness of microbial diversity within a sample can be analysed using different alpha-diversity indices: Chao1, Shannon, and Simpson were used in this present study and there were statistical differences between the species richness of the NTC and other brain areas across all indices. Differences in microbial richness were also detected between BA34-C and at least one other brain group by all indices used. Most differences in richness between groups were detected by Simpson calculation, with most control brain regions different from each other, suggesting differences between regions that were not detected when looking at overall relative abundance of taxa. The differences between the indices result from the use of different equations for calculating each index. The Shannon index calculates richness and evenness in a sample equally, whilst the Simpson calculation leans more towards evenness. In addition to this, these measures use different units (L Jost, 2006; Wagner *et al.*, 2018). By contrast, Chao1 takes into account richness but also emphasises the rarer species in the sample, giving them more weight in the calculation (Prehn-Kristensen *et al.*, 2018). By the Shannon and Simpson indices, LC-C had lower alpha diversity than other groups, whilst BA34-C had lower alpha diversity using the Chao1 index. The LC innervates many parts of the brain including the forebrain, basal ganglia, and cerebellum, and is involved in many bodily functions such as sleep regulation and memory consolidation (Madelung *et al.*, 2022).

The BA34 region is also involved in memory and emotion and receives neuronal projections from the LC (Canto *et al.*, 2008). It has been suggested that due to the many neuronal structures connecting LC to other areas, those areas would have a higher probability of developing LP as the LC is one of the areas affected with LP early; however, this is not seen in PD pathology and therefore the spread of LP is suggested to occur through other ways (Surmeier *et al.*, 2017). If there is microbial involvement in PD, the mechanisms of spread to different brain regions may also occur through other ways and not involving connected neuronal structures, possibly explaining why there was lower abundance or diversity in some parts of the brain compared to others.

It was only possible to perform statistical analysis of the beta diversity between groups consisting of three or more samples, which in this study were BA34-C, SN-C, and SN-PD. BA34-C was shown to be much less similar in taxonomic composition (high degree of beta diversity) as compared to the two SN groups, with very little difference between SN-C and SN-PD, meaning there were no statistical differences in the composition of these groups. This difference in diversity of BA34-C as compared to other groups could also be visualised by heatmap and by NMDS plot, in which BA34-C samples were plotted away from samples from other brain areas.

Brodmann area BA34 is part of the entorhinal cortex (BA28) and is involved in memory, emotion, and olfaction, and is connected to the hippocampus. Thus any cell destruction in this area results in anosmia (Strotzer, 2009). The differences in alpha and particularly beta diversity seen between BA34-C and the other groups may reflect the difference in the abundance profile, with BA34-C having a lower abundance of oral bacteria and a relatively high level of *Cutibacterium*. *Cutibacterium* is a commensal of skin and hair follicles and known to be associated with opportunistic infection and is also found in the olfactory tract. Its presence in the BA34 region could support an olfactory route for the entry of bacteria into the brain (Achermann *et al.*, 2014; Leheste *et al.*, 2017). This would support the hypothesis put forward by Braak and colleagues in their dual-hit hypothesis (Hawkes *et al.*, 2007). Alternatively, the data show that the mean levels of 16S copies/100 ng of BA34-C was the fourth highest out of all six brain areas examined, yet it had the lowest alpha diversity using Chao1 index and was different in abundance profile to other brain areas. This might allude to a 'normal' brain microbiome that has a low number of bacterial taxa but has specific species that are balanced and maintained by the host defence mechanisms (Link, 2021).

4.3.4 Significant differences in taxa abundance between SN-PD and SN-C

While there were no overall differences in abundance profiles between C and PD samples, between group species, variance statistics demonstrated a significant difference in bacterial composition between SN-PD and SN-C in the abundance of *Prevotella denticola,* a periodontal pathogen (Brown *et al.*, 2019). Further, the LefSe analysis found Bacteroidetes (of which *P. denticola* is a species) more abundant in SN-PD than SN-C and, interestingly, the SN region had the highest level of oral bacteria (>80%). In support of this finding, *Prevotella* was isolated from AD brains but not controls in the study by Siddiqui and colleagues, however it was not analysed down to species level (Siddiqui *et al.*, 2019). By contrast, *Prevotella* species were not found in any of the brain areas studied by Pisa or Emery and colleagues (Emery *et al.*, 2017; Pisa *et al.*, 2020). *Prevotella* is a genus common to both oral sites and GI tract, with most of oral origin, and has also been found to be implicated in peripheral infections such as those caused by dental extractions (Wu *et al.*, 2014, 2019). There is considerable evidence in the literature of *P. denticola* translocating from the oral cavity to cause infections in the periphery, including causing brain abscesses (Wu *et al.*, 2014; Macin *et al.*, 2017), with the nasal route and middle ear infection common causes of abscesses that can infect the frontal and temporal lobe respectively (Muzumdar *et al.*, 2011). The finding that *P. denticola* was significantly more abundant in SN-PD as compared to SN-C does add some support to the idea that periodontal pathogens may be involved in PD progression. This correlates with the population-based studies that have shown periodontal treatment is associated with a reduced risk of PD (Chen *et al.*, 2017, 2018).

No other major differences between PD and C groups were seen, which may be partially because there were not enough samples to group together for analysis in the second round of sequencing, but also because the samples used for controls were from patients who died from old age, when it is known the BBB becomes more compromised (Link, 2021). Furthermore, several controls had early signs of Braak tangle staging or other infarcts that could have also had some significance on the findings of this study. Alternatively, it could be that there is 'normal' bacterial presence in the brain, with a possible negligible shift in composition in disease.

4.3.5 Study limitations

The study involved extracting bacterial DNA from low biomass samples. Brain tissue was used for optimisation and a repeat sequencing run was done due to contamination of the first round of NGS. Because of this there were significantly fewer samples to send for sequencing in NGS2 and therefore

fewer brain areas with sufficient samples to compare between PD and C. For example, the BA34-C group was substantially different from other groups in bacterial abundance and alpha and beta diversity. However, there were no BA34-PD samples to compare it with, which would have been helpful.

Another limitation to studying brain areas impacted with neurodegeneration is that it is difficult to dissect the areas (such as SNpc, which has very little neuromelanin in PD samples) without potentially involving nearby areas, especially in the midbrain areas and BA34, which is harder to reach without dissecting areas around the required site.

Due to the COVID-19 pandemic, sequencing was undertaken by Eurofins, who use a different taxonomic assignment method and database to Novogene. The sequencing analyses, however, were very similar across the two and therefore should not be a significant limitation. Nevertheless, it is important to highlight different methodologies used in this study.

4.3.6 Conclusion

Parkinson's disease and healthy control post-mortem brain tissue were analysed using qPCR and 16S rRNA NGS for microbial content. Although the number of 16S copies were higher in PD samples than C overall, the difference did not reach statistical significance. There was no correlation between post-mortem delay and 16S levels, even after 40 hours.

An overwhelming majority of genera identified by NGS were derived from the oral cavity and the relative abundance across sample groups was very similar, with four of the top five genera being *Streptococcus, Haemophilus, Fusobacterium,* and *Porphyromonas*. However, no overall differences in relative abundance between brain areas or between C and PD groups were seen at this or higher taxonomic levels. Although there were no overall differences between health and disease, at the species level, *Prevotella denticola*, a periodontal pathogen that has been implicated in peripheral infections, was differentially represented between SN-PD and SN-C, and LefSe analysis also found phylum Bacteroidetes (of which *P. denticola* is a species) to be more abundant in SN-PD than SN-C. More work to confirm if this pathogen plays a role in PD neurodegeneration is needed.

There was one group, BA34-C, which had a different relative abundance pattern to the rest of the brain areas, with also lower alpha diversity and greater separation to other brain areas in beta-diversity analysis. BA34 is part of the entorhinal cortex (EC) and is affected by LP in Braak stages 3-4 (Braak *et al.*, 2004). It is highly innervated by neurons projecting from the LC and also from the basal

forebrain area where the olfactory bulb is located, which could point to a potential nasal route of different microorganisms. *Cutibacterium* was identified as being in the top five taxa across multiple samples, but particularly in LC-C, LC-PD and BA34-C and is a commensal of the olfactory system (Achermann *et al.*, 2014). This finding could suggest a nasal/oral route for bacterial infiltration into the brain, as posited by Braak and colleagues in their dual-hit hypothesis (Hawkes *et al.*, 2007, 2009). In a parallel study, blood from patients presenting to a dental hospital with either periodontitis or healthy gums was analysed using NGS. The relative abundance of taxa in blood was markedly different to that of brain groups, and very little blood content was measured in brain samples using a haemoglobin assay. It can therefore be inferred with some confidence that taxa seen in brain tissue were not derived from blood that may be present in white matter.

The findings in this study adds to the growing evidence of the presence of periodontal pathogens in the AD/PD brain, suggesting an oral/nasal route of entry to the brain. Further work is needed to confirm whether bacterial penetration into brain tissue initiates or exacerbates neurodegeneration with accumulation of α-synuclein as a response to bacterial invasion.

Future work

To develop this study further there are some additions that would be needed.

Discovering duration of disease for each donor, from age of diagnosis to age at death, would be advantageous for incorporating bacterial load assessment. This could determine whether long duration of the disease impacted on bacterial load. This would involve applying to the SWDBB for the donors' medical records and incorporating it into the qPCR analyses.

Furthermore, to determine any significance in bacterial load in brain areas where differences were seen, more samples would be needed to carry out qPCR, for example from SN-PD, BA38, BA34-PD BS, LC, and BA11.

The use of species specific primers in qPCR would also help determine quantity of the genera and species found in NGS analyses that could be of significance, for example *C. acnes* and *P. denticola.* This could help determine if there are clear differences in PD and C samples. Investigating the presence of fungal or viral candidates would also be an important element of assessing polymicrobial infection, and would add more evidence to a microbial theory of PD.

As the NGS analyses identified clear abundance differences in BA34-C, it would be beneficial to compare this with BA34-PD. Therefore, further work would involve having a comparison sample to determine any difference in this area between PD and C.

It was intended to analyse inflammation by inflammatory markers in brain tissue using Nanostring in this study. Unfortunately, due to the pandemic, this could not be undertaken. However, it would be incorporated into any future work so that it could be assessed whether there is a microbial-related inflammatory effect on the progression of PD.

References

Abusleme, L. *et al.* (2021) 'Microbial signatures of health, gingivitis, and periodontitis', *Periodontology 2000*, 86(1), pp. 57–78. Available at: https://doi.org/10.1111/prd.12362.

Achermann, Y. *et al.* (2014) '*Propionibacterium acnes*: From Commensal to opportunistic biofilm-associated implant pathogen', *Clinical Microbiology Reviews*, 27(3), pp. 419–440. Available at: https://doi.org/10.1128/CMR.00092-13.

Adler, C.H. (2005) 'Nonmotor complications in Parkinson's disease', *Movement Disorders*, 20(SUPPL. 11). Available at: https://doi.org/10.1002/mds.20460.

Agirman, G. and Hsiao, E.Y. (2021) 'SnapShot: The microbiota-gut-brain axis', *Cell*, 184(9), pp. 2524-2524.e1. Available at: https://doi.org/10.1016/j.cell.2021.03.022.

Aldridge, G.M. *et al.* (2018) 'Parkinson's disease dementia and dementia with Lewy bodies have similar neuropsychological profiles', *Frontiers in Neurology*, 9(123), pp. 1–8. Available at: https://doi.org/10.3389/fneur.2018.00123.

Alim, M.A. *et al.* (2002) 'Tubulin Seeds a-Synuclein Fibril Formation', *The Journal of Biological Chemistry*, 277(3), pp. 2112–2117. Available at: https://doi.org/10.1074/jbc.M102981200.

Alvarez, C.A. *et al.* (2020) 'Characterization of Polysaccharide A Response Reveals Interferon Responsive Gene Signature and Immunomodulatory Marker Expression', *Frontiers in Immunology*, 11(October), pp. 1–13. Available at: https://doi.org/10.3389/fimmu.2020.556813.

Angly, F.E. *et al.* (2014) 'CopyRighter: a rapid tool for improving the accuracy of microbial community profiles through lineage-specific gene copy number correction', *Microbiome*, 2(11), pp. 1–13.

Anis, E. *et al.* (2022) 'Endocrinology & Metabolism Digesting recent findings: gut alpha-synuclein, microbiome changes in Parkinson's disease', *Trends in Endocrinology & Metabolism*, 33, pp. 147–157. Available at: https://doi.org/10.1016/j.tem.2022.01.003.

Aubin, N. *et al.* (1998) 'Aspirin and Salicylate Protect Against MPTP-Induced Dopamine Depletion in Mice', *Journal of Neurochemistry*, 71, pp. 1635–1642.

Audshasai, T. *et al.* (2022) '*Streptococcus pneumoniae* rapidly translocates from the nasopharynx through the cribriform plate to invade and inflame the dura', *mBio*, 13(4).

Balestrino, R. and Schapira, A.H.V. (2020) 'Parkinson disease', *European Journal of Neurology*, 27, pp.

27–42. Available at: https://doi.org/10.1111/ene.14108.

Barbut, D., Stolzenberg, E. and Zasloff, M. (2019) 'Gastrointestinal Immunity and Alpha-Synuclein', *Journal of Parkinson's Disease*, 9. Available at: https://doi.org/10.3233/JPD-191702.

Barone, P., Erro, R. and Picillo, M. (2017) *Quality of Life and Nonmotor Symptoms in Parkinson ' s Disease*. 1st edn, *Nonmotor Parkinson's: The Hidden Face*. 1st edn. Elsevier Inc. Available at: https://doi.org/10.1016/bs.irn.2017.05.023.

Beach, T.G. and Adler, C.H. (2018) 'Importance of Low Diagnostic Accuracy for Early Parkinson's Disease', *Movement Disorders*, 33(10), pp. 155–1554. Available at: https://doi.org/10.1002/mds.27485.

Beatman, E.L. *et al.* (2016) 'Alpha-Synuclein Expression Restricts RNA Viral Infections in the Brain', *Journal of Virology*, 90(6), pp. 2767–2782. Available at: https://doi.org/10.1128/JVI.02949-15.Editor.

Bedarf, J.R. *et al.* (2021) 'Much ado about nothing? Off-target amplification can lead to false-positive bacterial brain microbiome detection in healthy and Parkinson's disease individuals', *Microbiome*, 9(1), pp. 1–15. Available at: https://doi.org/10.1186/s40168-021-01012-1.

Belshaw, R. and Katzourakis, A. (2005) 'BlastAlign: a program that uses blast to align problematic nucleotide sequences', *Bi*, 21(1), pp. 122–123. Available at: https://doi.org/10.1093/bioinformatics/bth459.

Benabid, A.L. (2003) 'Deep brain stimulation for Parkinson's disease', *Current opinion in Neurobiology*, 13, pp. 696–706. Available at: https://doi.org/10.1016/j.conb.2003.11.001.

Berg, D. *et al.* (2005) *"Pathophysiology: biochemistry of Parkinson's disease," in* Neurodegenerative Diseases: Neurobiology, Pathogenesis and Therapeutics. Cambridge: Cambridge University Press. Available at: https://doi.org/10.1017/CBO9780511544873.042.

Van Den Berge, S.A. *et al.* (2012) 'Dementia in Parkinson's disease correlates with α-synuclein pathology but not with cortical astrogliosis', *Parkinson's Disease*, 2012. Available at: https://doi.org/10.1155/2012/420957.

Betarbet, R., Sherer, T.B. and Greenamyre, T. (2005) 'Ubiquitin–proteasome system and Parkinson's diseases', *Experimental Neurology*, 191(1), pp. S17–S27.

Beyer, M.K. *et al.* (2001) 'Causes of death in a community-based study of Parkinson's disease', *Acta Neurologica Scandinavica*, 103, pp. 7–11.

Bieri, G., Gitler, A.D. and Brahic, M. (2018) 'Internalization, axonal transport and release of fibrillar forms of alpha-synuclein', *Neurobiology of Disease*, 109, pp. 219–225. Available at: https://doi.org/10.1016/j.nbd.2017.03.007.

Blair, J.A. *et al.* (2016) 'Individual case analysis of postmortem interval time on brain tissue preservation', *PLoS ONE*, 11(3), pp. 1–14. Available at: https://doi.org/10.1371/journal.pone.0151615.

Blauwendraat, C., Nalls, M.A. and Singleton, A.B. (2022) 'The genetic architecture of Parkinson's disease', 19(2), pp. 170–178. Available at: https://doi.org/10.1016/S1474-4422(19)30287-X.The.

Borghammer, P. *et al.* (2021) 'Neuropathological evidence of body-first vs. brain-first Lewy body disease', *Neurobiology of Disease*, 161(November), p. 105557. Available at: https://doi.org/10.1016/j.nbd.2021.105557.

Braak, H. *et al.* (2003) 'Staging of brain pathology related to sporadic Parkinson's disease', *Neurobiology of Aging*, 24(2), pp. 197–211. Available at: https://doi.org/10.1016/S0197-4580(02)00065-9.

Braak, H. *et al.* (2004) 'Stages in the development of Parkinson's disease-related pathology', *Cell and Tissue Research*, 318(1), pp. 121–134. Available at: https://doi.org/10.1007/s00441-004-0956-9.

Braak, H. and Braak, E. (1995) 'Staging of Alzheimer's Disease-Related Neurofibrillary Changes', *Neurobiology of Aging*, 16(3), pp. 271–278.

Branton, W.G. *et al.* (2013) 'Brain Microbial Populations in HIV/AIDS: a-Proteobacteria Predominate Independent of Host Immune Status', *PLoS ONE*, 8(1). Available at: https://doi.org/10.1371/journal.pone.0054673.

Bras, I.C. and Outeiro, T.F. (2021) 'Alpha-Synuclein: Mechanisms of Release and Pathology Progression in Synucleinopathies', *Cells*, 10(375), pp. 1–19.

Brissaud, E. (1899) Leçons sur les maladies nerveuses : deuxième série (Hôpital Saint-Antoine). Paris. Available at: https://wellcomecollection.org/works/enzzhqaj.

Bronstein, J.M. *et al.* (2011) 'Deep Brain Stimulation for Parkinson Disease', *Archives of Neurology*, 68(2), pp. 165–171. Available at: https://doi.org/10.1001/archneurol.2010.260.

Brown, J.L. *et al.* (2019) 'Polymicrobial oral biofilm models: Simplifying the complex', *Journal of Medical Microbiology*, 68(11), pp. 1573–1584. Available at: https://doi.org/10.1099/JMM.0.001063.

Brück, D. *et al.* (2016) 'Glia and alpha-synuclein in neurodegeneration: A complex interaction', *Neurobiology of Disease*, 85, pp. 262–274. Available at: https://doi.org/10.1016/j.nbd.2015.03.003.

Bruner, E. (2022) 'A network approach to the topological organization of the Brodmann map', *Anatomical Record*, 305(12), pp. 3504–3515. Available at: https://doi.org/10.1002/ar.24941.

Buckley, M.W. and Mcgavern, D.B. (2022) 'Immune dynamics in the CNS and its barriers during homeostasis and disease', *Immunological Reviews*, 306(December 2021), pp. 58–75. Available at: https://doi.org/10.1111/imr.13066.

Burke, R.E., Dauer, W.T. and Vonsattel, J.P.G. (2008) 'A Critical Evaluation of The Braak Staging Scheme for Parkinson's Disease', *Annals of Neurology*, 64(5), pp. 485–491. Available at: https://doi.org/10.1002/ana.21541.A.

Buset, S. *et al.* (2016) 'Are periodontal diseases really silent?A systematic review of their effect on quality of life', *Journal of Clinical Periodontology*, 43, pp. 333–344. Available at: https://doi.org/10.1111/jcpe.12517.

Calabrese, V. *et al.* (2018) 'Aging and Parkinson's Disease: Inflammaging, neuroinflammation and biological remodeling as key factors in pathogenesis', *Free Radical Biology and Medicine*, 115, pp. 80–91. Available at: https://doi.org/10.1016/j.freeradbiomed.2017.10.379.

Von Campenhausen, S. *et al.* (2005) 'Prevalence and incidence of Parkinson's disease in Europe', *European Neuropsychopharmacology*, 15(4), pp. 473–490. Available at: https://doi.org/10.1016/j.euroneuro.2005.04.007.

Canto, C.B., Wouterlood, F.G. and Witter, M.P. (2008) 'What does the anatomical organization of the entorhinal cortex tell us?', *Neural Plasticity*, 2008. Available at: https://doi.org/10.1155/2008/381243.

Carabotti, M. *et al.* (2015) 'The gut-brain axis: interactions between enteric microbiota, central and enteric nervous systems', *Annals of Gastroenterology*, 28, pp. 203–209.

Castillo, D.J. *et al.* (2019) 'The Healthy Human Blood Microbiome: Fact or Fiction?', *Frontiers in Cellular and Infection Microbiology*, 9(May), pp. 1–12. Available at: https://doi.org/10.3389/fcimb.2019.00148.

Chai, C. and Lim, K.-L. (2014) 'Genetic Insights into Sporadic Parkinson's Disease Pathogenesis', *Current Genomics*, 14(8), pp. 486–501. Available at: https://doi.org/10.2174/1389202914666131210195808.

Chapple, I. *et al.* (2015) 'Primary prevention of periodontitis: managing gingivitis', *Journal of Clinical Periodontology*, 42(16), pp. S71–S76. Available at: https://doi.org/10.1111/jcpe.12366.

Charcot, J. (1872) 'De la paralysie agitante', in *Oeuvres Complètes (t 1) Leçons sur les maladies du système nerveux*. London: New Sydenham Society, pp. 129–156.

Chatterjee, K. *et al.* (2020) 'Inflammasome and α-synuclein in Parkinson's disease: A cross-sectional study', *Journal of Immunology*, 338(October 2019), pp. 1–5.

Chaudhuri, K.R. *et al.* (2011) 'Parkinson's disease: The non-motor issues', *Parkinsonism and Related Disorders*, 17(10), pp. 717–723. Available at: https://doi.org/10.1016/j.parkreldis.2011.02.018.

Chelliah Sundramurthi, S. *et al.* (2022) 'Identification of blood-based biomarkers for diagnosis and prognosis of Parkinson's disease : A systematic review of proteomics studies', *Ageing Research Reviews*, 73(November 2021), p. 101514. Available at: https://doi.org/10.1016/j.arr.2021.101514.

Chen, C. *et al.* (2018) 'Dental Scaling Decreases the Risk of Parkinson's Disease: A Nationwide Population-Based Nested Case-Control Study', *Internation Journal of Environmental Research and Public Health*, 15. Available at: https://doi.org/10.3390/ijerph15081587.

Chen, C.K., Wu, Y.T. and Chang, Y.C. (2017) 'Periodontal inflammatory disease is associated with the risk of Parkinson's disease: A population-based retrospective matched-cohort study', *PeerJ*, (8), pp. 1–14. Available at: https://doi.org/10.7717/peerj.3647.

Chen, H. *et al.* (2003) 'Nonsteroidal Anti-inflammatory Drugs and the Risk of Parkinson Disease', *JAMA Neurology*, 60(8), pp. 1059–1064.

Chiara, G. De *et al.* (2012) 'Infectious Agents and Neurodegeneration', *Molecular Neurobiology*, 46, pp. 614–638. Available at: https://doi.org/10.1007/s12035-012-8320-7.

Cicciu, M. *et al.* (2012) 'Periodontal Health and Caries Prevalence Evaluation in Patients Affected by Parkinson's Disease', *Parkinson's Disease*, 2012, pp. 5–10. Available at: https://doi.org/10.1155/2012/541908.

Clark, D., Boutros, N. and Mendez, M. (2018) 'Brainstem', in *The Brain and Behaviour: An Introduction to Behavioural Neuroanatomy*. 4th edn. Cambridge: Cambridge University Press, pp. 151–163. Available at: https://doi.org/10.1017/9781108164320.

Claydon, N.. (2008) 'Current concepts in toothbrushing and interdental cleaning', *Periodontology 2000*, 48(1), pp. 10–22.

Connolly, B.S. and Lang, A.E. (2014) 'Pharmacological treatment of Parkinson disease: A review', *JAMA - Journal of the American Medical Association*, 311(16), pp. 1670–1683. Available at: https://doi.org/10.1001/jama.2014.3654.

Dando, S.J. *et al.* (2014) 'Pathogens penetrating the central nervous system: Infection pathways and the cellular and molecular mechanisms of invasion', *Clinical Microbiology Reviews*, 27(4), pp. 691–726. Available at: https://doi.org/10.1128/CMR.00118-13.

Daneman, R. and Prat, A. (2015) 'The Blood–Brain Barrier', *Cold Spring Harbor Perspectives in Biology*, 7, pp. 1–24.

Danzer, K.M. *et al.* (2012) 'Exosomal cell-to-cell transmission of alpha synuclein oligomers', *Molecular Neurodegeneration*, 7(42), pp. 1–18.

Delaney, C. and Campbell, M. (2017) 'The blood brain barrier: Insights from development and ageing', *Tissue Barriers*, 5(5). Available at: https://doi.org/10.1080/21688370.2017.1373897.

Devi, L. *et al.* (2008) 'Mitochondrial import and accumulation of α-synuclein impair complex I in human dopaminergic neuronal cultures and Parkinson disease brain', *Journal of Biological Chemistry*, 283(14), pp. 9089–9100. Available at: https://doi.org/10.1074/jbc.M710012200.

Dewhirst, F.E. *et al.* (2010) 'The human oral microbiome', *Journal of Bacteriology*, 192(19), pp. 5002–5017. Available at: https://doi.org/10.1128/JB.00542-10.

Dickson, D.W. *et al.* (2009) 'Neuropathological assessment of Parkinson's disease: refining the diagnostic criteria', *The Lancet Neurology*, 8(12), pp. 1150–1157. Available at: https://doi.org/10.1016/S1474-4422(09)70238-8.

Dickson, D.W. (2012) 'Parkinson's disease and parkinsonism: Neuropathology', *Cold Spring,Med, Harb Perspect*, 2(8), pp. 1–15.

Dickson, D.W. (2018) 'Neuropathology of Parkinson disease', *Parkinsonism and Related Disorders*, 46, pp. S30–S33. Available at: https://doi.org/10.1016/j.parkreldis.2017.07.033.

Dong, S. *et al.* (2022) 'Brain-gut-microbiota axis in Parkinson's disease: A historical review and future perspective', *Brain Research Bulletin*, 183(February), pp. 84–93. Available at: https://doi.org/10.1016/j.brainresbull.2022.02.015.

Dorsey, E.R. and Bloem, B.R. (2018) 'The Parkinson pandemic - A call to action', *JAMA Neurology*, 75(1), pp. 9–10. Available at: https://doi.org/10.1001/jamaneurol.2017.3299.

Doty, R.L. (2012) 'Olfactory dysfunction in Parkinson disease', *Nature Reviews Neurology*, 8, pp. 329–339.

Drevets, D.A. (1999) 'Dissemination of *Listeria monocytogenes* by infected phagocytes', *Infection and Immunity*, 67(7), pp. 3512–3517.

Dunn, N. *et al.* (2005) 'Association between dementia and infectious disease: Evidence from a case-control study', *Alzheimer Disease and Associated Disorders*, 19(2), pp. 91–94. Available at: https://doi.org/10.1097/01.wad.0000165511.52746.1f.

Edgar, R.C. (2004) 'MUSCLE: multiple sequence alignment with high accuracy and high throughput', *Nucleic Acids Research*, 32(5), pp. 1792–1797. Available at: https://doi.org/10.1093/nar/gkh340.

Edgar, R.C. *et al.* (2011) 'UCHIME improves sensitivity and speed of chimera detection', *Bioinformatics*, 27(16), pp. 2194–2200. Available at: https://doi.org/10.1093/bioinformatics/btr381.

Edgar, R.C. (2013) 'UPARSE: highly accurate OTU sequences from microbial amplicon reads', *Nature Methods*, 10(10). Available at: https://doi.org/10.1038/nmeth.2604.

Elbaz, A. *et al.* (2015) 'Epidemiology of Parkinson's disease', *Revue Neurologique*, 172(1), pp. 14–26. Available at: https://doi.org/10.1016/j.neurol.2015.09.012.

Emamzadeh, F.N. and Surguchov, A. (2018) 'Parkinson's disease: Biomarkers, treatment, and risk factors', *Frontiers in Neuroscience*, 12(AUG), pp. 1–14. Available at: https://doi.org/10.3389/fnins.2018.00612.

Emery, D.C. *et al.* (2017) '16S rRNA Next Generation Sequencing Analysis Shows Bacteria in Alzheimer's Post-Mortem Brain', *Frontiers in Aging Neuroscience*, 9(June), pp. 1–13. Available at: https://doi.org/10.3389/fnagi.2017.00195.

Emery, D.C. *et al.* (2021) 'Comparison of Blood Bacterial Communities in Periodontal Health and Periodontal Disease', *Frontiers in Cellular and Infection Microbiology*, 10(January), pp. 1–15. Available at: https://doi.org/10.3389/fcimb.2020.577485.

Emre, M. *et al.* (2007) 'Clinical diagnostic criteria for dementia associated with Parkinson's disease', *Movement Disorders*, 22(12), pp. 1689–1707. Available at: https://doi.org/10.1002/mds.21507.

Engelhart, M.J. *et al.* (2004) 'Inflammatory Proteins in Plasma and the Risk of Dementia: The Rotterdam Study', *Archives of Neurology*, 61(5), pp. 668–672. Available at: https://doi.org/10.1001/archneur.61.5.668.

Eren, A.M. *et al.* (2013) 'Oligotyping: differentiating between closely related microbial taxa using 16S rRNA gene data', *Methods in Ecology and Evolution*, 4, pp. 1111–1119. Available at: https://doi.org/10.1111/2041-210X.12114.

Eren, A.M. *et al.* (2015) 'Minimum entropy decomposition: Unsupervised oligotyping for sensitive partitioning of high-throughput marker gene sequences', *International Society for Microbial Ecology*, 9, pp. 968–979. Available at: https://doi.org/10.1038/ismej.2014.195.

Erny, D., Hrabe de Angelis, A.L. and Prinz, M. (2016) 'Communicating systems in the body: how microbiota and microglia cooperate', *Immunology*, 150, pp. 7–15. Available at: https://doi.org/10.1111/imm.12645.

Fahn, S. (2003) 'Description of Parkinson's Disease as a Clinical Syndrome', *New York Academy of Sciences*, 991, pp. 1–14.

Faria-pereira, A. and Morais, V.A. (2022) 'Synapses: The Brain's Energy-Demanding Sites', *International Journal of Molecular Sciences*, 23(3627). Available at: https://doi.org/https://doi.org/10.3390/ijms23073627.

Farrall, A.J. and Wardlaw, J.M. (2009) 'Blood – brain barrier: Ageing and microvascular disease – systematic review and meta-analysis', *Neurobiology of Aging*, 30, pp. 337–352. Available at: https://doi.org/10.1016/j.neurobiolaging.2007.07.015.

Ferrari, C.C. and Tarelli, R. (2011) 'Parkinson's Disease and Systemic Inflammation', *Parkinson's Disease*, 2011. Available at: https://doi.org/10.4061/2011/436813.

Fitzgerald, E., Murphy, S. and Martinson, H.A. (2019) 'Alpha-synuclein pathology and the role of the microbiota in Parkinson's disease', *Frontiers in Neuroscience*, 13(APR), pp. 1–13. Available at: https://doi.org/10.3389/fnins.2019.00369.

Forrester, J. V, Mcmenamin, P.G. and Dando, S.J. (2018) 'CNS infection and immune privilege', *Nature Reviews Neuroscience*, 19(november), pp. 655–671. Available at: https://doi.org/10.1038/s41583-018-0070-8.

Franceschi, C. *et al.* (2000) 'Inflamma-aging. An Evolutionary Perspective on Immunosenescence', *Annals of the New York Academy of Sciences*, 908, pp. 244–254.

Freeman, L.C. and P.-Y Ting, J. (2016) 'The pathogenic role of the inflammasome in neurodegenerative disease', *Journal of Neurochemistry*, 136, pp. 29–38. Available at: https://doi.org/10.1111/jnc.13217.

Fuente-Nunez, de la C. *et al.* (2018) 'Neuromicrobiology: How Microbes Influence the Brain', *ACS Chemical Neuroscience*, 9, pp. 141–150. Available at: https://doi.org/10.1021/acschemneuro.7b00373.

Gatz, M. *et al.* (2006) 'Potentially modifiable risk factors for dementia in identical twins', *Alzheimer's and Dementia*, 2, pp. 110–117. Available at: https://doi.org/10.1016/j.jalz.2006.01.002.

Gelb, D.J., Oliver, E. and Gilman, S. (1999) 'Diagnostic criteria for Parkinson disease', *Archives of Neurology*, 56(1), pp. 33–39. Available at: https://doi.org/10.1001/archneur.56.1.33.

George, S. *et al.* (2013) 'α-Synuclein: The long distance runner', *Brain Pathology*, 23(3), pp. 350–357. Available at: https://doi.org/10.1111/bpa.12046.

Gesi, M. *et al.* (2000) 'The role of the locus coeruleus in the development of Parkinson's disease', *Neuroscience and Biobehavioral Reviews*, 24, pp. 655–668.

Giguere, N. *et al.* (2019) 'Increased vulnerability of nigral dopamine neurons after expansion of their axonal arborization size through D2 dopamine receptor conditional knockout', *PLoS Genetics*, 15(8), pp. 1–26.

Glassing, A. *et al.* (2016) 'Inherent bacterial DNA contamination of extraction and sequencing reagents may affect interpretation of microbiota in low bacterial biomass samples', *Gut Pathogens*, 8(24), pp. 1–12. Available at: https://doi.org/10.1186/s13099-016-0103-7.

Goetz, C.G. (2011) 'The history of Parkinson's disease: Early clinical descriptions and neurological therapies', *Cold Spring Harbor Perspectives in Medicine*, 1(1), pp. 1–16. Available at: https://doi.org/10.1101/cshperspect.a008862.

Gomperts, S.N. (2016) 'Lewy Body Dementias: Dementia Bodies with Lewy Bodies and Parkinson Disease Dementia', *Continuum (Minneap Minn)*, 22(2), pp. 435–463. Available at: https://doi.org/10.1007/978-3-319-72938-1_14.

Gosney, M. *et al.* (2003) 'The incidence of oral Gram-negative bacteria in patients with Parkinson's disease', *European Journal of Internal Medicine*, 14(8), pp. 484–487. Available at: https://doi.org/10.1016/j.ejim.2003.09.009.

Govic, Y. Le *et al.* (2022) 'Pathogens infecting the central nervous system', *PLoS Pathogens*, 18(2), pp. 2–7. Available at: https://doi.org/https://doi.org/10.1371/journal.ppat.1010234.

Gowers, W.R. (1888) 'A Manual of Diseases of the Nervous System', *The American Journal of*

Psychology, 1(2), p. 346. Available at: https://doi.org/10.2307/1411377.

Guo, Y. *et al.* (2022) 'Brain regions susceptible to alpha-synuclein spreading', *Molecular Psychiatry*, 27, pp. 758–770. Available at: https://doi.org/10.1038/s41380-021-01296-7.

Habibi, M. (2017) *Dopamine receptors*, *The Curated Reference Collection in Neuroscience and Biobehavioral Psychology*. Elsevier. Available at: https://doi.org/10.1016/B978-0-12-809324-5.00551-4.

Hajishengallis, G. (2015) 'Periodontitis: From microbial immune subversion to systemic inflammation', *Nature Reviews Immunology*, 15(1), pp. 30–44. Available at: https://doi.org/10.1038/nri3785.

Hanaoka, A. and Kashihara, K. (2009) 'Increased frequencies of caries, periodontal disease and tooth loss in patients with Parkinson's disease', *Journal of Clinical Neuroscience*, 16(10), pp. 1279–1282. Available at: https://doi.org/10.1016/j.jocn.2008.12.027.

Haque, E. *et al.* (2020) 'Targeting the Microglial NLRP3 Inflammasome and Its Role in Parkinson's Disease', *Movement Disorders*, 35(1), pp. 20–33. Available at: https://doi.org/10.1002/mds.27874.

Hartmann, C.J. *et al.* (2019) 'An update on best practice of deep brain stimulation in Parkinson's disease', *Therapeutic Advancements in Neurological Disorders*, 12, pp. 1–20. Available at: https://doi.org/10.1177/1756286419838096.

Hawkes, C.H., Tredici, D. and Braak, H. (2009) 'Parkinson's Disease The Dual Hit Theory Revisited', *Annals of the New York Academy of Sciences*, 1170, pp. 615–622. Available at: https://doi.org/10.1111/j.1749-6632.2009.04365.x.

Hawkes, C.H., Tredici, K. Del and Braak, H. (2007) 'Review: Parkinson's disease: a dual-hit hypothesis', *Neuropathology and Applied Neurobiology*, 33, pp. 599–614. Available at: https://doi.org/10.1111/j.1365-2990.2007.00874.x.

Hawkes, C.H., Del Tredici, K. and Braak, H. (2010) 'A timeline for Parkinson's disease', *Parkinsonism and Related Disorders*, 16(2), pp. 79–84. Available at: https://doi.org/10.1016/j.parkreldis.2009.08.007.

Herrmann, K.M. Von *et al.* (2018) 'NLRP3 expression in mesencephalic neurons and characterization of a rare NLRP3 polymorphism associated with decreased risk of Parkinson's disease', *npjParkinson's Disease*, 24(November 2017). Available at: https://doi.org/10.1038/s41531-018-0061-5.

Holbrook, J.A. *et al.* (2021) 'Neurodegenerative Disease and the NLRP3 Inflammasome', *Frontiers in Pharmacology*, 12(March), pp. 1–15. Available at: https://doi.org/10.3389/fphar.2021.643254.

Holt, J.G. *et al.* (1994) *Bergey's Manual of Determinative Bacteriology*. Ninth edit. Baltimore: The Williams and Wilkins Comp.

Horliana, A.C.R.T. *et al.* (2014) 'Dissemination of periodontal pathogens in the bloodstream after periodontal procedures: A systematic review', *PLoS ONE*, 9(5), pp. 21–23. Available at: https://doi.org/10.1371/journal.pone.0098271.

Horz, H.-P. *et al.* (2008) 'Selective isolation of bacterial DNA from human clinical specimens', *Journal of Microbiological Methods*, 72(1), pp. 98–102.

Hu, X., Haas, J. and Lathe, R. (2021) 'The electronic tree of life (eTOL): a net of long probes to characterize the human microbiome from RNA-seq data', *Research Square* [Preprint]. Available at: https://doi.org/https://doi.org/10.21203/rs.3.rs-1208849/v1 License:

Hughes, D.T. and Sperandio, V. (2008) 'Inter-kingdom signalling: communication between bacteria and their hosts', *Nature Reviews Microbiology*, 6(2), pp. 111–120. Available at: https://doi.org/10.1038/nrmicro1836.Inter-kingdom.

Hussain, M., Stover, C.M. and Dupont, A. (2015) '*P. gingivalis* in periodontal disease and atherosclerosis - Scenes of action for antimicrobial peptides and complement', *Frontiers in Immunology*, 6(FEB), pp. 1–5. Available at: https://doi.org/10.3389/fimmu.2015.00045.

Ilievski, V. *et al.* (2018) 'Chronic oral application of a periodontal pathogen results in brain inflammation, neurodegeneration and amyloid beta production in wild type mice', *PLoS ONE*, 13(10), pp. 1–24. Available at: https://doi.org/10.1371/journal.pone.0204941.

Irwin, D.J., Lee, V.M.Y. and Trojanowski, J.Q. (2013) 'Parkinson's disease dementia: Convergence of α-synuclein, tau and amyloid-β pathologies', *Nature Reviews Neuroscience*, 14(9), pp. 626–636. Available at: https://doi.org/10.1038/nrn3549.

Jan, A. *et al.* (2021) 'The Prion-Like Spreading of Alpha-Synuclein in Parkinson's Disease: Update on Models and Hypotheses', *International Journal of Molecular Sciences*, 22, pp. 1–23.

Jankovic, J. and Tan, E.K. (2020) 'Parkinson's disease: etiopathogenesis and treatment', *Journal of Neurology Neurosurgery and Psychiatry*, 91(8), pp. 795–808. Available at: https://doi.org/10.1136/jnnp-2019-322338.

Jellinger, K.A. and Attems, J. (2006) 'Prevalence and impact of cerebrovascular pathology in Alzheimer's disease and parkinsonism', *Acta Neurologica Scandinavica*, 114, pp. 38–46. Available at: https://doi.org/10.1111/j.1600-0404.2006.00665.x.

Jellinger, K.A. and Korczyn, A.D. (2018) 'Are dementia with Lewy bodies and Parkinson's disease dementia the same disease?', *BMC Medicine*, 16(1), pp. 1–16. Available at: https://doi.org/10.1186/s12916-018-1016-8.

Jeong, E., Park, J.B. and Park, Y.G. (2021) 'Evaluation of the association between periodontitis and risk of Parkinson's disease: a nationwide retrospective cohort study', *Scientific Reports*, 11(1), pp. 1–8. Available at: https://doi.org/10.1038/s41598-021-96147-4.

Jha, M.K. and Morrison, B.M. (2018) 'Glia-neuron energy metabolism in health and diseases: New insights into the role of nervous system metabolic transporters', *Experimental Neurology*, 309(May), pp. 23–31. Available at: https://doi.org/10.1016/j.expneurol.2018.07.009.

Jo, S. *et al.* (2022) 'Oral and gut dysbiosis leads to functional alterations in Parkinson's disease', *npj Parkinson's Disease*, 8(1), pp. 1–12. Available at: https://doi.org/10.1038/s41531-022-00351-6.

Kamada, N. *et al.* (2013) 'Control of pathogens and pathobionts by the gut microbiota', *Nature Reviews Immunology*, 14(7), pp. 685–690. Available at: https://doi.org/10.1038/ni.2608.Control.

Karlsen, K.H. *et al.* (1999) 'Influence of clinical and demographic variables on quality of life in patients with Parkinson's disease', *Journal of Neurology Neurosurgery and Psychiatry*, 66(4), pp. 431–435. Available at: https://doi.org/10.1136/jnnp.66.4.431.

Karpinar, D.P. *et al.* (2009) 'Pre-fibrillar a-synuclein variants with impaired b-structure increase neurotoxicity in Parkinson's disease models', *The EMBO Journal*, 28(20), pp. 3256–3268. Available at: https://doi.org/10.1038/emboj.2009.257.

Kasen, A. *et al.* (2022) 'Upregulation of α-synuclein following immune activation: Possible trigger of Parkinson's disease', *Neurobiology of Disease*, 166.

Kennedy, M.A. *et al.* (1994) 'Relationship of oral microflora with oral health status in Parkinson's disease', *Special Care in Dentistry*, 14(4), pp. 164–168. Available at: https://doi.org/10.1111/j.1754-4505.1994.tb01125.x.

Kilian, M. *et al.* (2016) 'The oral microbiome - An update for oral healthcare professionals', *British Dental Journal*, 221(10), pp. 657–666. Available at: https://doi.org/10.1038/sj.bdj.2016.865.

Killinger, B.A. *et al.* (2018) 'The vermiform appendix impacts the risk of developing Parkinson's disease', *Science Translational Medicine*, 10(465). Available at: https://doi.org/10.1126/scitranslmed.aar5280.

Killinger, B.A. and Kordower, J.H. (2019) 'The interneuronal spread of alpha-synuclein- relevant or epiphenomenon?', *Journal of Neurochemistry*, 150, pp. 605–611. Available at: https://doi.org/10.1111/jnc.14779.

Kinane, D. and Attström, R. (2005) 'Advances in the pathogenesis of periodontitiss. Group B consensus report of the fifth European workshop in periodontology', *Journal of Clinical Periodontology*, 32(6), pp. 130–131.

Klein, M.O. *et al.* (2019) 'Dopamine: Functions, Signaling, and Association with Neurological Diseases', *Cellular and Molecular Neurobiology*, 39(1), pp. 31–59. Available at: https://doi.org/10.1007/s10571-018-0632-3.

Kobylecki, C. (2020) 'Update on the diagnosis and management of Parkinson's disease', *Clinical Medicine, Journal of the Royal College of Physicians of London*, 20(4), pp. 393–398. Available at: https://doi.org/10.7861/CLINMED.2020-0220.

Könönen, E., Gursoy, M. and Gursoy, U.K. (2019) 'Periodontitis: A multifaceted disease of tooth-supporting tissues', *Journal of Clinical Medicine*, 8(8). Available at: https://doi.org/10.3390/jcm8081135.

Kordower, J.H. *et al.* (2008) 'Lewy body – like pathology in long-term embryonic nigral transplants in Parkinson's disease', *Nature medicine*, 14(5), pp. 504–506. Available at: https://doi.org/10.1038/nm1747.

Kralik, P. and Ricchi, M. (2017) 'A basic guide to real time PCR in microbial diagnostics: Definitions, parameters, and everything', *Frontiers in Microbiology*, 8(FEB), pp. 1–9. Available at: https://doi.org/10.3389/fmicb.2017.00108.

Kumar, D.K.V. *et al.* (2016) 'Alzheimer's disease: the potential therapeutic role of the natural antibiotic amyloid- β peptide', *Neurodegenerative Disease Management*, 6(5), pp. 345–348.

L Jost (2006) 'Entropy and diversity', *Opinion*, 2, pp. 363–375.

Lee, E.Y. *et al.* (2020) 'Functional Reciprocity of Amyloids and Antimicrobial Peptides: Rethinking the Role of Supramolecular Assembly in Host Defense, Immune Activation, and Inflammation', *Frontiers in Immunology*, 11(July), pp. 1–15. Available at: https://doi.org/10.3389/fimmu.2020.01629.

Leheste, J.R. *et al.* (2017) '*P. acnes*-driven disease pathology: Current knowledge and future directions', *Frontiers in Cellular and Infection Microbiology*, 7(MAR), pp. 1–9. Available at: https://doi.org/10.3389/fcimb.2017.00081.

Li, X., Tronstad, L. and Olsen, I. (1999) 'Brain abscesses caused by oral infection', *Endodontics and Dental Traumatology*, 15(3), pp. 95–101. Available at: https://doi.org/10.1111/j.1600-9657.1999.tb00763.x.

Lie, G. *et al.* (2021) 'What's that smell? A pictorial review of the olfactory pathways and imaging assessment of the myriad pathologies that can affect them', *Insights into Imaging*, 12(7). Available at: https://doi.org/10.1186/s13244-020-00951-x.

Lill, C.M. (2016) 'Genetics of Parkinson's disease', *Molecular and Cellular Probes*, 30(6), pp. 386–396. Available at: https://doi.org/10.1016/j.mcp.2016.11.001.

Link, C.D. (2021) 'Is There a Brain Microbiome?', *Neuroscience Insights*, 16, pp. 1–5. Available at: https://doi.org/10.1177/26331055211018709.

Liu, G. *et al.* (2009) 'α-Synuclein is differentially expressed in mitochondria from different rat brain regions and dose-dependently down-regulates complex I activity', *Neuroscience Letters*, 454(3), pp. 187–192. Available at: https://doi.org/10.1016/j.neulet.2009.02.056.

Liu, T.C. *et al.* (2013) 'Increased risk of parkinsonism following chronic periodontitis: A retrospective cohort study', *Movement Disorders*, 28(9), pp. 1307–1308. Available at: https://doi.org/10.1002/mds.25359.

Lloyd-price, J., Abu-ali, G. and Huttenhower, C. (2016) 'The healthy human microbiome', *Genome Medicine*, 8(51), pp. 1–11. Available at: https://doi.org/10.1186/s13073-016-0307-y.

Lopes da Fonseca, T., Villar-piqué, A. and Outeiro, T.F. (2015) 'The Interplay between Alpha-Synuclein Clearance and Spreading', *Biomolecules*, 5, pp. 435–471. Available at: https://doi.org/10.3390/biom5020435.

Louveau, A. *et al.* (2017) 'Understanding the functions and relationships of the glymphatic system and meningeal lymphatics', *The Journal of Clinical Investigation*, 127(9), pp. 3210–3219.

Lu, X. *et al.* (2019) 'Transcellular traversal of the blood-brain barrier by the pathogenic *Propionibacterium acnes*', *Journal of Cellular Biochemistry*, 120(5), pp. 8457–8465. Available at: https://doi.org/10.1002/jcb.28132.

Luca, A., Calandra, C. and Luca, M. (2018) 'Molecular Bases of Alzheimer's Disease and Neurodegeneration: The Role of Neuroglia', *Aging and Disease*, 9(6), pp. 1134–1152.

Luo, S.X. and Huang, E.J. (2016) 'Dopaminergic Neurons and Brain Reward Pathways From Neurogenesis to Circuit Assembly', *The American Journal of Pathology*, 186(3), pp. 478–488. Available at: https://doi.org/10.1016/j.ajpath.2015.09.023.

Lusk, R.W. (2014) 'Diverse and widespread contamination evident in the unmapped depths of high throughput sequencing data', *PLoS ONE*, 9(10). Available at: https://doi.org/10.1371/journal.pone.0110808.

Luth, E.S. *et al.* (2014) 'Soluble, prefibrillar α-synuclein oligomers promote complex I-dependent, Ca2+-induced mitochondrial dysfunction', *Journal of Biological Chemistry*, 289(31), pp. 21490–21507. Available at: https://doi.org/10.1074/jbc.M113.545749.

Lutz, H. *et al.* (2020) 'Effects of Extended Postmortem Interval on Microbial Communities in Organs of the Human Cadaver', *Frontiers in Microbiology*, 11(December), pp. 1–11. Available at: https://doi.org/10.3389/fmicb.2020.569630.

Lyra, P. *et al.* (2020) 'Parkinson's Disease, Periodontitis and Patient-Related Outcomes: A Cross-Sectional Study', *medicina*, 56(383), pp. 1–11.

Macin, S. *et al.* (2017) 'Mastoiditis, brain abscess and sinus thrombosis as complications of chronic otitis media: A case report', *Jundishapur Journal of Microbiology*, 10(2), pp. 0–3. Available at: https://doi.org/10.5812/jjm.41352.

Madelung, C.F. *et al.* (2022) 'Locus Coeruleus Shows a Spatial Pattern of Structural Disintegration in Parkinson's Disease', *Movement Disorders*, 37(3), pp. 479–489. Available at: https://doi.org/10.1002/mds.28945.

Magoc, T. and Salzberg, S.L. (2011) 'FLASH: fast length adjustment of short reads to improve genome assemblies', *Bioinformatics*, 27(21), pp. 2957–2963. Available at: https://doi.org/10.1093/bioinformatics/btr507.

Di Maio, R. *et al.* (2016) 'α-synuclein binds to TOM20 and inhibits mitochondrial protein import in Parkinson's disease', *Science Translational Medicine*, 8(342), pp. 1–15. Available at: https://doi.org/10.1126/scitranslmed.aaf3634.

Mak, T.N. *et al.* (2012) '*Propionibacterium acnes* host cell tropism contributes to vimentin-mediated invasion and induction of inflammation', *Cellular Microbiology*, 14(11), pp. 1720–1733. Available at:

https://doi.org/10.1111/j.1462-5822.2012.01833.x.

Malpartida, A.B. *et al.* (2021) 'Mitochondrial Dysfunction and Mitophagy in Parkinson's Disease: From Mechanism to Therapy', *Trends in Biochemical Sciences*, 46(4), pp. 329–343.

Manfredsson, F.P. *et al.* (2019) 'Induction of alpha-synuclein pathology in the enteric nervous system of the rat and non-human primate results in gastrointestinal dysmotility and transient CNS pathology', *Neurobiology Disorders*, 112, pp. 106–118. Available at: https://doi.org/10.1016/j.nbd.2018.01.008.Induction.

Mapunda, J.A. *et al.* (2022) 'How Does the Immune System Enter the Brain?', *Frontiers in Immunology*, 13(February), pp. 1–15. Available at: https://doi.org/10.3389/fimmu.2022.805657.

Marques, O. and Outeiro, T.F. (2012) 'Alpha-synuclein: from secretion to dysfunction and death', *Cell Death and Disease*, 3(7), pp. e350-7. Available at: https://doi.org/10.1038/cddis.2012.94.

Marsh, L. (2013) 'Depression and Parkinson's Disease: Current Knowledge', *Current Neurology and Neuroscience Reports*, 13(12). Available at: https://doi.org/10.1007/s11910-013-0409-5.

Marsh, P.D. and Zaura, E. (2017) 'Dental biofilm: ecological interactions in health and disease', *Journal of Clinical Periodontology*, 44, pp. S12–S22. Available at: https://doi.org/10.1111/jcpe.12679.

Marsili, L., Rizzo, G. and Colosimo, C. (2018) 'Diagnostic criteria for Parkinson's disease: From James Parkinson to the concept of prodromal disease', *Frontiers in Neurology*, 9(MAR), pp. 1–10. Available at: https://doi.org/10.3389/fneur.2018.00156.

Martinez-Martin, P. *et al.* (2015) 'Assessing the non-motor symptoms of Parkinson's disease: MDS-UPDRS and NMS Scale', *European Journal of Neurology*, 22(1), pp. 37–43. Available at: https://doi.org/10.1111/ene.12165.

De Marzi, R. *et al.* (2016) 'Loss of Dorsolateral Nigral Hyperintensity on 3.0 Tesla Susceptibility-Weighted Imaging in Idiopathic Rapid Eye Movement Sleep Behavior Disorder', *Annals of Neurology*, 70, pp. 1026–1030. Available at: https://doi.org/10.1002/ana.24646.

McKeith, I.G. *et al.* (2017) 'Diagnosis and management of dementia with Lewy bodies', *Neurolo*, 89, pp. 1–14. Available at: https://www.ncbi.nlm.nih.gov/pubmed/28592453.

Mcmanus, R.M. and Heneka, M.T. (2017) 'Role of neuroinflammation in neurodegeneration: new insights', *Alzheimer's Research and Therapy*, 9(14), pp. 1–7. Available at: https://doi.org/10.1186/s13195-017-0241-2.

Meade, R.M., Fairlie, D.P. and Mason, J.M. (2019) 'Alpha-synuclein structure and Parkinson's disease', *Molecular Neurodegeneration*, 14(1), pp. 1–14. Available at: https://doi.org/10.1186/s13024-019-0329-1.

Medawar, P.. (1947) 'Immunity to homologous grafted skin. III . The fate of skin homografts transplanted to the brain, to subcutaneous tissue, and to the anterior chamber of the eye.', *The British Journal of Experimental Pathology*, 29(1), pp. 58–69.

Meder, D. *et al.* (2019) 'The role of dopamine in the brain - lessons learned from Parkinson's disease', *NeuroImage*, 190(October 2018), pp. 79–93. Available at: https://doi.org/10.1016/j.neuroimage.2018.11.021.

Meyle, J. and Chapple, I. (2015) 'Molecular aspects of the pathogenesis of periodontitis', *Periodontology 2000*, 69(1), pp. 7–17. Available at: https://doi.org/10.1111/prd.12104.

Midwood, I. *et al.* (2019) 'Patients' perception of their oral and periodontal health and its impact: a cross-sectional study in the NHS', *British Dental Journal*, 227(7), pp. 587–593. Available at: https://doi.org/10.1038/s41415-019-0721-9.

Mihaila, D. *et al.* (2018) 'The oral microbiome of early stage Parkinson's disease and its relationship with functional measures of motor and non-motor function', *PLoS ONE*, 14(6), pp. 1–24. Available at: https://doi.org/10.1371/journal.pone.0218252.

Miller, D.B. and Callaghan, J.P.O. (2014) 'Biomarkers of PD - Present and Future', *Metabolism*, 64(3), pp. S40–S46. Available at: https://doi.org/10.1016/j.metabol.2014.10.030.Biomarkers.

Miller, I.N. and Cronin-Golomb, A. (2010) 'Gender differences in Parkinson's Disease: Clinical characteristics and cognition', *Movement Disorders*, 25(16), pp. 2695–2703. Available at: https://doi.org/10.1002/mds.23388.GENDER.

Miranda-saksena, M. *et al.* (2018) 'Infection and Transport of Herpes Simplex Virus Type 1 in Neurons: Role of the Cytoskeleton', *Viruses*, 10(92), pp. 1–20. Available at: https://doi.org/10.3390/v10020092.

Miriam, F.M. and William, O.C. (2017) 'The lung microbiome in health and disease', *Clinical Medicine*, 17(6), pp. 525–529.

Molteni, M. and Rossetti, C. (2017) 'Neurodegenerative diseases: The immunological perspective', *Journal of Neuroimmunology*, 313(November), pp. 109–115. Available at: https://doi.org/10.1016/j.jneuroim.2017.11.002.

Montagne, A. *et al.* (2015) 'Blood-Brain Barrier Breakdown in the Aging Human Hippocampus', *Neuron*, 85(2), pp. 296–302. Available at: https://doi.org/10.1016/j.neuron.2014.12.032.Blood-Brain.

Moore, T.J., Glenmullen, J. and Mattison, D.R. (2014) 'Reports of Pathological Gambling, Hypersexuality, and Compulsive Shopping Associated With Dopamine Receptor Agonist Drugs', 22314(12), pp. 1930–1933. Available at: https://doi.org/10.1001/jamainternmed.2014.5262.

Moussaud, S. *et al.* (2014) 'Alpha-synuclein and tau: teammates in neurodegeneration?', *Molecular Neurobiology*, 9(43), pp. 1–14.

Mucci, L.A. *et al.* (2004) 'Birth Order, Sibship Size, and Housing Density in Relation to Tooth Loss and Periodontal Disease: A Cohort Study among Swedish Twins', *American Journal of Epidemiology*, 159(5), pp. 499–506. Available at: https://doi.org/10.1093/aje/kwh063.

Mulak, A. and Bonaz, B. (2015) 'Brain-gut-microbiota axis in Parkinson's disease', *World Journal of Gastroenterology*, 21(37), pp. 10609–10620. Available at: https://doi.org/10.3748/wjg.v21.i37.10609.

Muzumdar, D., Jhawar, S. and Goel, A. (2011) 'Brain abscess: An overview', *International Journal of Surgery*, 9(2), pp. 136–144. Available at: https://doi.org/10.1016/j.ijsu.2010.11.005.

Nadkarni, M.A. *et al.* (2002) 'Determination of bacterial load by real-time PCR using a broad-range (universal) probe and primers set', *Microbiology*, 148, pp. 257–266. Available at: papers3://publication/uuid/720C1476-57B5-40A2-AC1C-EA8708B08F2E.

Nakayama, Y., Washio, M. and Mori, M. (2004) 'Oral Health Conditions in Patients with Parkinson's Disease', *Journal of Epidemiology*, 14(5), pp. 143–150.

Nazir, M. *et al.* (2020) 'Global Prevalence of Periodontal Disease and Lack of Its Surveillance', *Scientific World Journal*, 2020. Available at: https://doi.org/10.1155/2020/2146160.

Norsted, E., Gomuc, B. and Meister, B. (2008) 'Protein components of the blood–brain barrier (BBB) in the mediobasal hypothalamus', *Journal of Chemical Neuroanatomy*, 36, pp. 107–121. Available at: https://doi.org/10.1016/j.jchemneu.2008.06.002.

Noyce, A.J. *et al.* (2016) 'The prediagnostic phase of Parkinson's disease', *J Neurol Neurosurg Psychiatry*, 87, pp. 871–878. Available at: https://doi.org/10.1136/jnnp-2015-311890.

O'Hara, D.M., Kalia, S.K. and Kalia, L. V (2020) 'Methods for detecting toxic α -synuclein species as a biomarker for Parkinson ' s disease', *Critical Reviews in Clinical Laboratory Sciences*, 57(5), pp. 291–

307. Available at: https://doi.org/10.1080/10408363.2019.1711359.

Oertel, W. and Schulz, J.B. (2016) 'Current and experimental treatments of Parkinson disease: A guide for neuroscientists', *Journal of Neurochemistry*, 139, pp. 325–337. Available at: https://doi.org/10.1111/jnc.13750.

Ogata, A. *et al.* (1997) 'A rat model of Parkinson's disease induced by Japanese encephalitis virus', *Journal of Neurovirology*, 3(2), pp. 141–147. Available at: https://doi.org/10.3109/13550289709015803.

Ogrendik, M. (2013) 'Rheumatoid arthritis is an autoimmune disease caused by periodontal pathogens', *International Journal of General Medicine*, 6, pp. 383–386. Available at: https://doi.org/10.2147/IJGM.S45929.

Oliva, R. *et al.* (2021) 'Remodeling of the Fibrillation Pathway of α -Synuclein by Interaction with Antimicrobial Peptide LL-III', *Chemistry Europe*, 27, pp. 11845–11851. Available at: https://doi.org/10.1002/chem.202101592.

Ong, L.K., Walker, F.R. and Nilsson, M. (2017) 'Is Stroke a Neurodegenerative Condition? A Critical Review of Secondary Neurodegeneration and Amyloid-beta Accumulation after Stroke', *AIMS Medical Science*, 4(1), pp. 1–16. Available at: https://doi.org/10.3934/medsci.2017.1.1.

Opara, J.A. *et al.* (2012) 'Quality of life in Parkinson's disease.', *Journal of medicine and life*, 5(4), pp. 375–381. Available at: https://doi.org/10.5005/jp/books/10538_43.

Orad, R.I. and Shiner, T. (2022) 'Differentiating dementia with Lewy bodies from Alzheimer's disease and Parkinson's disease dementia: an update on imaging modalities', *Journal of Neurology*, 269(2), pp. 639–653. Available at: https://doi.org/10.1007/s00415-021-10402-2.

Otomo-Corgel, J. *et al.* (2012) 'State of the science: Chronic periodontitis and systemic health', *Journal of Evidence-Based Dental Practice*, 12(3 SUPPL.), pp. 20–28. Available at: https://doi.org/10.1016/S1532-3382(12)70006-4.

Outeiro, T.F. *et al.* (2019) 'Dementia with Lewy bodies: An update and outlook', *Molecular Neurodegeneration*, 14(1), pp. 1–18. Available at: https://doi.org/10.1186/s13024-019-0306-8.

Outeiro, T.F. (2019) 'LRRK2, alpha-synuclein , and tau: partners in crime or unfortunate bystanders?', *Biomedical Society Transactions*, 47(3), pp. 827–838. Available at: https://doi.org/https://doi.org/10.1042/BST20180466.

Packer, M. *et al.* (2009) 'The potential benefits of dental implants on the oral health quality of life of people with Parkinson's disease', *Gerodontology*, 26(1), pp. 11–18. Available at: https://doi.org/10.1111/j.1741-2358.2008.00233.x.

Pang, S.Y.Y. *et al.* (2019) 'The interplay of aging, genetics and environmental factors in the pathogenesis of Parkinson's disease', *Translational Neurodegeneration*, 8(1), pp. 1–11. Available at: https://doi.org/10.1186/s40035-019-0165-9.

Parahitiyawa, N.B. *et al.* (2009) 'Microbiology of Odontogenic Bacteremia: beyond Endocarditis', *Clinical Microbiology Reviews*, 22(1), pp. 46–64. Available at: https://doi.org/10.1128/CMR.00028-08.

Paredes-rodriguez, E. *et al.* (2020) 'The Noradrenergic System in Parkinson's Disease', *Frontiers in Pharmacology*, 11(435), pp. 1–13. Available at: https://doi.org/10.3389/fphar.2020.00435.

Parent, M. and Parent, A. (2010) 'Substantia Nigra and Parkinson's Disease: A Brief History of Their Long and Intimate Relationship', *The Canadian Journal of Neurological Sciences*, 37, pp. 313–319.

Park, S.-P. *et al.* (2016) 'Functional characterization of alpha-synuclein protein with antimicrobial activity', *Biochemical and Biophysical Research Communications*, 478(2), pp. 924–928.

Parkinson, J. (1817) *An essay on the shaking palsy*. London: Sherwood, Neely, and Jones. Available at: https://wellcomecollection.org/works/dds3xw6y.

Parkkinen, L., Pirttilä, T. and Alafuzo, I. (2008) 'Applicability of current staging/ categorization of a-synuclein pathology and their clinical relevance', *Acta Neurologica*, 115, pp. 399–407. Available at: https://doi.org/10.1007/s00401-008-0346-6.

Pereira, P.A.B. *et al.* (2017) 'Oral and nasal microbiota in Parkinson's disease', *Parkinsonism and Related Disorders*, 38, pp. 61–67. Available at: https://doi.org/10.1016/j.parkreldis.2017.02.026.

Persidsky, Y. *et al.* (2006) 'Blood–brain Barrier: Structural Components and Function Under Physiologic and Pathologic Conditions', *Journal of Neuroimmune Pharmacology*, 1, pp. 223–236. Available at: https://doi.org/10.1007/s11481-006-9025-3.

Peterson, S.N. *et al.* (2013) 'The Dental Plaque Microbiome in Health and Disease', *PLoS ONE*, 8(3). Available at: https://doi.org/10.1371/journal.pone.0058487.

Pisa, D., Alonso, R. and Carrasco, L. (2020) 'Parkinson's disease: A comprehensive analysis of fungi and bacteria in brain tissue', *International Journal of Biological Sciences*, 16(7), pp. 1135–1152.

Available at: https://doi.org/10.7150/ijbs.42257.

Pisa, Di. *et al.* (2017) 'Polymicrobial Infections in Brain Tissue from Alzheimer's Disease Patients', *Scientific Reports*, 7(1), pp. 1–14. Available at: https://doi.org/10.1038/s41598-017-05903-y.

Poewe, W. (2008) 'Non-motor symptoms in Parkinson's disease', *European Journal of Neurology*, 15, pp. 14–20. Available at: https://doi.org/10.1016/j.bbrc.2016.08.052.

Politis, M. *et al.* (2010) 'Parkinson's Disease Symptoms: The Patient's Perspective', *Movement Disorders*, 25(11), pp. 1646–1651. Available at: https://doi.org/10.1002/mds.23135.

Popescu, B.O. *et al.* (2009) 'Blood-brain barrier alterations in ageing and dementia', *Journal of the Neurological Sciences*, 283, pp. 99–106. Available at: https://doi.org/10.1016/j.jns.2009.02.321.

Postuma, R.B. *et al.* (2015) 'MDS clinical diagnostic criteria for Parkinson's disease', *Movement Disorders*, 30(12), pp. 1591–1601. Available at: https://doi.org/10.1002/mds.26424.

Pradeep, A.R. *et al.* (2015) 'Clinical evaluation of the periodontal health condition and oral health awareness in Parkinson's disease patients', *Gero*, 32, pp. 100–106. Available at: https://doi.org/10.1111/ger.12055.

Prehn-Kristensen, A. *et al.* (2018) 'Reduced microbiome alpha diversity in young patients with ADHD', *PLoS ONE*, 13(7), pp. 1–19. Available at: https://doi.org/10.1371/journal.pone.0200728.

Public Health England (2020) *National Dental Epidemiology Programme for England - Oral health survey of adults attending general dental practices 2018*. Available at: https://assets.publishing.service.gov.uk/government/uploads/system/uploads/attachment_data/file/891208/AiP_survey_for_England_2018.pdf.

Qian, Y. *et al.* (2018) 'Detection of microbial 16S rRNA gene in the blood of patients with Parkinson's disease', *Frontiers in Aging Neuroscience*, 10(MAY), pp. 1–11. Available at: https://doi.org/10.3389/fnagi.2018.00156.

Quast, C. *et al.* (2013) 'The SILVA ribosomal RNA gene database project: improved data processing and web-based tools', *Nucleic Acids Research*, 41(November 2012), pp. 590–596. Available at: https://doi.org/10.1093/nar/gks1219.

Radak, D. *et al.* (2017) 'Apoptosis and Acute Brain Ischemia in Ischemic Stroke', *Current Vascular Pharmacology*, 15(2), pp. 115-122(8).

Rambaran, R.N. and Serpell, L.C. (2008) 'Amyloid fibrils Abnormal protein assembly', *Prion*, 2(3), pp.

112–117.

Reeve, A., Simcox, E. and Turnbull, D. (2014) 'Ageing and Parkinson's disease: Why is advancing age the biggest risk factor?', *Ageing Research Reviews*, 14(1), pp. 19–30. Available at: https://doi.org/10.1016/j.arr.2014.01.004.

Ren, L. *et al.* (2018) 'Nonsteroidal anti-inflammatory drugs use and risk of Parkinson disease', *Medicine*, 97(37).

Rey, N.L., Wesson, D.W. and Brundin, P. (2018) 'The olfactory bulb as the entry site for prion-like propagation in neurodegenerative diseases', *Neurobiology of Disease*, 109, pp. 226–248. Available at: https://doi.org/10.1016/j.nbd.2016.12.013.The.

Rhee, S.H., Pothoulakis, C. and Mayer, E.A. (2009) 'Principles and clinical implications of the brain-gut-enteric microbiota axis', *Nature Reviews Gastroenterology and Hepatology*, 6(5), pp. 306–314. Available at: https://doi.org/10.1038/nrgastro.2009.35.

Riel, D. Van, Verdijk, R. and Kuiken, T. (2015) 'The olfactory nerve: A shortcut for influenza and other viral diseases into the central nervous system', *The Journal of Pathology* [Preprint], (October 2017). Available at: https://doi.org/10.1002/path.4461.

Rocha Sobrinho, H.M. da *et al.* (2018) 'TLR4 and TLR2 activation is differentially associated with age during Parkinson's disease', *Immunological Investigations*, 47(1), pp. 71–88. Available at: https://doi.org/10.1080/08820139.2017.1379024.

Rodriguez, R.D. and Grinberg, L.T. (2015) 'Argyrophilic grain disease An underestimated tauopathy', *Dementia Neuropsychology*, 9(1), pp. 2–8. Available at: https://doi.org/10.1590/S1980-57642015DN91000002.

Salter, S.J. *et al.* (2014) 'Reagent and laboratory contamination can critically impact sequence-based microbiome analyses', *BMC Biology*, 12(1), pp. 1–12. Available at: https://doi.org/10.1186/s12915-014-0087-z.

Sampson, T.R. *et al.* (2016) 'Gut Microbiota Regulate Motor Deficits and Neuroinflammation in a Model of Parkinson's Disease', *Cell*, 167(6), pp. 1469–1480. Available at: https://doi.org/10.2174/1568026615101503282234 28.

Santos-García, D. and De La Fuente-Fernández, R. (2013) 'Impact of non-motor symptoms on health-related and perceived quality of life in Parkinson's disease', *Journal of the Neurological Sciences*, 332(1–2), pp. 136–140. Available at: https://doi.org/10.1016/j.jns.2013.07.005.

Sanz, M. *et al.* (2020) 'Periodontitis and cardiovascular diseases: Consensus report', *Journal of Clinical Periodontology*, 47(August 2019), pp. 268–288. Available at: https://doi.org/10.1111/jcpe.13189.

Scannapieco, F.A. (2013) 'The oral microbiome: Its role in health and in oral and systemic infections', *Clinical Microbiology Newsletter*, 35(20), pp. 163–169. Available at: https://doi.org/10.1016/j.clinmicnews.2013.09.003.

Scheperjans, F. *et al.* (2015) 'Gut Microbiota Are Related to Parkinson's Disease and Clinical Phenotype', *Movement Disorders*, 30(3), pp. 9–12. Available at: https://doi.org/10.1002/mds.26069.

Schloss, P.D. *et al.* (2009) 'Introducing mothur: Open-Source, Platform-Independent, Community-Supported Software for Describing and Comparing Microbial Communities', *Applied and Environmental Microbiology*, 75(23), pp. 7537–7541. Available at: https://doi.org/10.1128/AEM.01541-09.

Schwartz, M. and Cahalon, L. (2022) 'The vicious cycle governing the brain–immune system relationship in neurodegenerative diseases', *Current Opinion in Immunology*, 76. Available at: https://doi.org/https://doi.org/10.1016/j.coi.2022.102182.

Schwarz, J., Heimhilger, E. and Storch, A. (2006) 'Increased periodontal pathology in Parkinson's disease', *Journal of Neurology*, 253, pp. 608–611. Available at: https://doi.org/10.1007/s00415-006-0068-4.

Scott, K.M. *et al.* (2018) 'A systematic review and meta-analysis of alpha synuclein auto-antibodies in Parkinson's disease', *Frontiers in Neurology*, 9(OCT), pp. 1–11. Available at: https://doi.org/10.3389/fneur.2018.00815.

Senatorov Jr, V. V *et al.* (2019) 'Blood-brain barrier dysfunction in aging induces hyperactivation of TGFß signaling and chronic yet reversible neural dysfunction', *Science Translational Medicine*, 11(521). Available at: https://doi.org/https://doi.org/10.1126/scitranslmed.aaw8283.

Seyfried, T.N. *et al.* (2018) 'Sex-Related Abnormalities in Substantia Nigra Lipids in Parkinson's Disease', *ASN Neuro*, 10. Available at: https://doi.org/10.1177/1759091418781889.

Sharma, L.K., Lu, J. and Bai, Y. (2009) 'Mitochondrial Respiratory Complex I: Structure, Function and Implication in Human Diseases', *Current Medicinal Chemistry*, 16(10), pp. 1266–1277.

Sharon, G. *et al.* (2016) 'The Central Nervous System and the Gut Microbiome', *Cell*, 167(4), pp. 915–932. Available at: https://doi.org/10.1016/j.cell.2016.10.027.

Sherwin, E., Dinan, T.G. and Cryan, J.F. (2018) 'Recent developments in understanding the role of the gut microbiota in brain health and disease', *Annals of the New York Academy of Sciences*, 17, pp. 5–25. Available at: https://doi.org/10.1111/nyas.13416.

Shibley, R. *et al.* (2008) 'Quality of life in Parkinson's disease: The relative importance of the symptoms', *Movement Disorders*, 23(10), pp. 1428–1434. Available at: https://doi.org/10.1002/mds.21667.

Shoemark, D. and Allen-Birt, S. (2017) 'Bacterial burden in disease, aging and Alzheimer's', in *Handbook of Infection and Alzheimer's Disease*, pp. 133–149.

Siddiqui, H. *et al.* (2019) 'High Throughput Sequencing Detect Gingivitis And Periodontal Oral Bacteria In Alzheimer's Disease Autopsy Brains', *Neuro Research*, 1(1). Available at: https://doi.org/10.35702/nrj.10003.

Singhal, G. *et al.* (2014) 'Inflammasomes in neuroinflammation and changes in brain function: a focused review', *Frontiers in Neuroscience*, 8(October), pp. 1–13. Available at: https://doi.org/10.3389/fnins.2014.00315.

Song, Y. *et al.* (2020) 'The Effect of Estrogen Replacement Therapy on Alzheimer's Disease and Parkinson's Disease in Postmenopausal Women: A Meta-Analysis', *Frontiers in Neuroscience*, 14(March), pp. 1–13. Available at: https://doi.org/10.3389/fnins.2020.00157.

Soscia, S.J. *et al.* (2010) 'The Alzheimer's Disease-Associated Amyloid b-Protein Is an Antimicrobial Peptide', *PLoS ONE*, 5(3), pp. 1–10. Available at: https://doi.org/10.1371/journal.pone.0009505.

Souza, M. *et al.* (2000) 'Dityrosine Cross-linking Promotes Formation of Stable a-Synuclein Polymers', *The Journal of Biological Chemistry*, 275(24), pp. 18344–18349. Available at: https://doi.org/10.1074/jbc.M000206200.

Spagnuolo, C., Moccia, S. and Russo, G.L. (2018) 'Anti-inflammatory effects of flavonoids in neurodegenerative disorders', *European Journal of Medicinal Chemistry*, 153, pp. 105–115. Available at: https://doi.org/10.1016/j.ejmech.2017.09.001.

Spillantini, M.G. *et al.* (1998) 'α-Synuclein in filamentous inclusions of Lewy bodies from Parkinson's disease and dementia with Lewy bodies', *Proceedings of the National Academy of Sciences of the United States of America*, 95(11), pp. 6469–6473. Available at: https://doi.org/10.1073/pnas.95.11.6469.

Stein, P.S. *et al.* (2007) 'Tooth loss, dementia and neuropathology in the Nun study', *The Journal of*

the American Dental Association, 138(10), pp. 1314–1322. Available at: https://doi.org/10.14219/jada.archive.2007.0046.

Stolzenberg, E. *et al.* (2017) 'A Role for Neuronal Alpha-Synuclein in Gastrointestinal Immunity', *Journal of Innate Immunity*, 9, pp. 456–463. Available at: https://doi.org/10.1159/000477990.

Strotzer, M. (2009) 'One century of brain mapping using Brodmann areas', *Clinical Neuroradiology*, 19(3), pp. 179–186. Available at: https://doi.org/10.1007/s00062-009-9002-3.

Strowig, T. *et al.* (2012) 'Inflammasomes in health and disease', *Nature*, 481. Available at: https://doi.org/10.1038/nature10759.

Subramaniam, S.R. *et al.* (2014) 'Region specific mitochondrial impairment in mice with widespread overexpression of alpha-synuclein', *Neurobiology of Disease*, 70, pp. 204–213. Available at: https://doi.org/https://doi.org/10.1016/j.nbd.2014.06.017.

Surmeier, D.J., Obeso, J.A. and Halliday, G.M. (2017) 'Selective neuronal vulnerability in Parkinson disease', *Nature Reviews Neuroscience*, 18(2), pp. 101–113. Available at: https://doi.org/10.1038/nrn.2016.178.

Thanvi, B.R. and Lo, T.C.N. (2004) 'Long term motor complications of levodopa: Clinical features, mechanisms, and management strategies', *Postgraduate Medical Journal*, 80(946), pp. 452–458. Available at: https://doi.org/10.1136/pgmj.2003.013912.

The NHS Information Centre Dental and Eye Care Team (2009) 'Adult Dental Health Survey 2009 – First Release', pp. 1–19. Available at: http://goo.gl/2rcR1C%5Cnhttp://www.dhsspsni.gov.uk/adultdentalhealthsurvey_2009_firstrelease.pdf.

Tomás, I. *et al.* (2012) 'Periodontal health status and bacteraemia from daily oral activities: systematic review/meta-analysis', *Journal of Clinical Periodontology*, 39, pp. 213–228. Available at: https://doi.org/10.1111/j.1600-051X.2011.01784.x.

Tredici, K. Del and Braak, H. (2020) 'To stage, or not to stage', *Current Opinion in Neurobiology*, 61, pp. 10–22. Available at: https://doi.org/10.1016/j.conb.2019.11.008.

Tretiakoff, C. (1919) *Contribution a l'etude de l'anatomie pathologique du locus nigerde Soemmering avec quelques dedutions relatives a la pathogenie des troubles dutonus musculaire et de la maladie de Parkinson*. University of Paris.

Trutti, A.C. *et al.* (2019) 'Functional neuroanatomical review of the ventral tegmental area', *NeuroImage*, 191(January), pp. 258–268. Available at: https://doi.org/10.1016/j.neuroimage.2019.01.062.

Tysnes, O.B. and Storstein, A. (2017) 'Epidemiology of Parkinson's disease', *Journal of Neural Transmission*, 124(8), pp. 901–905. Available at: https://doi.org/10.1007/s00702-017-1686-y.

Tyson, T., Steiner, J.A. and Brundin, P. (2016) 'Sorting out release, uptake and processing of alpha-synuclein during prion-like spread of pathology', *Journal of Neurochemistry*, 139, pp. 275–289. Available at: https://doi.org/10.1111/jnc.13449.

Valdes, A.M. *et al.* (2018) 'Role of the gut microbiota in nutrition and health', *BMJ (Online)*, 361, pp. 36–44. Available at: https://doi.org/10.1136/bmj.k2179.

Valdinocci, D. *et al.* (2017) 'Potential Modes of Intercellular α -Synuclein Transmission'. Available at: https://doi.org/10.3390/ijms18020469.

Vanle, B. *et al.* (2018) 'NMDA antagonists for treating the non-motor symptoms in Parkinson's disease', *Translational Psychiatry*, 8(1). Available at: https://doi.org/10.1038/s41398-018-0162-2.

Veazey, C. (2005) 'Prevalence and Treatment of Depression in Parkinson's Disease', *Journal of Neuropsychiatry*, 17(3), pp. 310–323. Available at: https://doi.org/10.1176/appi.neuropsych.17.3.310.

Villafane, G. *et al.* (2007) 'Chronic high dose transdermal nicotine in Parkinson's disease: an open trial', *European Journal of Neurology*, 14, pp. 1313–1316. Available at: https://doi.org/10.1111/j.1468-1331.2007.01949.x.

Villafane, G. *et al.* (2018) 'High-dose transdermal nicotine in Parkinson's disease patients: a randomized, open-label, blinded-endpoint evaluation phase 2 study', *European Journal of Neurology*, 25(1), pp. 120–127. Available at: https://doi.org/10.1111/ene.13474.

Wade, W.G. (2013) 'The oral microbiome in health and disease', *Pharmacological Research*, 69(1), pp. 137–143. Available at: https://doi.org/10.1016/j.phrs.2012.11.006.

Wagner, B.D. *et al.* (2018) 'On the use of diversity measures in longitudinal sequencing studies of microbial communities', *Frontiers in Microbiology*, 9(MAY). Available at: https://doi.org/10.3389/fmicb.2018.01037.

Wang, Q. *et al.* (2007) 'Naive Bayesian Classifier for Rapid Assignment of rRNA Sequences into the

New Bacterial Taxonomy', *Applied and Environmental Microbiology*, 73(16), pp. 5261–5267. Available at: https://doi.org/10.1128/AEM.00062-07.

Wang, W. *et al.* (2015) 'Role of pro-inflammatory cytokines released from microglia in Alzheimer's disease', *Annals of Translational Medicine*, 3(10), pp. 1–15. Available at: https://doi.org/10.3978/j.issn.2305-5839.2015.03.49.

Wise, R.A. (2009) 'Roles for nigrostriatal-not just mesocorticolimbic-dopamine in reward and addiction', *Trends in Neurosciences*, 32(10), pp. 517–524. Available at: https://doi.org/10.1016/j.tins.2009.06.004.

Wong, Y.C. and Krainc, D. (2017) 'α-synuclein toxicity in neurodegeneration: mechanism and therapeutic strategies', *Nature medicine*, 23(2). Available at: https://doi.org/10.1038/nm.4269.

Wu, J.S., Kuo, C.Y. and Wu, J. Der (2019) '*Prevotella denticola* septic embolic cerebral infarction after difficult lower wisdom tooth extraction', *Journal of Dental Sciences*, 14(4), pp. 426–427. Available at: https://doi.org/10.1016/j.jds.2019.04.006.

Wu, P.C. *et al.* (2014) '*Prevotella* brain abscesses and stroke following dental extraction in a young patient: A case report and review of the literature', *Internal Medicine*, 53(16), pp. 1881–1887. Available at: https://doi.org/10.2169/internalmedicine.53.1299.

Yang, Q. *et al.* (2015) 'Evaluation of suitable control genes for quantitative polymerase chain reaction analysis of maternal plasma cell-free DNA', *Molecular medicine reports*, 12(5), pp. 7728–7734. Available at: https://doi.org/10.3892/mmr.2015.4334.

Yilmaz, R. *et al.* (2019) 'Biomarkers of Parkinson's disease: 20 years later', *Journal of Neural Transmission*, 126(7), pp. 803–813. Available at: https://doi.org/10.1007/s00702-019-02001-3.

Yu, M.B. *et al.* (2018) 'Extracellular Vimentin Modulates Human Dendritic Cell Activation', *Molecular Immunology*, 104, pp. 37–46. Available at: https://doi.org/10.1016/j.molimm.2018.09.017.Extracellular.

Zhan, X. *et al.* (2017) 'Gram-negative bacterial molecules associate with Alzheimer disease pathology', *Neurology*, 88(24), p. 2338. Available at: https://doi.org/10.1212/WNL.0000000000004048.

Zhou, R. *et al.* (2011) 'A role for mitochondria in NLRP3 inflammasome activation', *Nature*, 469, pp. 221–227. Available at: https://doi.org/10.1038/nature09663.

Zhou, R.M. *et al.* (2010) 'Molecular interaction of a-synuclein with tubulin influences on the polymerization of microtubule in vitro and structure of microtubule in cells', *Molecular Biology Reports*, 37, pp. 3183–3192. Available at: https://doi.org/10.1007/s11033-009-9899-2.